Utilising Chlorophyll Fluorescence to Assess the Variability of Phytoplankton Biomass and Productivity in the North-West European Shelf Seas

James Edward Fox

A thesis submitted for the Degree of
Doctor of Philosophy in Marine Biology

Department of Biological Sciences

University of Essex

October 2017

Thesis Abstract

Marine primary productivity by phytoplankton drives the conversion of CO_2 into organic carbon, thus supporting key marine ecosystem services such as biogeochemical nutrient cycles and fisheries. Therefore, the ability to accurately quantify and predict the environmental influences that govern this process is of paramount importance. Through surveying and experimental approaches, I investigated the variability of phytoplankton physiology and biomass across a range of light and nutrient environments. I found that growth and physiological responses differ in geographically distinct regimes of nutrient limitation across the North Sea. Variable nutrient stoichiometry across the region could therefore lead to alternative growth and productivity rates that reflect the populations suited to the different conditions. Fast repetition rate fluorometry (FRRf) measurements of photosystem II (PSII) characteristics during a spring bloom were shown to change with hydrography and community composition. Thus, providing further support that the physiological state of PSII can be used as an indicator of bloom status and community composition. FRRf-derived productivity parameters were also measured and shown to change in response to changes in taxonomy. Through geostatistical approaches the spatial distribution of phytoplankton was characterised during a spring bloom. I show both *in situ* and satellite sampling approaches possess the ability to capture mesoscale variability in phytoplankton distribution, but ocean colour estimates lose accuracy in highly heterogenous conditions. This thesis provides a step towards capturing the extent of spatial and temporal variability in phytoplankton stocks and rates in temperate shelf seas, in part, by providing a better understanding of the strengths and limitations of the use of fluorescence-based measurements.

Acknowledgments

First, I would like to offer my sincere gratitude to my supervisors Richard Geider, Etienne Low-Décarie and Rodney Forster for their inspiration and guidance over the past four years.

I'd also like to thank all members of the algal physiology group, past and present, for their feedback and thoughtful discussion; Phil Siegel and Kirralee Baker for the enthusiasm and time they always offered to discuss all things phytoplankton; Phil Davey and John Green for their patience and technical assistance in the collection of pigment and nutrient data; Veronique Creach for cruise opportunities and assistance in flow cytometry analysis; all the scientists and crew of the RV *Cefas endeavour* and RRS *Discovery* who always made going to sea a fantastic experience; all the regulars of department football who endured my competitive nature over the years!

Finally, I would like to thank all my friends and family for the continuous source of encouragement. Special thanks go to my parents and Ana, your love and support keep me going.

Table of Contents

Abbreviation	Abbreviation Definition	Unit
FRRf	Fast Repetition Rate fluorometry	
ETR	Electron Transfer Rate	
PAR	Photosynthetically active radiation	µmol photons m^{-2} s^{-1}
PSII	Photosystem II	
RCII	Reaction centre of PSII	
RLC	Rapid light curve	
NSV	Normalised Stern-Volmer coefficient	
NPQ	Non-photochemical quenching	dimensionless
ΔNPQ	The maximum range of NPQ measured over a fluorescence light curve	dimensionless
F_o', F', F_m'	Minimal, steady state and maximal fluorescence yields measured in actinic light	dimensionless
F_v	Variable fluorescence in darkness (= F_m - F_o)	dimensionless
F_q'	Change in fluorescence yield under actinic light (F_m' - F')	dimensionless
F_v/F_m	Maximum photochemical efficiency of PSII in dark adapted state	dimensionless
F_q'/F_m'	Operating efficiency of PSII	dimensionless
σ_{PSII}	Functional cross section of Photosystem II	nm^2
aETR	Absolute electron transport rate	e^- $RCII^{-1}$ s^{-1}
ETR_{max}	Maximum Electron Transport Rate	e^- $RCII^{-1}$ s^{-1}
α	Maximum light-utilisation coefficient	
E_k	Light required to saturate photosynthesis	µmol photons m^{-2} s^{-1}
DY029	Celtic Sea cruise, 2015	
CEND1417	North Sea cruise, 2014	
CEND1518	North Sea cruise, 2015	
CCS	Central Celtic Sea station	
YDay	Year day. The day of year where January 1st is day 1	
SML	Surface mixed layer	
BML	Bottom mixed layer	
SFC	Scanning Flow Cytometry	
Chl b	Chlorophyll b	
Allo	Alloxanthin	
Fuco	Fucoxanthin	
Per	Peridinin	
Zea	Zeaxanthin	
Allo	Alloxanthin	
Hex	19'-hexanoyloxyfucoxanthin	
But	19'-butanoyloxyfucoxanthin	

PPC	Photoprotective carotenoids
PSC	Photosynthetically active carotenoids

List of Figures

Supplementary Figures

List of Tables

Supplementary Tables

Declaration of the Contribution to Each Chapter

Chapter 1

I conceived and wrote this introductory chapter.

Chapter 2

All data for this chapter were collected during a cruise to the North Sea in 2015. I was responsible for the conception of the experimental design, conducting the incubation experiments, data analysis and write-up. Analysis for dissolved inorganic nutrients, chlorophyll by ultra-high-performance liquid chromatography (UPLC) and FRRf were carried out by myself. Analysis for POC were carried out by myself and Dannielle Berry (University of Essex). Flow cytometry sample collection and processing was carried out by myself with assistance from Dr Veronique Creache (Cefas) who carried out the cluster analysis and kindly offered the data. My cruise time and the funding for pigment analysis (samples sent to DHI) was made possible thanks to funding from the HighRoc project, obtained by Dr Rodney Forster (University of Hull) and Dr Veronique Creache.

Chapter 3

All data for this chapter were collected during a cruise to the Celtic Sea as part of the Shelf Sea Biogeochemistry program (NERC & DEFRA funded). I was responsible for the conception of the experimental design, data analysis and write-up. Collection and data analysis for the fast repetition rate fluorometry (FRRf) was carried out by myself. I analysed the CTD data, which was made available following processing and quality control by Dr Joanne Hopkins (National Oceanography Centre Liverpool). The collection and processing of complete and size-fractionated fluorometric chlorophyll

was carried out by myself Glen Tarran (Plymouth Marine Laboratories) and Alex Poulson (Herriot-Watt University). Flow cytometry sample collection, processing and cluster analysis was carried Dr Glen Tarran who kindly offered the data. Macronutrient sample collection and processing was carried Malcolm Woodward (Plymouth Marine Laboratories) who kindly offered the data. Remote sensing data was provided by the NERC Earth Observation Data Acquisition and Analysis Service (NEODAAS).

Chapter 4

All data for this chapter were collected during a cruise to the Celtic Sea as part of the Shelf Sea Biogeochemistry program (NERC & DEFRA funded). I was responsible for the conception of the experimental design, data analysis and write-up of the chapter. Collection and data analysis for FRRf was carried out by myself. I analysed the underway data which was made available, following processing and quality control, by the British Oceanographic Data Centre (BODC). The collection and processing of complete and size-fractionated fluorometric chlorophyll was carried out by myself Glen Tarran (Plymouth Marine Laboratories) and Alex Poulton (Herriot Watt University). Remote sensing data was provided by the NERC Earth Observation Data Acquisition and Analysis Service (NEODAAS).

Chapter 5

I conceived and wrote this chapter.

Chapter 1 : Introduction

This introductory chapter provides a context for the work presented throughout the thesis. It discusses the importance of quantifying phytoplankton photosynthesis in the marine environment and how phytoplankton rates and stocks are controlled by environmental factors. It also presents the techniques used to measure photosynthesis and the model regions in which data collection took place. Concluding with a summary of the overall research objective of this project.

1.1. The Importance of Marine Photosynthesis

Through the cycling and regeneration of essential elements, the ocean provides a buffering system that lessens the impacts of the changing climate (Bauer *et al*. 2013). Despite contributing less than 1% of the earth's photosynthetic biomass, it is estimated that marine phytoplankton are responsible for almost half of the biospheres annual primary production and subsequently the fixation of 40-60 Tg of CO_2 into organic carbon per year (Falkowski *et al*. 2004; Worden *et al*. 2015).

At present, phytoplankton physiology is still insufficiently characterised for the climate models and remote sensing approaches used to quantify and monitor productivity over regional and global scales. To address this issue and achieve greater understanding of primary productivity we are required to (i) obtain primary productivity measurements at high temporal and spatial resolution and (ii) account for the natural variability in phytoplankton physiology in response to the environmental controls of photosynthesis. The efforts made to address these requirements are discussed henceforth and begin with a description of photosynthesis.

1.2. Photosynthesis

Photosynthesis is the process by which autotrophic organisms utilise solar energy to form organic carbon required for growth (Eqn. 1.1; Falkowski & Raven, 2013).

$$CO_2 + H_2O + 8\,photons \rightarrow CH_2O + H_2O + O_2 \quad \text{Eqn. 1.1}$$

The first stage of photosynthesis is referred to as the 'light' reactions, during which photons are absorbed and utilised to generate energy conserving compounds (Eqn. 1.2). The products of the light reactions are subsequently utilised to reduce CO_2 to organic carbon compounds through the 'dark' reactions (Eqn. 1.3).

$$2H_2O + 2NADP^+ + 3ADP + 3P_i + 8\,photons \rightarrow O_2 + 2H^+ + 2NADPH + 3\,ATP \quad \text{Eqn. 1.2}$$

$$CO_2 + NADPH + 2H^+ + 3\,ATP \rightarrow CH_2O + H_2O + NADP^+ + 3ADP + 3P_i \quad \text{Eqn. 1.3}$$

The ensemble of bio-chemical components that facilitate these reactions constitute the *photosynthetic apparatus*. In eukaryotic cells, the photosynthetic apparatus for the light reactions is formed of organelles (chloroplasts), which contain alternating layers of lipoprotein membranes (thylakoids) responsible for light capture (Falkowski & Raven, 2013). Embedded within the thylakoid membrane, the light harvesting apparatus is composed of two membrane-bound photosystems (PSI and PSII), each containing a light-capturing antenna and reaction centre (RCI and RCII). Following light absorption by the pigments of the antennae, excitation energy is passed to the specialised protein complex of each reaction centre (P680 in RCII and P700 in RC1) where photochemistry takes place.

Light energy is preferentially absorbed into the lower energy P680 of PSII, where it raises the energy of an electron, allowing charge separation to take place. The free electron is immediately captured by a closely associated electron transfer chain (ETC) and is replaced by an electron derived from the splitting of a water molecule. The electron flow along the ETC follows the 'Z-scheme' (Fig. 1.1), providing the energy required for the enzymatic reaction of $NADP^+$ to NADPH; and the proton gradient required for ATP synthesis via photophosphorylation.

These high-energy compounds (ATP and NADPH) are then available for the fixation of CO_2, through a series of enzyme-catalysed reactions during the Calvin cycle (MacIntyre *et al.* 2000).

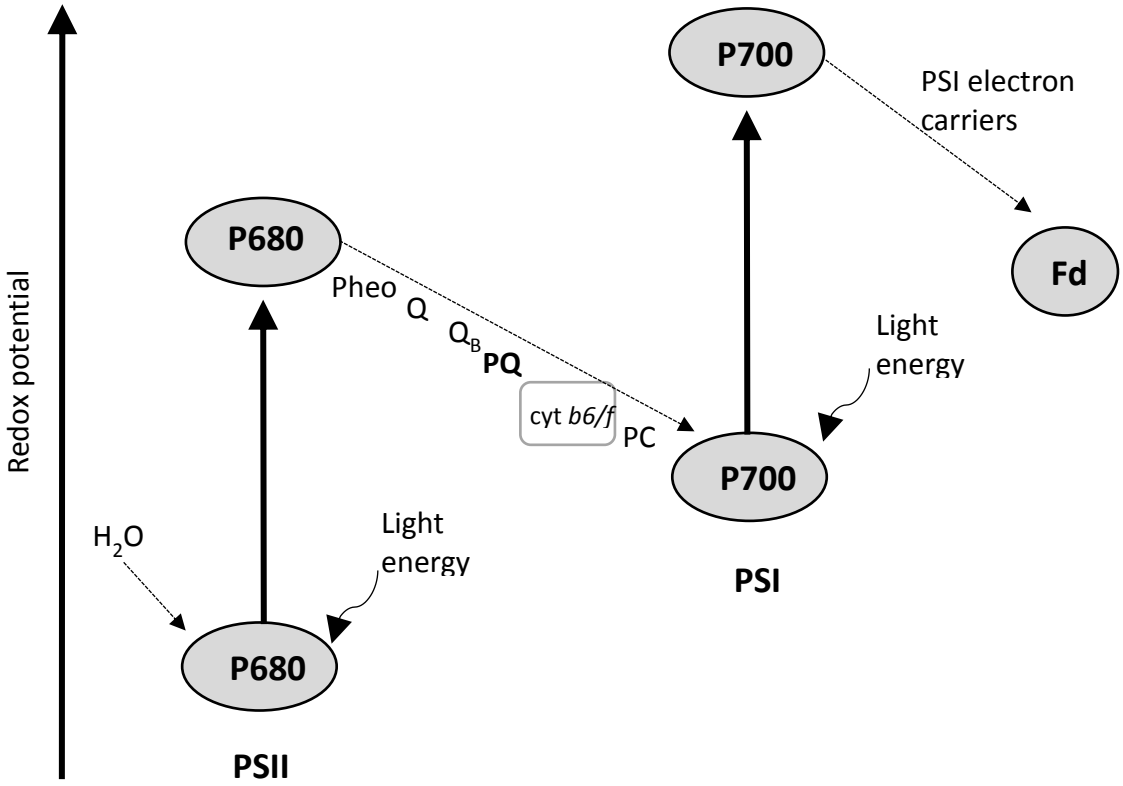

Figure 1.1. The Z-scheme depicting electron transport during photosynthesis.

The rates of each step in the photosynthesis process are controlled by different environmental factors and these factors combine to control primary productivity and phytoplankton growth.

1.3. Environmental Controls of Phytoplankton Growth and Photosynthesis

Through the process of photosynthesis, phytoplankton are reliant on the availability of nutrients and light, leading to suppressed growth and productivity in oligotrophic or light-limited environments (Geider *et al.* 2001; Arrigo, 2005; Moore, 2014). This thesis focusses largely on how phytoplankton photophysiology responds in a range of light and nutrient conditions, and subsequently, how this influences growth and photosynthesis.

Light

In the marine environment, light availability is never constant and phytoplankton are subjected to fluctuant regimes that vary over seasons, days or minutes (Bailey & Grossman, 2008). As a result, photosynthetic organisms are required to optimise their capacity for light absorption at low light intensities. Whilst, at the same time minimising the potential for excess excitation energy, which can damage the photosynthetic apparatus (Long *et al*. 1994; Niyogi & Truong, 2013). These photoprotective methods, can be employed over the short-term (photo-regulation), medium-term (photo-acclimation) or long-term (photo-adaptation) in response to extreme light exposure.

Photo-regulation consists of very short-term responses such as the dissipation of excess energy in the chlorophyll pigment through a non-radiative pathway (Milligan

et al. 2012). The dissipation of excess energy as heat during light harvesting involves the de-excitation of chlorophyll cells; referred to as non-photochemical quenching (NPQ; Müller *et al*. 2001).

Photo-acclimation describes the physiological responses over short-term timescales of hours or minutes. These processes include changes in the number of photosynthetic reaction centres, the chlorophyll:carbon ratio, light harvesting pigments and a decrease in the size of the PSII antennae (MacIntyre *et al.* 2002; Moore *et al.* 2006; Robison and Warner, 2006; Ragni *et al.* 2008).

Evolutionary adaptation has led different groups of phytoplankton to obtain a series of phenotypic traits which leave them genetically suited to a specific environmental regime (Falkowski and LaRoche, 1991; Falkowski *et al.* 2004).

The measurement of photoprotective mechanisms at high temporal resolution will subsequently lead to the better prediction of photo-physiological responses to changing light conditions and is an important step towards the improved estimation of primary productivity. The techniques available to make such measurements are discussed later in this chapter.

Nutrients

The availability of nutrients is essential for the growth of marine phytoplankton and is a constraint on the potential yield of biomass or growth rate of individual cells in limiting concentrations (Arrigo, 2005; Moore *et al*. 2013). Nitrogen (N) and phosphorus (P) are required for the synthesis of key substrates involved in photosynthesis (Berges *et al.* 1996; Mills *et al.* 2004), whilst iron and other trace

metals are essential reducing agents during the ETC (Greene *et al.* 1991; Moore *et al.* 2007).

Traditional concepts of nutrient limitation (Liebig's or Blackmans law) imply a single nutrient plays a limiting role in the accumulation of biomass (Blackman, 1903). Yet, in the surface waters of the modern ocean, no single nutrient could be considered limiting in isolation; giving rise to a focus on the co-limiting influence of multiple elements (Saito *et al.* 2008; Harpole *et al.* 2011; Moore *et al.* 2013). Nutrient co-variability was first explored by Alfred Redfield, who noted the elemental composition of N, P and C in seawater was strikingly similar to that of plankton (Redfield, 1958). The 'Redfield ratio' of 106C:16N:1P has since become an important stoichiometric concept in ocean biogeochemistry, used for nutrient based calculations and in productivity models. Despite this, it is well established that the proportions may alter according to the nutritional status and taxonomic composition of the phytoplankton community (Geider and La Roche, 2002).

Reliable and extensive datasets are required to improve the understanding of how these environmental factors combine to control phytoplankton stocks and rates in the marine environment.

1.4. Measuring Phytoplankton Physiology and Productivity

Net primary production (NPP) is the difference between autotrophic photosynthesis and respiration, also defined as the amount of photosynthetically fixed organic carbon available to the first heterotrophic level in an ecosystem (Field *et al*. 1998). As a result, it is a major component in the global carbon cycle and a key regular in energy transfer and ecosystem processes. Oceanic NPP is dominated by marine phytoplankton and

occurs in the sunlit waters of the euphotic zone. Contemporary approaches stem from the calculation of global NPP as a simple function of available energy for photosynthesis, the absorbed photosynthetically active solar radiation (APAR), and an average light utilisation efficiency coefficient (ε) (Eqn. 1.4).

$$\mathrm{NPP} = \mathrm{APAR} \times \varepsilon \qquad \text{Eqn. 1.4}$$

Quantifying phytoplankton productivity through incubation-based methods can be achieved through the measurement of photosynthetic rates over a range of light levels (P vs. E). Through the calculation of parameters associated with the shape of a P vs. E curve (Fig. 1.2), insight can be gained into both the photosynthetic performance and photoacclimation state of phytoplankton (Ralph and Gademann, 2005; Cruz and Serôdio, 2008). The P vs. E parameters, as defined by Sakshaug *et al*. (1997), are detailed below.

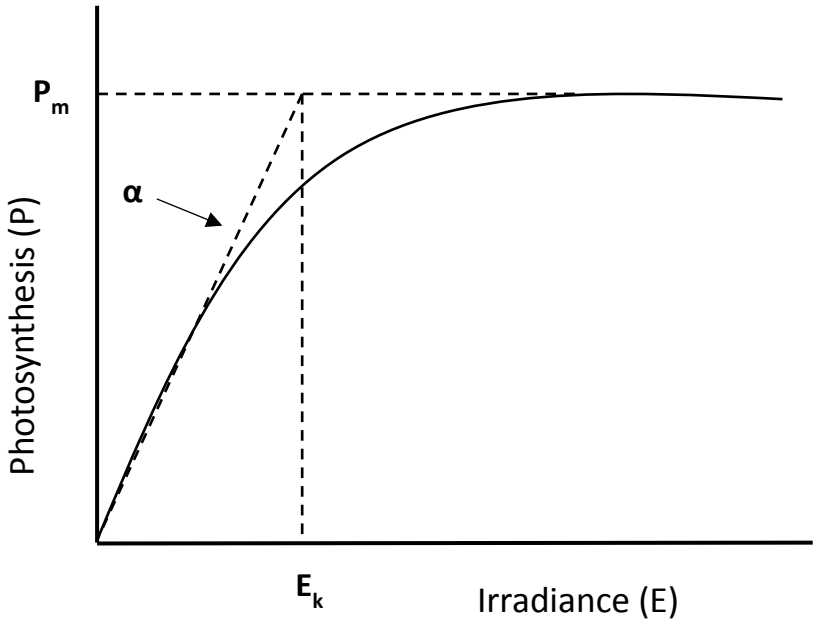

Figure 1.2. Photosynthesis vs. Irradiance (P vs. E) curve with parameters.

The initial linear slope of a P vs. E curve provides an index of the *maximum light utilisation coefficient* (α) and represents the region of the curve where light is the rate-limiting substrate in photosynthesis. The *light-saturated photosynthetic rate* (P_m), denotes the point at which a further increase in irradiance will not yield an increase in photosynthesis. The *light saturation index* (E_k) is the intercept between the initial slope and P_m, reflecting the point that light limited photosynthetic-rate and photochemical energy conversion are balanced.

Common methods used to measure photosynthetic-rate in phytoplankton include carbon fixation and oxygen evolution (Ruben *et al.* 1941; Nielsen, 1952). In the former, cells are incubated, following the addition of a known concentration of bicarbonate labelled with the radioisotope ^{14}C. This allows the user to determine the rate of carbon fixation by calculating the amount of ^{14}C assimilated into tissues (Nielsen, 1952). An alternate method is to measure the O_2 evolved during the light reactions using membrane inlet mass spectrometry (MIMS) or electrodes. Disadvantages of these traditional measurement techniques include the need to bottle incubate samples, which is time consuming and can lead to artefacts termed 'bottle effects' and the relatively limited application of the methods over time and space (Venrick *et al.* 1977; Fogg and Calvario-Martinez, 1989).

Previously, uncertainty in the measurement of global NPP was primarily caused by the scarcity of these *in situ* field measurements. Over the past two decades however, the increased deployment of ocean monitoring satellites has provided unprecedented spatial and temporal coverage but shifted the uncertainty in NPP estimates to the accuracy of satellite-derived ocean colour observations and how effectively they can be scaled (Silsbe *et al*. 2016).

1.4.1. Satellite-based Approaches to Estimating NPP

Satellite-based estimates of chlorophyll concentration profoundly enriched our understanding of global phytoplankton distribution by providing a spatially and temporally cohesive picture of biomass variability, which *in situ* sampling approaches could only partially resolve (O'Reilly *et al.* 1998). The ability to determine global biomass (using chlorophyll as a proxy) and incident light also provided the necessary components to estimate global primary production (Field *et al*. 1998). This was achieved initially through models including variations of the Vertically Generalized Production Model (Eqn. 1.5; VPGM); where the simple model discussed in section 1.4 (Eqn. 1.4) is expanded to account for observed variables and ε is parameterised from thousands of ^{14}C-based field measurements adjusted to account for the effects of temperature and water stress (Behrenfeld and Falkowski, 1997). As described by Field et al. (1998) the fundamental equation for the VGPM is

$$\mathrm{NPP} = C_{\mathrm{sat}} \cdot Z_{\mathrm{eu}} \cdot f(\mathrm{PAR}) \cdot P_{\mathrm{opt}}^{\mathrm{b}}(T) \qquad \text{Eqn. 1.5}$$

where C_{sat} the satellite-derived, near-surface estimation of phytoplankton chlorophyll, Z_{eu} is the depth to which light is able to support photosynthesis, f(PAR). Describes the fraction of the water column from the surface to Z_{eu} in which photosynthesis is light saturated and P_{opt}^{b} is the maximum chlorophyll-specific carbon fixation rate, estimated as a function of sea surface temperature. Using satellite derived estimates of phytoplankton biomass (chlorophyll from ocean colour as a proxy) and it's parameterised physiological status the development of the VGPM allowed the effective partitioning of the factors that affect primary production into

those that influence the relative vertical distribution of primary production (P_z) and those that control the P_{opt}^{b}, however, it also highlighted the importance of increased understanding of phytoplankton ecology and photophysiology and their influence on light harvesting capacity and photoacclimation. To achieve this, initial steps were taken through the development of a carbon-based productivity model (CbPM) which accounted for potential alterations in the chlorophyll to carbon ratios in response to physiological dependencies of light, nutrients and temperature (Behrenfeld *et al.* 2005; Westberry *et al.* 2008). These approaches have greatly improved our understanding of the climate-driven trends in primary productivity, but there are still global and regional patterns of photophysiological responses that remain largely unexplained (Behrenfeld *et al*. 2006; Behrenfeld *et al*. 2006a; O'Malley *et al*. 2014).

In the past decade a number of studies have attempted to remotely assess the physiological status and light-use efficiencies of phytoplankton utilising solar-induced chlorophyll fluorescence (Huot *et al*. 2005; Behrenfeld *et al*. 2009; Huot *et al*. 2013). However, these algorithms would benefit from more *in situ* calibration data, collected at high spatial and temporal resolution, to provide a mechanistic understanding of how photophysiology influences productivity. As discussed in the previous section, current approaches are spatially limited, so alternative methods are required.

These approaches rely on *in situ* measurements of physiology to calibrate and inform the empirical algorithms used to convert satellite observations of phytoplankton biomass into primary production (Behrenfeld & Falkowski, 1997). The current techniques used to obtain these *in situ* measurements of physiology are time consuming and yield relatively few data; limiting our ability to assess how they change over time and space in response to different environmental conditions. To achieve

the aforementioned requirements for improved primary productivity estimation (section 1.1) we rely on (i) sampling techniques that can obtain phytoplankton physiology and biomass data at high resolution and (ii) the necessary auxiliary measurements required to accurately interpret this data.

1.4.2. Chlorophyll Fluorescence

Fluorescence has commonly been used to assess the standing stocks and rates of phytoplankton in the marine environment, with many advantages that include the rapid and non-destructive examination of phytoplankton physiology and biomass (Kolber and Falkowski, 1993; Suggett *et al.* 2001; Moore *et al.* 2006; Robinson *et al.* 2014; Houliez *et al.* 2017). The concept of photochemistry and chlorophyll

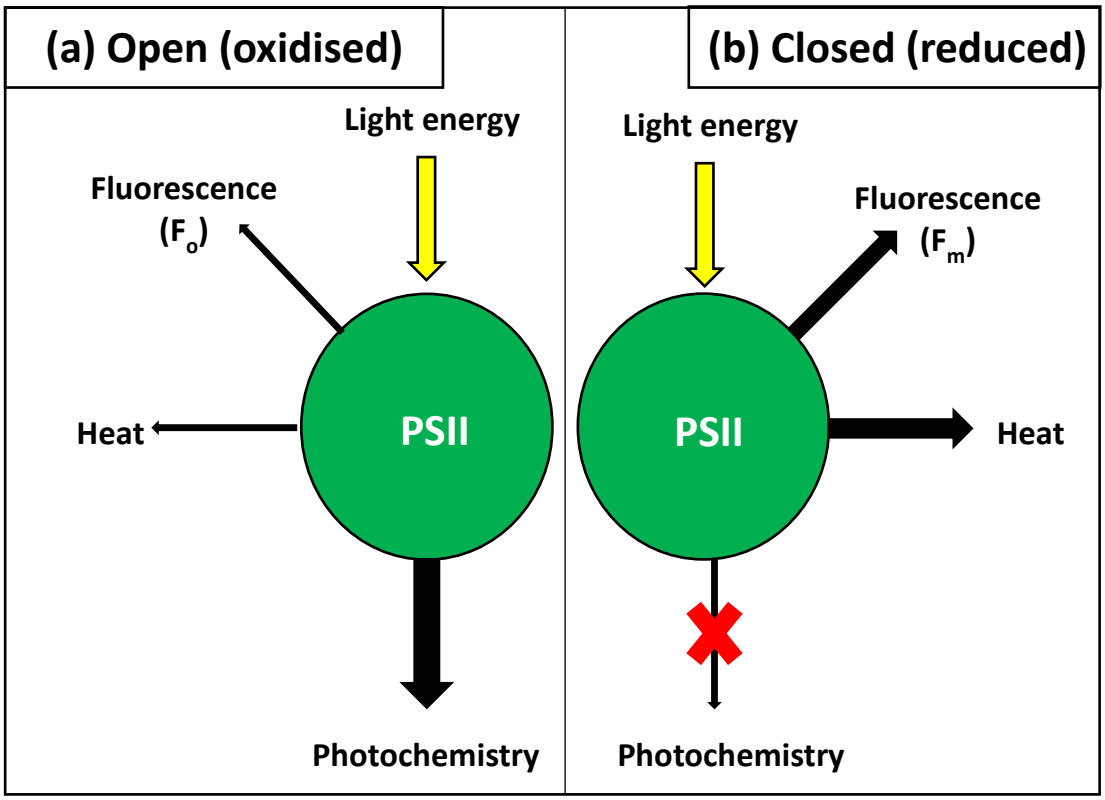

Figure 1.3. The de-excitation pathways for absorbed energy by PSII when reaction centres are **(a)** open (oxidised) and available to accept an electron and **(b)** closed (reduced) and photochemistry cannot take place

fluorescence yield is based on the understanding that the de-excitation of absorbed light energy takes place through one of three competing pathways, controlled by the redox state of the primary electron acceptor of PSII, quinone Q_A (Suggett *et al.* 2004). When Q_A is oxidised the reaction centre is said to be open and is available to accept an electron (Fig. 1.3). When Q_A is reduced, photochemistry cannot take place and excess light energy is dissipated as chlorophyll fluorescence or through non-photochemical quenching (NPQ) as heat (Baker, 2008).

Several techniques allow the measurement of these three competing pathways but for the purpose of this thesis, fast repetition rate fluorometry (FRRf) is now described.

FRRf

Using FRRf, a series of short high-intensity flashlets of light are used to determine the relative amount of reduced Q_A and the extent to which photosynthesis is light-limited or light-saturated (Kolber *et al.* 1998; Oxborough *et al.* 2012). Prior to measurement, samples are typically kept in a low light environment to allow the relaxation of NPQ and the re-oxidation of the Q_A. Under these conditions, photochemistry occurs with high efficiency and the fluorescence yield is minimal (F_o). Following the saturating sequence (typically 100 ~1µs flashlets), all the reactions centres will close and the maximal fluorescence yield (F_m) is reached (Fig. 1.4). The difference between F_m and F_o is termed the variable fluorescence yield (F_v) and when normalised to F_m can be used as an estimate of the maximum quantum efficiency of PSII (F_v/F_m, ϕ_{PSII}). Based on laboratory studies the maximum value of F_v/F_m is perceived to be 0.65 (units are dimensionless); deviations away from this maximum are

considered indicative of variation in the fraction of functional RCIIs (Suggett *et al*. 2009a).

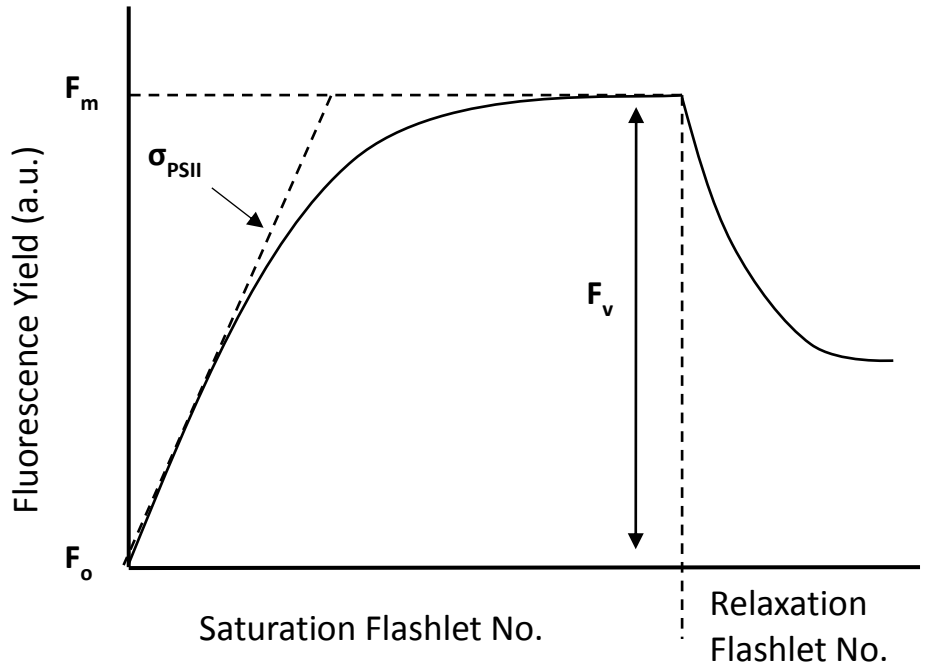

Figure 1.4. Fluorescence induction and relaxation in response to excitation flashlets, measured by FRRf

The rate of increase in fluorescence yield from F_o to F_m represents the rate of PSII light saturation. This is referred to as the PSII effective absorption cross-section (σ_{PSII}). Values of σ_{PSII} describe the functional 'target area' of the light harvesting antenna and can be interpreted as a measure of likelihood that photon absorption will result in photochemistry. A series of sub-saturating flashes can be used to measure the decrease in fluorescence yield which corresponds with the re-opening of the reaction centres as electrons are passed from Q_A to the plastoquinone pool (PQ). The rate at which the relaxation fluorescence yield falls signifies the maximum rate of electron transfer ($1/\tau$) from PSII to PSI.

P vs. E parameters can be obtained using FRRf by measuring F_v/F_m over an actinic light gradient. However, unlike traditional incubation techniques which

provide insight into the entire process of photosynthesis (^{14}C and O_2-evolution), FRRf measures the processes associated with PSII. As such, in contrast to a ^{14}C-dervied E_k which represents the light level at which the rate of photochemistry is balanced with that of whole electron transport, an FRRf-derived E_k instead represents the light level at which PSII becomes saturated.

Calculation of the absolute rate of electron transfer through the PSII reaction centres can be achieved using FRRf as follows:

$$ETR^{RCII} = 0.6023 \cdot a^{PSII} \cdot \left[F_q'/F_m'\right] \cdot E \qquad \text{Eqn. 1.6}$$

where ETR^{RCII} is the rate of charge separation by RCII (units of s^{-1} $RCII^{-1}$), $a^{PSII} = \sigma_{PSII}/(F_v/F_m)$ is the optical cross-section of PSII (units of nm^2 $RCII^{-1}$), where both σ_{PSII} and F_v/F_m are measured after dark-acclimation prior to generating the P vs. E curve, F_q'/F_m' is the operating efficiency of PSII under actinic illumination, E is the photosynthetic photon flux density (units of µmol photons m^{-2} s^{-1}) and the constant 0.6023 is Avogadro's number divided by 10^{24} to allow ETR^{RCII} to be reported in units of inverse time (units of s^{-1} $RCII^{-1}$).

Throughout the course of this study P vs. E parameters were calculated from light-dependent changes in ETR^{RCII} calculated at multiple light-steps before being fitted to a function adapted from the Webb model (Eqn. 1.7; Webb, 1974) as discussed in Silsbe & Kronkamp (2012):

$$Webb\ model\ \ (ETR^{RCII}) = \ \alpha \cdot \frac{E}{E_K} \cdot \left[1 - \left(\frac{E}{E_K}\right)\right] \qquad \text{Eqn. 1.7}$$

where α represents the initial light-limited slope, E_K represents the light saturation parameter and the maximum light-saturated ETR^{RCII} (ETR_{max}) is calculated as $E_K \cdot \alpha$. In

principle, FRRf-derived measurements of ETR^{RCII} can be used to estimate rates of gross O_2-evolution or CO_2 uptake by applying a conversion factor that accounts the physiological processes that decouple the ETR and O_2 evolution/CO_2 fixation (Lawrenz *et al.* 2013; Robinson *et al*. 2014). Over the past three decades the application of fluorescence techniques to measure productivity parameters and physiology have advanced significantly through the continued development of FRRf algorithms and instrumentation. The foremost benefit of FRRf as a means to obtain P vs E parameters *in situ* is the ability to sample at high resolution over space and time in areas of variable biomass with the overarching objective of using these data to better parameterise productivity algorithms and models used with satellite data products (Moore et al. 2003; Moore et al. 2006; Suggett et al. 2009b).

Attempts have been made to compare and calibrate the alternative methods of measuring PP through *in situ* and *in vitro* studies using both FRRf and traditional techniques, yielding results that show estimates of GPP through FRRf measurements to be consistent with comparative independent measurements of PP through C^{14} and evolved O_2, although FRRf measurements did provide a two-fold increase in estimates (Suggett et al. 2001; Smyth et al. 2004; Robinson et al. 2009). This study suggested potential differences to a number of factors including uncertainty over the calculation and expectation of the number of functional PSII reaction centres per unit chlorophyll (n_{PSII}) which has shown variable results amongst eukaryotes and cyanobacteria (Falkowski and Kolber, 1995; Berges *et al.* 1996). Unlike many of these studies, this thesis focussed on the spatio-temporal variability of FRRf-derived P vs E parameters rather than gross productivity estimates and the prevailing factors that contribute to widespread variability. Although multi-spectral instrumentation was utilised, all FRRf-parameters

reported throughout the thesis were collected with an actinic excitation source of blue LEDs (centred at 458 nm).

Chlorophyll Fluorometry

Whilst fluorescence-derived P vs. E parameters could be utilised to further inform and parameterise the photophysiological elements in remote sensing productivity algorithms, chlorophyll fluorometers can also provide an important validation dataset for the development and groudtruthing of ocean colour algorithms (Sathyendranath *et al.* 2017). Ocean colour is a key component in some satellite productivity calculations but gaps have been identified in the determination of phytoplankton biomass from space (Lin *et al.* 2016). These include poor match-ups between satellite and *in situ* observations of phytoplankton community, a lack of uncertainty estimates provided with satellite data and the limited applicability of satellite algorithms for determining phytoplankton composition in coastal waters (Bracher *et al.* 2017). The use of *in vivo* passive and active fluorescence techniques allows oceanographers to measure the biomass and distribution of marine phytoplankton, frequently in time and space, leading to the regular incorporation of fluorometers into ecological monitoring systems (Falkowski & Kiefer 1985; Sauzède *et al*. 2015). This has led to the assembly of a substantial dataset that can be used to assess the accuracy of satellite measurements of ocean colour, particularly in coastal regions where optical properties are difficult to determine (Tilstone *et al.* 2005).

This thesis utilised FRRf and chlorophyll fluorometers to obtain *in situ* measurements of phytoplankton biomass and productivity parameters. These data were analysed to investigate the accuracy of satellite determinations of chlorophyll biomass and shed light on the prevailing environmental controls of P vs E parameters.

1.5. Study Regions

This study is focussed on shelf seas. Despite constituting ~8% of the oceanic surface area, shelf seas are disproportionately productive, estimated to account for 10-30% of annual marine production and up to 50% of the organic carbon that is supplied to the deep ocean (Thomas *et al*. 2004; Bauer *et al*. 2013). The biological activity that drives this carbon fixation also plays an important role in buffering anthropogenic nutrient loading (eutrophication) and supporting substantial fisheries (Frank *et al.* 2007; Burson *et al.* 2016; Grosse *et al.* 2017). Such importance has led to increased investigation to quantify the role of shelf sea regions in the global biological carbon pump with particular focus on the environmental controls on primary productivity variability (Moore *et al.* 2003; Borges *et al.* 2005; Hickman *et al.* 2012).

1.6. Thesis Objectives

The broad objective of this thesis is to address the requirements for an improved understanding of phytoplankton productivity and distribution discussed in **section 1.1** of this chapter. To achieve this, high-resolution measurements of photosynthetic parameters were measured across a range of light and nutrient environments, to investigate the limiting effects on physiology discussed in **section 1.3**. To obtain these high-resolution data, the fluorescence techniques discussed in **section 1.4** were employed in the North-West European shelf seas. This thesis also aims to utilise these high-resolution techniques to assess the accuracy of satellite estimations in the determination of phytoplankton distribution. The objective is addressed through the chapters of this thesis, which are summarised below.

In **chapter two**, the influence of nutrient limitation on phytoplankton photophysiology and growth is tested.

In **chapter three**, P vs. E parameters are measured at high-spatial resolution using FRRf and auxiliary measurements are used to explain the prevailing factor driving the observed variability.

In **chapter four**, high-resolution fluorescence data are analysed alongside satellite estimates of phytoplankton biomass to compare the ability of each technique in capturing the variability of phytoplankton distribution

In **chapter five**, the broader significance of key findings from previous chapters are recounted and future research directions are put forward

Chapter 2 : Patterns of Phytoplankton Growth and Photophysiology in Contrasting Nutrient Regimes

2.1. Introduction

The availability of nutrients is essential for the growth of marine phytoplankton and is a constraint on the potential yield of biomass or growth rate of individual cells in limiting concentrations (Arrigo, 2005; Moore *et al*. 2013). Historically, the inorganic macronutrients nitrate (N) and phosphate (P) were viewed as the prevailing limiting resources in phytoplankton growth, supressing photosynthetic activity and primary production in large areas of the upper ocean (Cullen, 1991). Traditional concepts of nutrient limitation (Liebig's or Blackmans law) imply a single nutrient plays a limiting role in the accumulation of biomass but it is increasingly common to see an expansion to more than one nutrient, often defined by the term 'co-limitation' (Saito *et al.* 2008).

The concept of co-limitation at a community-level is defined in Harpole *et al*. (2011) as a combination of mechanisms that cause species to be simultaneously or independently limited by multiple nutrients. The study highlights the necessity for clarifying terminology associated with nutrient co-limitation, setting out to address and define the mechanisms that could lead to the different types. For example, the growth of organisms can be considered co-limited in the case of substitutional nutrients because it can be parameterised as a function of two or more key nutrients (Saito *et al*. 2008; Pahlow and Oschiles, 2009; Harpole *et al*. 2011). Co-limitation at a community introduces a further layer of complexity with the consideration that natural communities are composed of numerous species with shared or individual adaptations to limiting ecological factors. This can lead to a situation where there may be a community of species all limited by different nutrients, or in contrast, a community where the community is comprised of functionally equivalent species

whereby all individuals are co-limited by the same nutrient/substrate (Harpole *et al*. 2011)

Experimental investigations of resource control over phytoplankton communities often employ nutrient addition bioassays to test for individual or multiple nutrient stress on phytoplankton communities (Mills *et al.* 2004; Moore *et al.* 2008; Suggett *et al.* 2009). This approach has associated caveats, such as, the removal of grazing pressure or "bottle effects" (Fogg & Calvario-Martinez, 1989). Nevertheless, it is important in developing our understanding of co-limitation in phytoplankton communities, following the simultaneous relief of one or more nutrients. This is particularly important in coastal regions, areas often subject to eutrophication through fluvial deposition, which can lead to unbalanced stoichiometry (Grosse *et al*. 2017b). Shelf seas that possess large areas of coastline are often impacted the most; with unbalanced nutrient loads disrupting the ratio of dissolved inorganic N:P. This leads to different regimes of nutrient limitation with major consequences for the composition, productivity and growth of the phytoplankton community (Abrantes *et al.* 2016; Burson *et al.* 2016).

The hydrography of the North Sea varies greatly due to the influence of water from the North Atlantic and Baltic Sea, as well as fluvial input from surrounding land masses. The distribution and circulation of these intrusive water bodies play important roles in supporting the planktonic communities across the North Sea; particularly during the summer months following the onset of thermal stratification in the central and northern regions. A strong thermocline and reduced vertical mixing commonly lead to nutrient depletion in the surface mixed layer, resulting in a steady

decline in phytoplankton biomass and changes in community (Weston *et al.* 2005; Muylaert *et al.* 2006; Greenwood *et al.* 2010)

The hydrography also influences phytoplankton community structure and light harvesting strategy with different taxonomic groups possessing a higher capacity to adapt to the highly fluctuant light conditions found in turbulent waters, such as those of the southern North Sea. As a result, a geographic trend in the composition of phytoplankton functional types (defined by size classes or accessory pigments) can be seen during the summer months (Ford *et al.* 2017). Diatoms are found in the turbid mixed coastal regions in the south, prymnesiophytes in the stratified central regions and chlorophytes in the north-west boundary where the North Sea meets the North Atlantic.

In this study, seven nutrient-addition bioassay experiments were performed during a cruise to the North Sea to examine the effects of nutrient addition on phytoplankton communities found across the study region. The objectives of this chapter were to (1) determine the response of phytoplankton growth and photophysiology over short term incubations (48 h), following the relief of nutrient limitation and (2) use the bioassays to further interpret *in situ* data and establish how environmental drivers influence spatial changes observed in phytoplankton physiology.

2.2. Methods

2.2.1. General Sampling and Nutrient Bioassay Experiments

Data were collected on board the RV *Cefas Endeavour* (CEND_1815) during a research cruise to the North Sea, between the 9th of August and 3rd of September 2015 (Fig.

2.1). Seawater for the nutrient bioassay experiments was collected pre-dawn from the vessel's underway supply and passed through a 200 µm mesh before filling the 1.2 L polycarbonate (Nalgene) incubation bottles. From this time point (T0), samples were taken for high performance liquid chromatography (HPLC), flow cytometry, fast repetition rate fluorometry (FRRf), dissolved inorganic nutrients (DIN) and particulate organic carbon (POC). Incubation bottles were then either left as controls (n = 4) or spiked with nutrients, added alone and or in combination, at concentrations of F/2 algal growth medium (8.82 x 10^{-4} M $NaNO_3$, 3.62 x 10^{-5} M NaH_2PO_4, 1.06 x 10^{-4} M Na_2SiO_3; Guillard 1975). Treatment one (N+PSi) comprised of nitrogen (N), silicate (Si) and phosphorus (P) addition as well as F/2 trace metals (TM) and vitamins (V). Treatment two (PSi) also contained P, Si, V and TM but no N. Treatment three (N+) consisted of an N only addition. For each treatment, a total of four bottles were incubated. Following nutrient spiking the all treatment and control bottles were sealed and placed in an on-deck incubator to allow cooling by near-surface seawater from the underway deck supply. The FerryBox system measured changes in temperature over the course of the incubations, whilst a PAR sensor on the ship's bridge provided daily irradiance profiles.

Endpoint (48 h) samples were taken for chlorophyll, dissolved inorganic nutrients (DIN), particulate organic carbon (POC) and FRRf following the incubation period (Suppl. Table. 2.1). In-between experiments all bottles and sampling equipment were thoroughly rinsed and acid-washed. An Orion 3-star benchtop pH meter (Thermo Scientific, MA, USA) was used to measure the pH of all treatment bottles at the start (T0) and end (48 h) of all experiments; no significant changes were recorded.

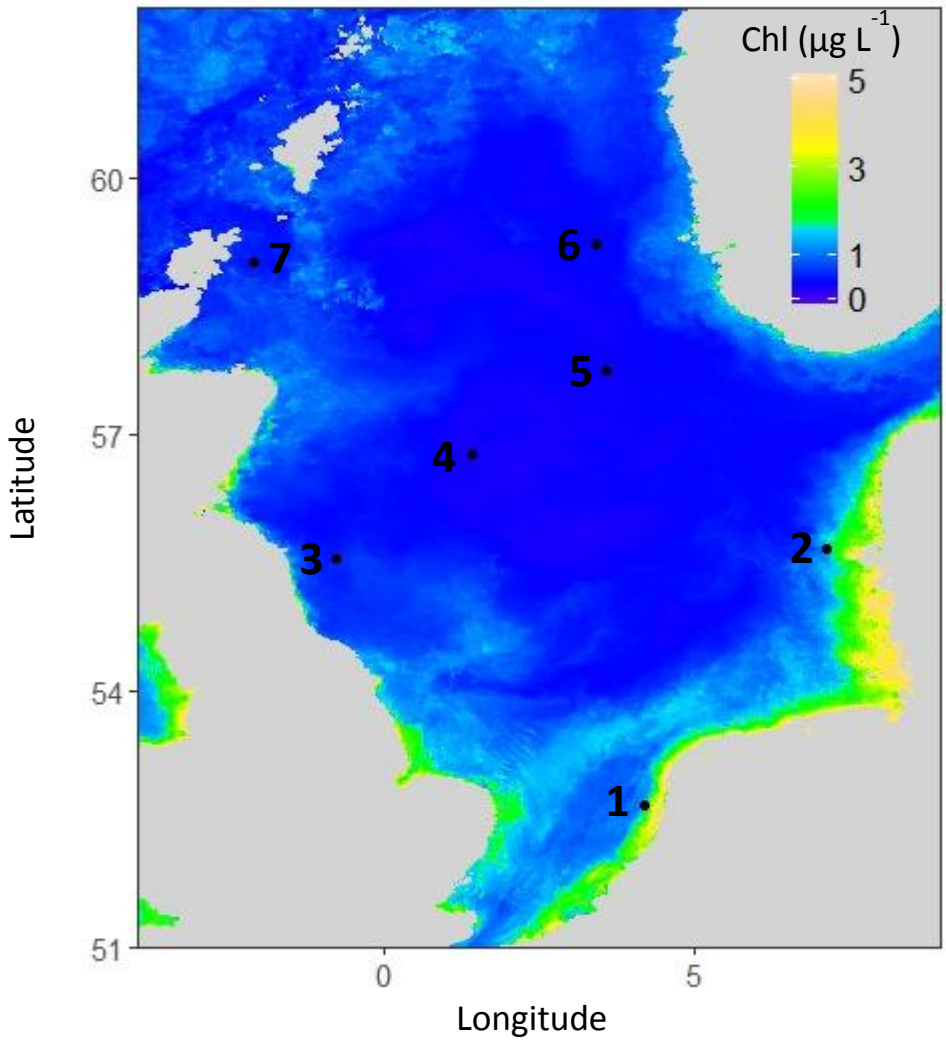

Figure 2.1. The experimental sites (labelled 1-7) sampled during a cruise aboard the RV Cefas Endeavour between the 9th of August and 3rd of September 2015. Background is a MODIS satellite-derived chlorophyll concentration composite for the period of the cruise (01-31 August 2015).

2.2.2. Nutrient Concentration

Seawater samples for DIN were obtained by syringe-filtering water (100 – 300 ml) through a pre-combusted (400^{o}C for 6 hours) 25 mm Whatman® glass-fibre filter (GF/F; nominal pore size of 0.7 µm). The filtrates were immmediately frozen at -80 ^{o}C until analysis at the Unviersity of Essex and the filters kept for the determination of particulate organic (POC).

Samples were analysed using a segmented, colorimetric AA3 H3 Autoanalyzer (SEAL Analytical, Wisconsin, U.S) with four analytical channels (nitrate+nitrite passed through a cadmium column, phosphate, silicate, ammonia). Lower range detection limits for the instrument are stated by the manufacturer as 0 - 0.3 to 0 - 2.75 mg L^{-1} for nitrate, 0 - 1.7 to 0-7.5 mg L^{-1} for phosphate, 0-6 to 0-60 mg L^{-1} and 0-0.25 to 0-5 mg L^{-1} for ammonia.

2.2.3. Particulate Organic Carbon (POC)

Filters collected for POC were immediately frozen at -80 ^{o}C until analysis at the Unviersity of Essex. The filters were thawed and dried before being acidified using 1 mol HCL to remove inorganic carbon. They were then processed using a Shimadzu TOC-V_{csh} total organic carbon analyser (McKew *et al*. 2011).

2.2.4. Phytoplankton Pigments and Community Structure

Water samples for phytoplankton pigment composition at T0 were collected in clean Nalgene bottles and filtered through 47 mm Whatman® GF/F filters before immediate storage at -80 ^{o}C. A selection of 55 samples, including all but one (4) of the experimental sites, were selected and sent for pigment analysis using high

performance liquid chromatography (HPLC) at the DHI Institute for Water and Environment (Hørsholm, Denmark) (Schlüter *et al*. 2011). Pigment data were statistically analysed and quality assured (QA) following the methods of Aiken *et al.* (2009). Upon completion of QA, data from two stations were removed due to an unusual ratio of total chlorophyll *a* to accessory pigments.

To examine potential differences in community composition, 7 diagnostic marker pigments were selected and compared as a ratio of their cumulative total. Taxon-specific marker pigments were used as proxies for phytoplankton functional type following the methods of Aiken *et al*. (2009) and Brewin *et al*. (2010). The 7 marker pigments (and taxonomic grouping) were chlorophyll b (Chlb, chlorophytes), zeaxanthin (Zea, cyanophytes), alloxanthin (Allo, cryptophytes), 19'-butanoyloxyfucoxanthin (But, chrysophytes), 19'-hexanoyloxyfucoxanthin (Hex, prymnesiophytes), peridinin (Per, dinoflagellates) and fucoxanthin (Fuc, diatoms). In total, these diagnostic marker pigments comprised >85% of the total photosynthetic carotenoids present in all samples (excluding chlorophyll a and c's).

Experimental samples for chlorophyll concentration at T0 and endpoint (48 h) were filtered through 25 mm Whatman® GF/F filters before immediate storage at -80 ^{o}C until later analysis at the University of Essex. Pigments were extracted into 98% methanol - buffered with 2% ammonium acetate (0.5 M, pH 7.2) – by sonication following the methods of van Leeuwe *et al*. (2006). Extracts were then filtered through a 0.2 μm polytetrafluoroethylene (PTFE) membrane syringe filter to remove cell debris before ultra-performance liquid chromatography (UPLC) was carried out using a Waters® *ACQUITY*™ UPLC system, Waters C_8 column and Waters Eλ photodiode array absorption detector (Waters, MA, USA). Pigment separation was performed using an

aqueous pyridine (0.25 M, pH 5) mobile phase and followed a modified method from Zapata *et al*. (2000). The peak area for chlorophyll was calibrated against known concentrations of a chlorophyll *a* standard (C5753-1MG, Sigma).

Scanning Flow cytometry

Sea-water samples for scanning flow cytometry (SFC) analysis were collected and preserved in 1% glutaraldehyde before storage at -80 ^{o}C until, analysis at Cefas Laboratories (Lowestoft, UK). Samples were thawed at 4^{o}C before analysis using a Cytosense™ scanning flow cytometer (Cytobuoy, NL). Sample processing and cluster analysis followed the methods of Thyssen *et al*. (2015), but will be described here in short.

The forward (FWS) and side scatter (SWS) signals as well as red, orange or yellow fluorescence (FLR, FLO, FLY respectively) signals were measured for chains or individual cells following particle separation by laminar flow. A set of spherical beads with different diameters was analysed along with the sample, in known quantities, to evaluate the control and calibration of the instrument. This allowed the definition of size-estimated calibration curves between total FWS (in arbitrary units, a.u.) and actual bead size. This set included 1, 6, 20, 45 and 90 µm sized yellow-green fluorescence beads from Polyscience Fluoresbrite microspheres and 10 µm orange fluorescence beads from Invitrogen polystyrene FluoroSpheres.

The phytoplankton community was described using several two-dimensional cytograms built with the Cytoclus® software. For each autofluorescing phytoplankton cell analysed, the integrated value of FLR pulse shape (total red fluorescence (TFLR), in a.u.) was calculated. The TFLR (cm^{-3}) of each resolved phytoplankton cluster was

summed and used as a proxy for biomass to analyse differences in the community structure between sites.

2.2.5. Fast Repetition Rate fluorometry

A multi-spectral FRRf (*FastOcean™*, Chelsea Technologies Group - CTG - Ltd, UK) fitted with an integrated FastAct™ bench-top unit (CTG Ltd) was used to measure the photophysiology of nutrient-enriched and natural phytoplankton communities. Samples were dark-acclimated at source temperature for a minimum of 30 minutes before single-turnover FRRf measurements were made using a 32-sequence protocol of 100 1.1 µs saturation flashes at 2.8 µs intervals followed by 40 µs relaxation flashes at 50 µs intervals. Data were processed using software provided by the instrument manufacturer (FASTpro8 V1.0.5, CTG Ltd) with the minimum (F_o) and maximum (F_m) fluorescence and effective absorption cross section provided by fitting single acquisition data to the Kolber-Prášil-Falkowski (KPF) model (Kolber *et al.* 1998).

The dark-acclimated maximum quantum yield of photochemistry (F_v/F_m) was calculated as F_m- F_o/F_m. Syringe filtered (0.2 µm Acrodisc) seawater samples were measured after all RLCs to calculate the contribution of fluorescence from non-algal dissolved material ("the blank"; Cullen & Davis, 2003). Using the same FRRf settings as the unfiltered sample, 5 single turnover acquisitions were made for each experimental site. The average of these measurements was then calculated from all repetitions and found to be minimal in all sample blanks, contributing between 5-10% of the measured signal (Supp. fig. 2.1). Non-linearity in instrument settings (gain and LED intensity) was normalised by the FASTpro8 software using a chlorophyll-in-acetone correction and further characterised using a chlorophyll-in-acetone dilution

series conducted post-cruise with results showing effective correction over a range of gain and LED intensities.

P vs. E parameters were obtained via FRRf using rapid light curves (RLC) run at the start and end of the incubation period. Each consisted of 14 x 120 s light steps, with the PAR progressively increasing from 11 to 1610 µmol photons m^{-2} s^{-1}. At each light step the fluorescence under actinic light (F'), the maximum fluorescence under actinic light (F_m') and the parameters F_q'/F_v', F_v'/F_m' and F_q'/F_m' were obtained (Table 2.1). NPQ was calculated as the normalised Sterm-Volmer coefficient (Eqn. 2.1), defined as:

$$NPQ_{NSV} = \left(\frac{Fm'}{Fv'}\right) - 1 = \left(\frac{Fo'}{Fv'}\right) \qquad \text{Eqn. 2.1}$$

where NPQ_{NSV} is the ratio of the nonphotochemical dissipation in the light-adapted state to the rate constant for photochemistry (McKew *et al.* 2013). The absolute rate of photosynthetic electron transfer (Eqn. 2.2) through photosystem II (PSII) reaction centres was calculated using Eqn. 1.6. P vs. E parameters for PSII turnover were calculated from light-dependent changes in ETR^{RCII} at each light-step by fitting a function (Eqn. 1.7) adapted from Webb *et al*. (1974) to the RLC data, using the R package "phytotools" (Silsbe, 2015), as defined in section 1.4.3.

2.2.6. Statistical Analysis

Treatment means from the experiments were compared using a one-way ANOVA and Tukey-Kramer (T-K, p <0 .05) post-hoc test to determine the significant differences between the treatment groups. Pearson's correlation (r) was used to measure the linear association of parameters. Principal component analysis (PCA) was carried out

using the “stats” package in R. The data for the PCA were log-transformed and centred for normality.

The log response ratio (RR; the ratio of the mean outcome in an experimental group to that in the control group) is often used in experimental ecology as a measure of effect magnitude on treatment populations from different environments (Hedges *et al.* 1999; Elser *et al.* 2007). In this study log RR was used to assess the proportionate change in growth and photophysiology following the addition of nutrients. Data are given as natural-log transformed response ratios (RR) in which the response variable is divided by the value of the control treatment.

2.3. Results

2.3.1. Initial Conditions of the Experimental Sites

The geographic distance between study sites resulted in substantial variability in the biotic and abiotic conditions (Table 2.1). Principal component analysis (PCA) was carried out to characterise the variability observed in the environmental parameters (temperature, salinity, N, P and Si) measured at T0. The first two components of the PCA accounted for ~89% of the variability between the sample stations and revealed three distinct clusters of stations, separated by differences in nutrient concentration and physical conditions (Fig. 2.2). Two clusters contained sites 1 – 6 where nutrient values were all close to detection limit; these six sites were therefore separated primarily by changes in temperature and salinity (Table 2.1).

Table 2.1. Initial conditions at the sites of the bioassay experiments.

Site	**1**	**2**	**3**	**4**	**5**	**6**	**7**
Date	09-Aug	12-Aug	16-Aug	19-Aug	22-Aug	28-Aug	02-Sep
Temp (^{o}C)	18.11	17.12	15.21	14.81	14.62	14.62	12.10
Sal (ppt)	34.86	32.72	34.58	34.89	35.06	34.35	35.05
$NO3^{-}$ (µM L^{-1})	0.43	0.48	0.26	0.38	0.65	0.34	2.44
$PO4^{-}$ (µM L^{-1})	0.13	0.06	0.09	0.01	0.03	0.05	0.32
Si (µM L^{-1})	0.64	1.41	0.25	0.13	1.01	0.25	1.10
Chl (µg L^{-1})	0.68	0.88	0.66	0.39	0.42	0.31	0.55
N:P	3.31	8.00	2.89	38.00	21.67	6.80	7.63
Si:N	1.49	2.94	0.96	0.34	1.55	0.74	0.45
Si:P	4.92	23.50	2.78	13.00	33.67	5.00	3.44
Total Depth	20	30	100	98	65	193	66

The first cluster contained sites 1 and 2, which were characterised by low nutrient availability and warmer average water temperatures (17.6 ^{o}C). This cluster will hereafter be referred to as WNP (warm-nutrient-poor). The second nutrient poor cluster contained sites 3 – 6 where the water temperature was slightly cooler on average (14.8 ^{o}C). This cluster will be referred to as CNP (cool-nutrient-poor). The final site (7) was distinctly different from the previous six, with N and P concentrations 5-fold higher than the average of the other 6 sites. The water temperature at 7 was much lower (12.1 ^{o}C) than the other two cluster averages. This site will therefore be referred to as the cold-nutrient-rich (CNR) site. Si concentration showed no geographical trend and did not correlate with temperature or salinity. Chlorophyll at all sites was low but ranged nearly 3-fold between the highest (site 2) and lowest (site 6) concentrations.

Phytoplankton Size and Community Composition

The results of the SFC analysis revealed differences in the community composition and some variation in the size structure of the experimental communities. SFC cluster

analysis identified 5 distinct components based on their optical fingerprints and were labelled as such: Pico, Syn, Nano, Crypto and Micro. The Pico and Syn component were both highly abundant in cell number, contributing between 75-90% across the experimental sites. Despite this, they were only dominant contributors to community biomass (derived from SFC fluorescence) at the CNR station (7); accounting for 70 % (Fig. 2.3a).

In contrast, the CNP sites were largely composed (~70% or more) of Nano and Syn components but did not show a consistent trend in composition. The WNP were largely composed of the Pico (~30-40%) and Nano (~50-60%) cells with the remaining community made up of the Syn and Micro components. The dominance of the Nano

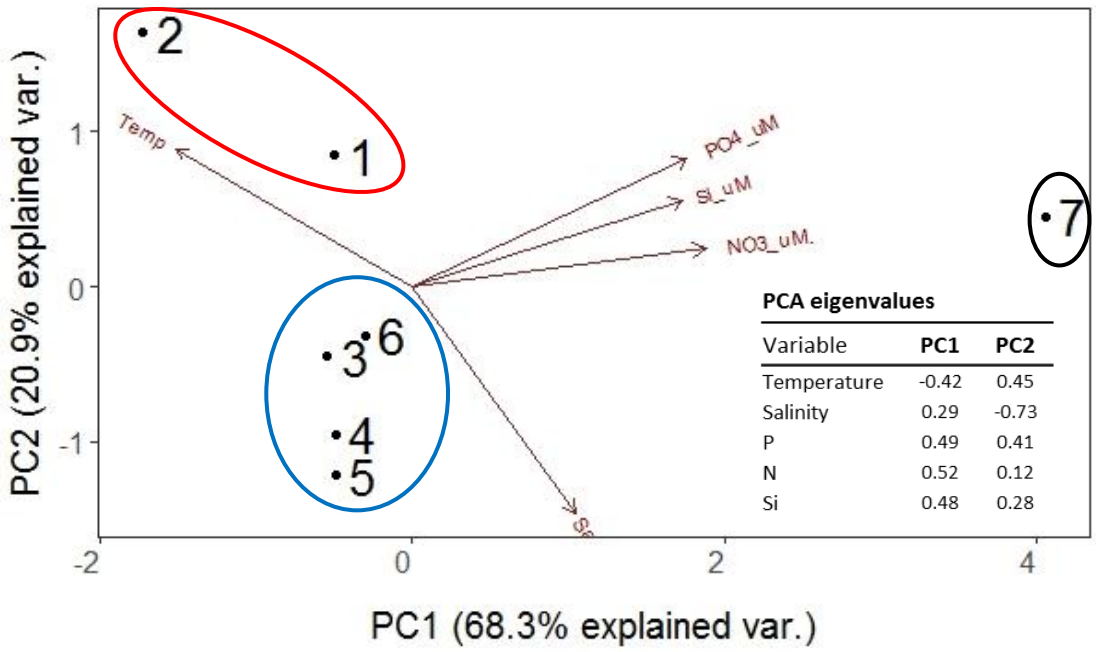

Figure 2.2. A principal component analysis (PCA) ordination for environmental parameters measured at the seven experimental sites. Selected parameters were temperature, salinity, nitrate, phosphate and silicate. Data were scaled and centred prior to analysis. 68.3% of the variance in data was explained by the principal component 1 (PC1) with the second (PC2) accounting for a further 20.9%.

and Pico components was reflected in the size range at all experimental sites, with > 75% of the measured particles between 2-5 µm.

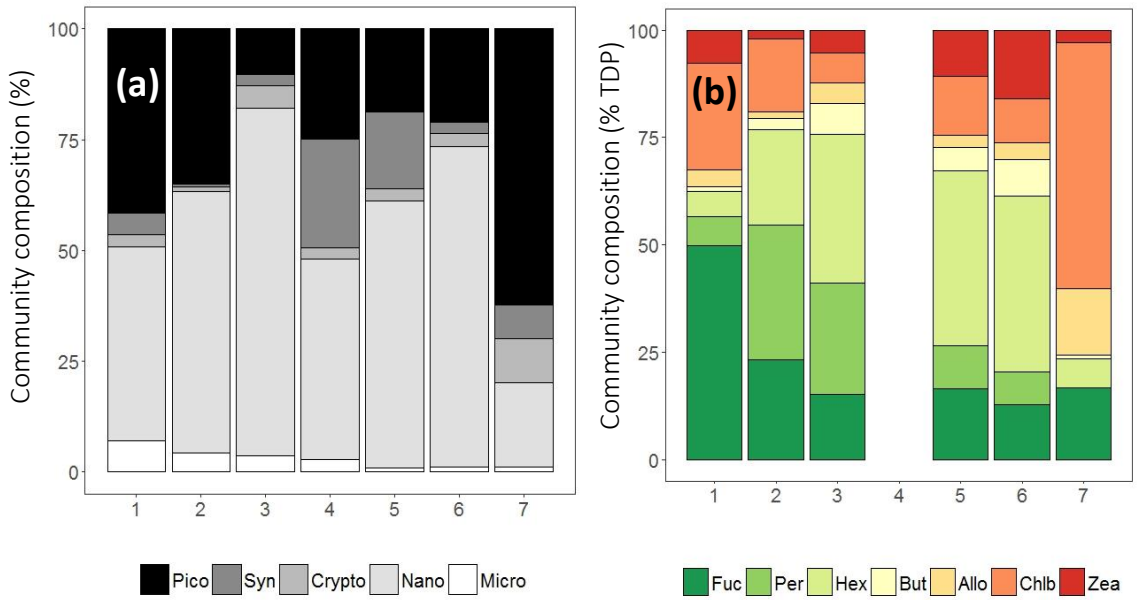

Figure 2.3. Taxonomic composition of the phytoplankton community at the start of the experiments, determined using scanning flow cytometry (SFC) and pigment composition. **(a)** The % community composition of the five distinct phytoplankton types identified using SFC. **(b)** The % composition of diagnostic marker pigments to the cumulative total. Pigments were identified using HPLC and are as follows: 19'-butanoyloxyfucoxanthin (But, chrysophytes), 19'-hexanoyloxyfucoxanthin (Hex, prymnesiophytes), peridinin (Per, dinoflagellates) and fucoxanthin (Fuc, diatoms), zeaxanthin (Zea, cyanophytes), chlorophyll b (Chlb, chlorophytes), alloxanthin (Allo, cryptophytes).

Phytoplankton pigment composition

Changes in the diagnostic marker pigments provided further insight into the composition of the different communities. The CNR (site 7) site was largely composed of chlorophyll b suggesting the large Pico component observed in the flow cytometry data comprised of chlorophytes. Hex was the most abundant (~30-35%) pigment across the CNP sites but no site was dominated by one pigment, but site 3 did show a higher proportion of peridinin than the other two CNP sites (Fig. 2.3b). Site 2 of the

WNP cluster showed a similar pigment composition to site 3 with a slightly higher proportion of fucoxanthin and chlorophyll b whilst the other WNP site (1) had a large proportion of fucoxanthin, potentially indicating the presence of diatoms.

2.3.2. PSII and Light Response Parameters

Following the incubation (48 h), PSII characteristics (F_v/F_m and σ_{PSII}) were found to differ in all experiments indicating nutrient availability was an influential factor on photophysiology of the experimental phytoplankton communities. Values of σ_{PSII} and F_v/F_m were found to negatively co-vary across all experiments and were highly correlated ($r = -0.70$, $n = 28$, $p < 0.001$), suggesting that common factors were responsible for much of the variability observed between the two parameters.

F_v/F_m values in the all treatments differed significantly from the controls in 4 of the 7 experiments and exhibited positive and negative responses to nutrient addition (Fig. 2.4). The most striking result was observed following the addition of PSi, added alone or as N+PSi, which resulted in a significantly higher F_v/F_m at sites 4 and 7 relative to the control. The addition of N alone, resulted in a significant F_v/F_m in the community of site 5 whilst site 6 only saw significant change following the addition of N+PSi but no response to either added alone.

Nutrient addition was found to have a greater effect on the σ_{PSII} values of experimental samples, with 6 of the 7 sites showing treatment responses at 48 h. The addition of N, either alone or as N+PSi, resulted in significant lower values of σ_{PSII} compared to controls at site 1 whilst the addition of PSi added alone or with N saw the same response at site 7. The addition of N+PSi at four other sites (2, 3, 4 and 6) all resulted in a significant decrease in σ_{PSII} compared to the controls and other

treatments revealing co-limitation of two or more substrates at these stations (Fig. 2.4).

The range of non-photochemical quenching measured over a light response curve (ΔNPQ) also showed significant changes in most of the experiments, generally decreasing following the addition of one or more nutrients. The most consistent result

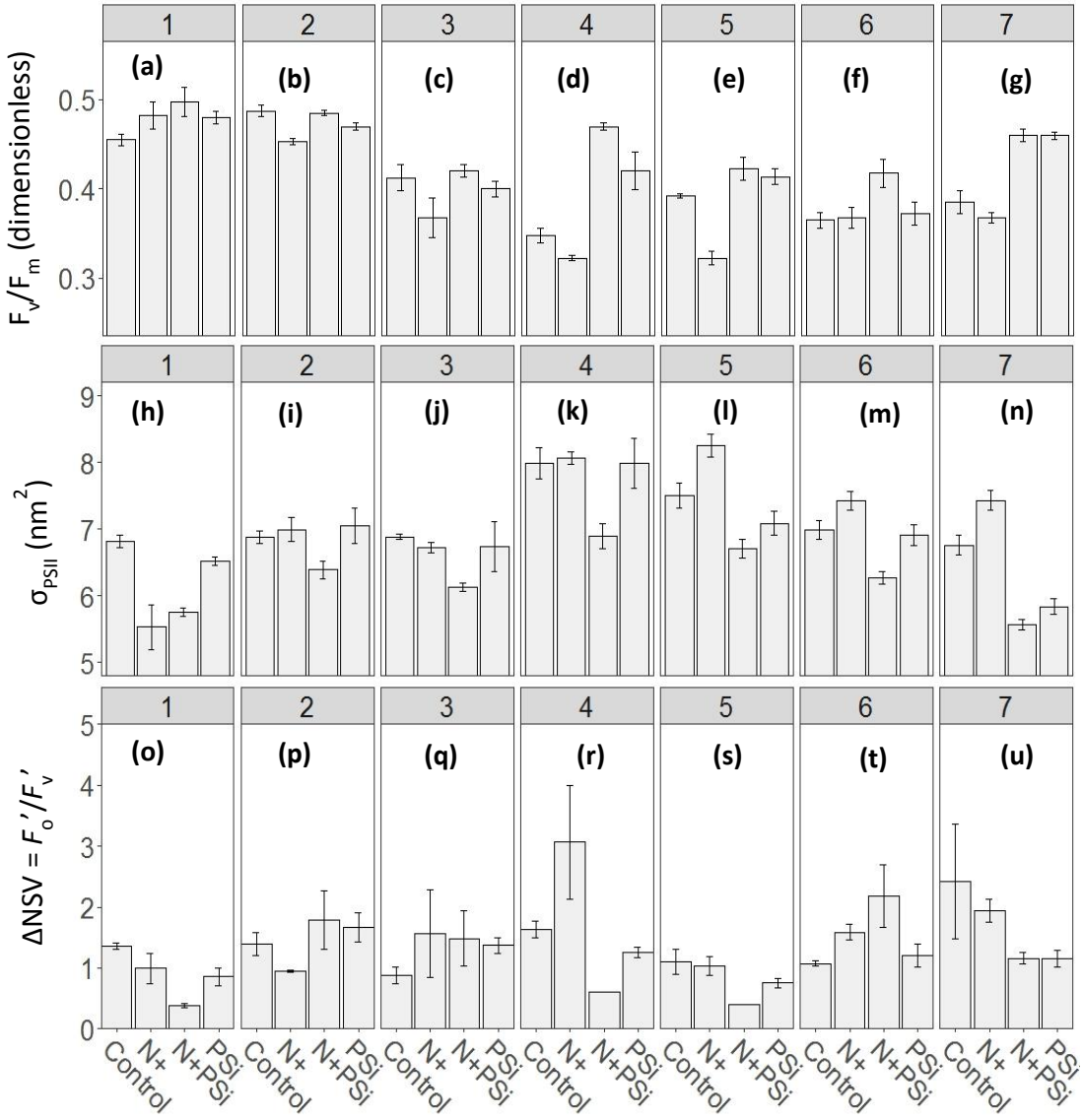

Figure 2.4. Changes in photosystem II characteristics measured following nutrient addition in the seven bioassay experiments. Measurements were made using FRRf following dark acclimation **(a-g)** the maximum quantum yield of photochemistry (F_v/F_m) **(h-n)** the functional cross section of Photosystem II (σ_{PSII}) and **(o-u)** the range of NPQ_{NSV} (ΔNSV) over a rapid light curve. Shown are means (± 1 s.e., n = 4) except **(r)**-**(f)** where range is not indicated (n = 2). All data shown are from the endpoint (48 h).

was a decrease in ΔNPQ following the addition of N+PSi (observed in sites 1, 4 and 5). Despite this, the lone addition of N (site 2) or PSi (site 7) also resulted in significant changes.

Modelled light-response (P vs. E) parameters also showed patterns of nutrient limitation in several of the experiments (Fig. 2.5). FRRF-based estimates of the light utilisation efficiency (α) decreased significantly following the addition of N added alone or as N+PSi at site 1 whilst the opposite response to the same treatments was observed at site 6. The addition of PSi added alone or with N resulted in a significant increase in the α of the community at site 5. Inconclusive trends were observed at sites 2 and 7, the former increasing significantly under N and PSi and the latter under both PSi treatments.

The saturating irradiance (E_K) changed significantly in three experiments, generally decreasing following nutrient addition. Site 1 was the only experiment where E_K increased significantly compared to the controls and this occurred following the addition of N+PSi. A decrease following the addition of PSi either alone or with N significantly decreased the values of sites 4 and 5 whilst the same response for N was observed in site 6. Changes in the maximum electron transfer rate (ETR_{max}) showed the least response of any measured parameter but did increase significantly following the addition of N+PSi at site 1 whilst decreasing following the addition of PSi (alone or with N) at site 5.

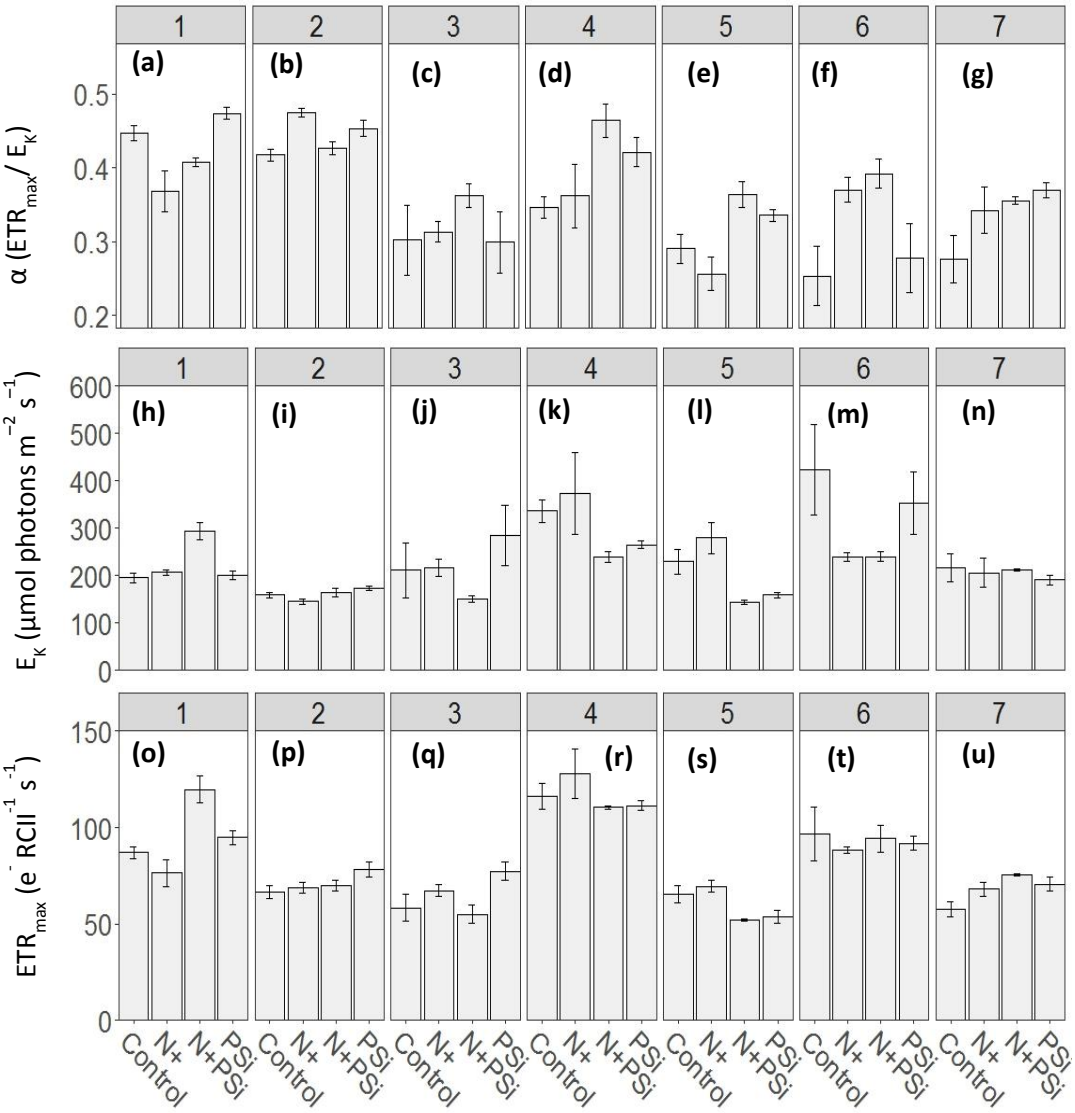

Figure 2.5. Light response (P vs. E) parameters following nutrient addition in the seven bioassay experiments. Data are derived from FRRf rapid light curves using a Webb (1974) model fit **(a-g)** the maximum light utilisation efficiency (α) **(h-n)** the saturating irradiance (E_K) and **(o-u)** the maximum electron transfer rate (ETR_{max}). Shown are means (± 1 s.e., n = 4). All data shown are from the endpoint (48 h).

2.3.3. Growth and Physiology

Growth, measured as chlorophyll accumulation, occurred in all the experiments apart from site 5 (Fig. 2.6). The addition of N in combination with P and Si resulted in the largest response with as much as a 4-fold increase compared to the controls, however,

the prevailing limiting resource varied between experiments with evidence of N-limitation (site 2), P/Si-limitation (site 7) and various patterns of co-limitation (sites 1, 3, 4, 6) observed across the sites. A clear independent co-limitation response was observed at site 1 where significant chlorophyll accumulation occurred independently after N and P/Si addition (ANOVA, T-K, p <0.01), but most prominently following N+PSi enrichment (ANOVA, T-K, p <0.001). Sites 3 and 6 also showed signs of synergistic co-limitation following the addition of N+PSi, although no significant increases (compared to controls) were found after the addition of N or P/Si alone. Responses at site 4 represent simultaneous co-limitation in which an increase in chlorophyll only occurred when all resources (N+PSi) were added in combination.

The influence of nutrient addition on POC was lesser in comparison to the changes in chlorophyll. The most significant change was observed following the addition of N+PSi at site 1, with a 2-fold increase in POC taking place compared to the control and other treatments. The only other significant change took place following the addition of PSi at site 3 which resulted in a decrease in POC compared to the other treatments and control.

The POC:chlorophyll showed strong responses to nutrient addition. The POC:chlorophyll values of control samples in both sites 1 and 2 were up to 2-fold higher than all treatments which did not differ significantly. The control was also significantly higher than both PSi and N+PSi treatments at site 6 and was similar to the N+ treatment which differed significantly from the N+PSi but not the PSi treatment.

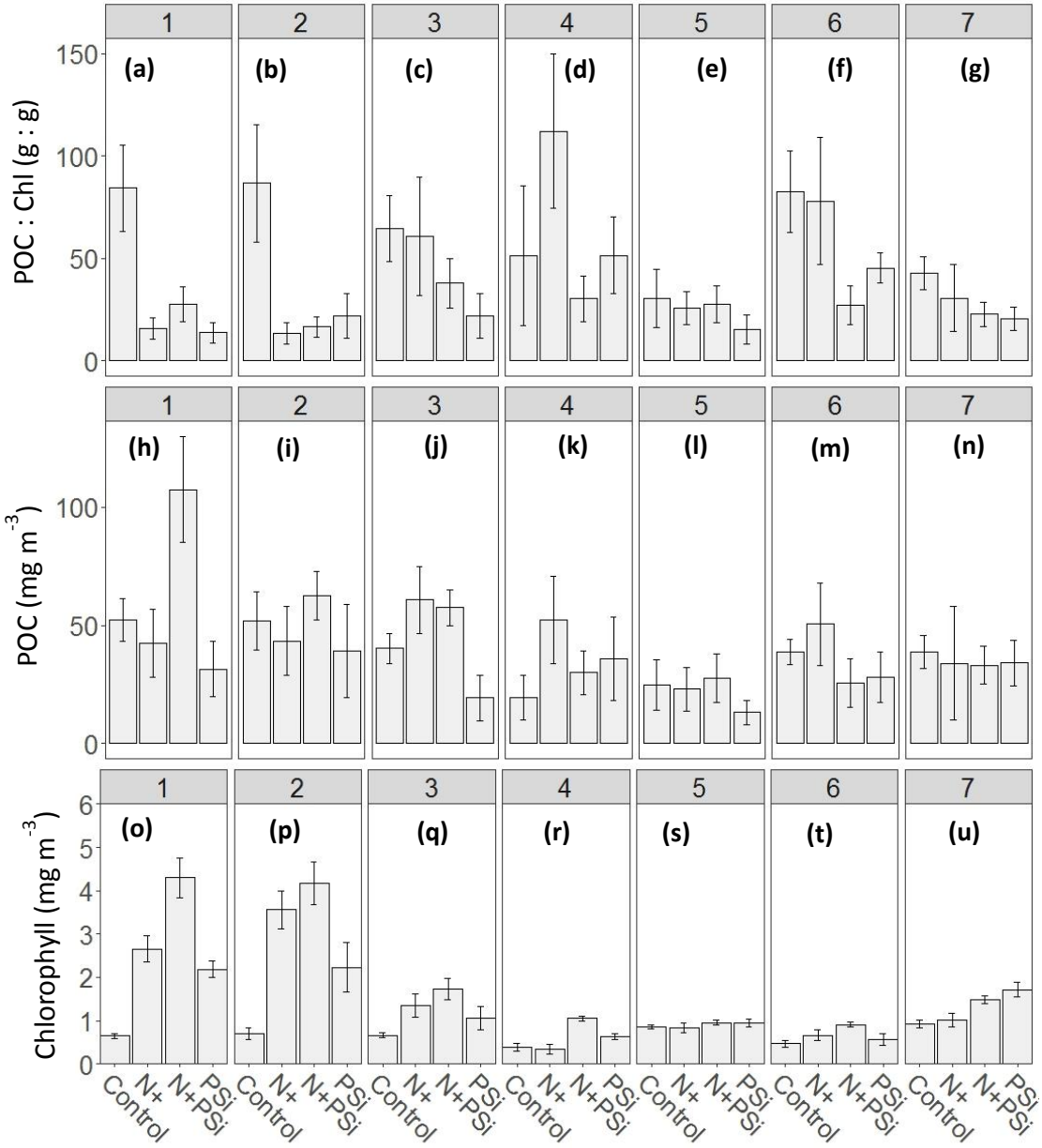

Figure 2.6. Growth and physiology response to nutrient addition in the seven bioassay experiments (**a-g)** particulate organic carbon (POC):chlorophyll **(h-n)** POC concentration **(o-u)** chlorophyll concentration. Shown are means (± 1 s.e., n = 4). All data shown are from the endpoint (48 h).

2.3.4. Response Relative to Initial Conditions

The results of the 7 experiments clearly identified that nutrient limitation influenced the physiology and growth of the phytoplankton communities. Yet, no consistent

response was found across the experimental sites, possibly caused by the different starting conditions (e.g. nutrient concentration, temperature). The N+PSi addition was the only treatment to elicit a significant response in all the measured parameters. Therefore, it was used to examine how initial conditions influenced the community response to nutrient addition. This was done using the log RR (as discussed in section 2.2.6) (Fig. 2.7 & Fig. 2.8).

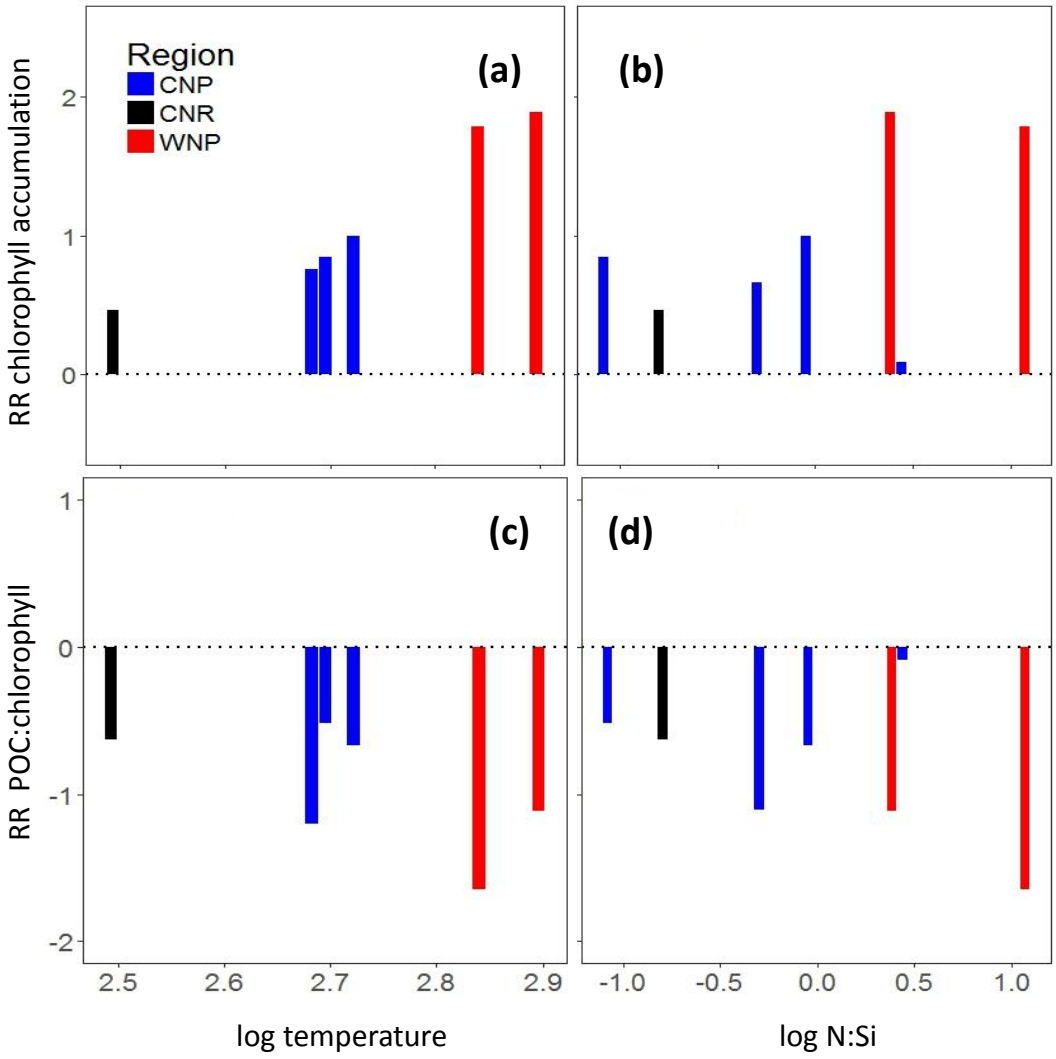

Figure 2.7. Log response ratio of phytoplankton growth and physiology following nutrient enrichment of nitrate, phosphate and silicate. For methods of y-axis calculation see section 2.2.7. The x-axis represents the initial conditions of the seven experiments **(a)** The change in community chlorophyll concentration versus temperature **(b)** The change in community chlorophyll concentration versus N:Si **(c)** the POC:chlorophyll versus temperature and **(d)** the POC:chlorophyll versus Si:N

The log RR of each physiology and growth measurements were plotted along a gradient of starting environmental parameters. The environmental parameters selected were: temperature, N:P, N:Si, Si:P and the nano:pico for cell number and biomass. The nano:pico was calculated using the summed biomass and cell numbers for the pico (Pico & Syn) and nano (Nano & Crypto) components identified using SFC.

The log RR analysis showed differences in the ratio of dissolved inorganic nutrients as the prevailing factor driving changes in growth and physiology; temperature and community composition were also influential. The magnitude of change observed in both chlorophyll accumulation and the POC:chlorophyll were seemingly driven by the initial N:Si. At the two WNP sites the N:Si was ~1 or greater. Here, chlorophyll accumulation increased compared to the control and was markedly higher than the CNP and CNR sites where the N:Si was less than 1 (Fig. 2.7). This was reflected in the POC:chlorophyll which was lower in all the CNP and CNR sites apart

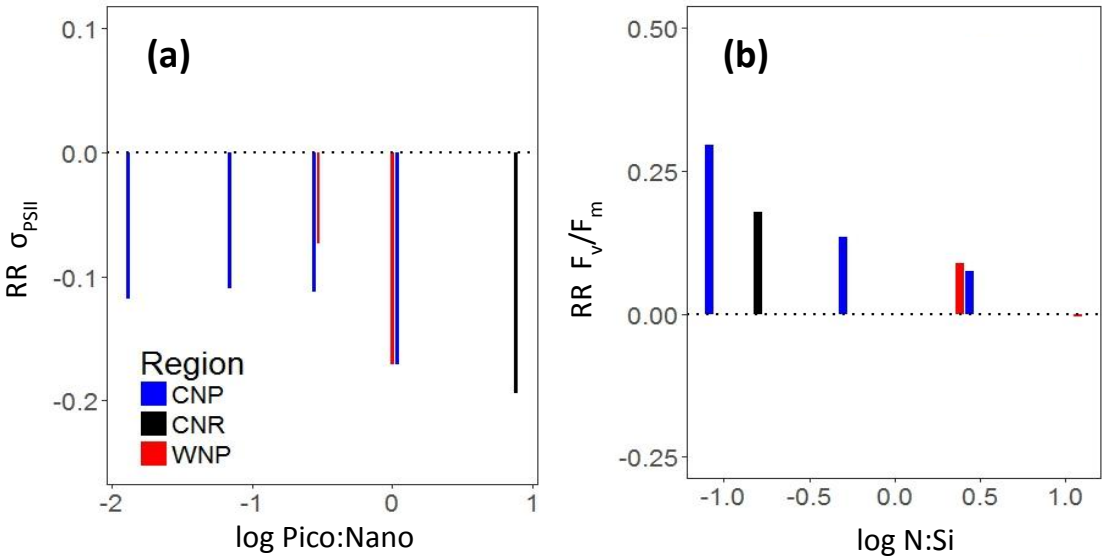

Figure 2.8. Log response ratio of phytoplankton photophysiology following nutrient enrichment of nitrate, phosphate and silicate. The x-axis represents the initial conditions of the seven experiments **(a)** the functional cross section of Photosystem II (σ_{PSII}) versus changes in taxonomy and **(b)** the maximum quantum yield of photochemistry (F_v/F_m) versus differences in N:Si

from site 3. Chlorophyll accumulation also showed a much greater response in warm conditions.

The N:Si was also found to effect PSII characteristics, with the largest increases in F_v/F_m occurring at the sites with high N:Si values (Fig. 2.8). σ_{PSII} values showed no identifiable trend with nutrient availability, but were lower at the stations with a pico:nano of 1 or greater (Fig. 2.8). Despite changes in PSII characteristics the FRRf-derived P vs. E parameters showed no significant environmental drivers; although, the WNP sites did respond differently to nutrient addition compared to the CNP and CNR sites (Supp. fig. 2.2).

2.4. Discussion

This study provides evidence that geographically different regimes of nutrient limitation and co-limitation exist across the North Sea, influencing the growth and photophysiology of phytoplankton communities. Nutrient-limited phytoplankton growth is a common occurrence in temperate shelf sea regions over the summer months, brought about by the development of thermal stratification (van Leeuwen *et al.* 2015).

Evidence of stratification and nutrient depletion was found across many of the 60 stations visited in this study. However, several stations were also found to have anomalously high nutrient concentration. These stations were often located in shallow or coastal areas, where the physical structure of the water column differs from other regions; due to the influence of external water bodies or riverine input. The CNR site (7) was amongst these anomalous stations and was located in the north-west region of the North Sea, where North Atlantic water enters the basin before

moving along the east coast of the UK. However, at present there is a significant lack of knowledge about nutrient dynamics across the entire North Sea with most studies focussed on coastal regions influenced by fluvial outputs (Artioli *et al.* 2008; Lenhart *et al.* 2010; Grizzetti *et al.* 2012).

Model observations reveal oceanic water input leads to a decrease in water temperature and increased nutrient concentration; resulting in widespread differences in the community composition (Ford *et al.* 2017). This is in keeping with the findings of this study which showed the phytoplankton community composition at the CNR site, was distinctly different from both the WNP and CNP sites, due to the dominance of picoplankton. However, the experimental sites in the two nutrient poor clusters also differed in the biotic and abiotic conditions, with the variability seemingly driven by coastal proximity.

Three of the experimental sites were in coastal regions and were characterised by both WNP (sites 1 and 2) and CNP (site 3) conditions. Coastal areas of the North Sea are strongly influenced by riverine input and particularly susceptible to damaging anthropogenic influence (e.g. eutrophication); leading to unbalanced nutrient loading, increased sedimentation from organic material and changes in species composition (Lenhart *et al*. 2010; Burson *et al*. 2016; Grosse *et al*. 2017b). The two sites of the WNP region were located in a problem area (PA), highlighted by a 2003 OSPAR report into eutrophication status of the North Sea (OSPAR, 2003). The nutrient concentration in the WNP was not found to be eutrophic and was similar to the central and northern regions. However, the high N:Si revealed an unbalanced nutrient stoichiometry that seemingly allowed nano-sized (2-5 μm) diatoms and dinoflagellates to dominate the community in these areas. In contrast, the community

composition of the non-coastal regions was more mixed. The true extent of the diatom dominance may not have been captured by the flow cytometry, as they may have formed large chains.

The differences in community and abiotic conditions was shown to influence the potential growth response of the phytoplankton community, following the addition of all growth-limiting nutrients (N+PSi treatment). Reasons for the large growth response in the WNP sites, compared to the other two clusters, could include the turbid nature of the region, grazer activity and the initial community composition. Phytoplankton growth in this shallow region of the North Sea is supressed through self-shading or light attenuation by silt (Lenhart *et al.* 2010; Burson *et al.* 2016). Removal from turbid conditions could be attributed to the large growth response. In this region, unbalanced nutrient loading has also led to an offshore gradient of nutrient limitation. Resulting in P and Si limited phytoplankton growth nearshore, the co-limitation of N and P in the transitional region and N limitation in the offshore waters.

Differences in the prevailing limiting nutrient were observed in the two WNP sites, but cannot be attributed to location as the community composition also differed. As such, this study shows that growth in diatom-dominated community from nutrient-poor, warm coastal region of the southern North Sea is co-limited by both Si/P and N whilst a mixed dinoflagellate-diatom community in similar conditions is N-limited. The results of the CNP sites do not provide conclusive evidence for a primary growth-limiting nutrient. The CNR station was unusual as nutrient concentrations were not found at levels expected to be limiting but clear P or Si limited growth was still observed. It could potentially be explained by a recent mixing event which

resulted in an influx of nutrients. The response of these treatments to N+PSi and PSi additions suggests a limiting substrate of either P or Si.

2.4.1. FRRf in Different Nutrient Limited Phytoplankton Communities

An inverse relationship between F_v/F_m and σ_{PSII} was observed and has been shown to occur when PSII function becomes compromised by nutrient starvation (Kolber *et al*. 1988; Sugget *et al*. 2009). The response of F_v/F_m was found to be mixed. F_v/F_m values for N+ treatment bottles were found to decrease in multiple experiments. These findings are consistent with open ocean studies that saw an increase in chlorophyll but no response or a decrease in F_v/F_m following N addition (Behrenfeld *et al*. 2006). It has been postulated that this response could be driven by an increased synthesis of phycobilisomes, resulting in an artificially high F_o and decreased F_v/F_m (Suggett *et al*. 2009), but only if the community is dominated by cyanobacteria which are driving the response.

2.4.2. Study Limitations

Due to the short incubation period, it is most likely the observed changes in experiments are a result of the nutrient addition and not changes in community. Small shifts are possible but could be attributed to incubation settings such as light dosage and water temperature (Beardall *et al.* 2001). The focus of this study was to investigate the limiting effects of N on the growth and physiology of natural phytoplankton communities. Due to limited space in the on-deck incubator (16 bottles) a fully-factorial experimental design was not possible and restricted the investigation into the effects of P and Si addition.

2.5. Conclusion

Different regimes of nutrient limitation found across the North Sea. Following nutrient addition, the phytoplankton communities from these different sites all showed increased biomass but the largest increase was in the areas where N:Si was highest, which typically allows diatoms to dominate the population. The largest response coincided with the sites where the microphytoplankton and fucoxanthin (diatom marker pigment) were most abundant. PSII characteristics also responded differently according to initial conditions and conform to previous findings that identify F_v/F_m as an indicator of nutrient stress and σ_{PSII} with a taxonomic signature. Despite this the PE parameters did not differ according to initial taxonomy or nutrient condition

2.6. Supplementary Information

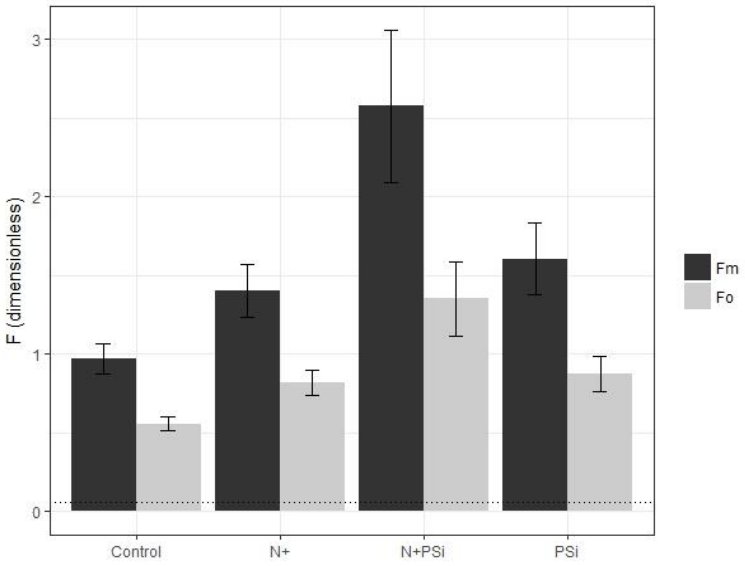

Supplementary Figure 2.1. FRRf measurements of fluorescence for experimental samples. The dashed line indicates the average blank. Displayed data taken from all timepoints.

Supp. table. 2.1. Measurements made at start and end points of each of the seven bioassay experiments.

Measurement	Start (T0)	End point (48 h)
Chlorophyll (UPLC)	✓	✓
Particulate organic carbon	✓	✓
Pigment composition (HPLC)	✓	X
Taxonomy (Flow cytometry)	✓	X
Dissolved inorganic nutrients	✓	X
Photophysiology (FRRf)	✓	✓

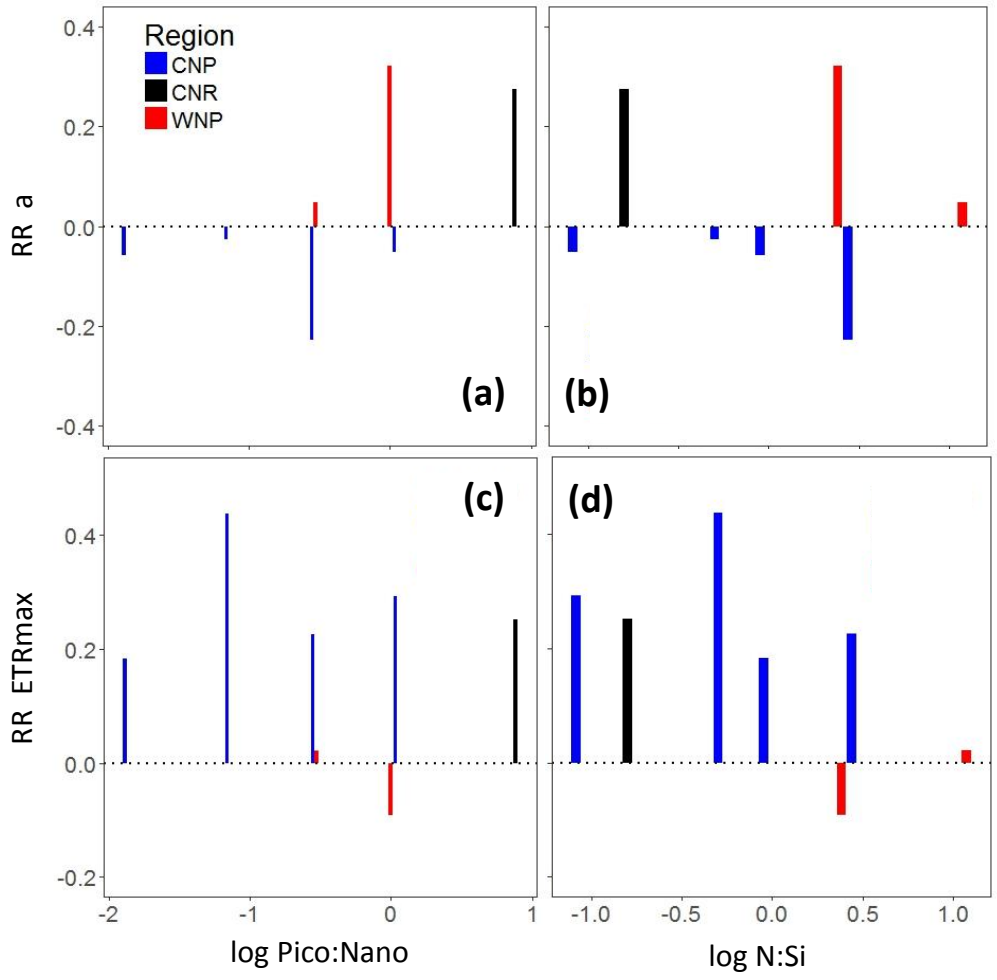

Supplementary Figure 2.2. Log response ratios of light response (P vs. E) parameters following nutrient enrichment of nitrate, phosphate and silicate. Data are given as natural-log transformed response ratios (RR). The x-axis represents the initial conditions of the seven experiments **(a)** the maximum light utilisation efficiency (α_{RCII}) versus pico:nano **(b)** the α_{RCII} versus N:Si **(c)** the maximum electron transfer rate (ETR_{max}) versus pico:nano and **(d)** the ETR_{max} versus N:Si

Chapter 3：Variability of Photosynthetic Properties During a Spring Bloom

3.1. Introduction

The Northwest European shelf is amongst the most studied continental shelf systems and is highly efficient at inorganic carbon capture, acting as a sink throughout the year (Thomas *et al.* 2004; Chen *et al.* 2013). The most significant period of shelf sea carbon cycling takes place during the springtime phytoplankton bloom, which is responsible for a large proportion of the ~1.3 Gt C yr^{-1} exported from the North Atlantic (Sanders *et al.* 2014). This annual carbon export event typically follows the alleviation of low light conditions and is characterised by a sustained biomass accumulation in nutrient-enriched waters (Behrenfeld and Boss, 2014; Daniels *et al.* 2015).

The factors that govern the onset and magnitude of spring blooms remain a subject of debate, with the oldest argument formed around Sverdrup's (1953) "Critical Depth Hypothesis" over 60 years ago. This theory was formulated on the premise that phytoplankton growth, limited by vertical mixing and limited light, can outweigh the losses following the shoaling of the mixed layer to a depth shallower than the critical depth horizon. Recent studies have started to call into question the physical controls over bloom formation and dynamics, and instead postulate that climatic forcing and food-web shifts are the driving forces behind bloom formation (Behrenfeld, 2010; Behrenfeld & Boss 2014; Franks, 2015).

Despite the lack of consensus on blooms initiation and dynamics it remains an extensively studied topic of research, with a multitude of studies conducted both *in situ* and using satellite-derived data products or models (Mahadevan *et al.* 2012; Teeling *et al.* 2012; Brunet *et al.* 2013). Although the latter provide a spatial and temporal resolution that cannot be matched by *in situ* studies, they lack the ability to

address the complex nature of phytoplankton community structure and physiology; and subsequently these controls over growth and productivity (Daniels *et al.* 2015).

At present, bio-optical techniques are the only method that can be employed *in situ* to measure both phytoplankton biomass and photophysiology at high resolution and have previously been employed autonomously to gather data over large spatial areas (Kavanaugh *et al.* 2014; Robinson *et al.* 2014). Active fluorometry allows non-invasive, instantaneous measurements of phytoplankton photosynthetic rates that can be used to provide insight into how marine productivity varies both spatially and temporally. Thus, advancing our understanding of how phytoplankton acclimation and adaptation contribute to changes in primary productivity and bloom status (Suggett *et al.* 2001; Moore *et al.* 2005, 2006).

The main objectives of this study were (i) to use FRRf to examine the spatial and temporal variability of phytoplankton photophysiology over the course of a spring bloom in the central Celtic Sea and (ii) determine the prevailing environmental factor (nutrient concentration, phytoplankton taxonomy, physical conditions) that drives the variability in photophysiological measurements.

3.2. Methods

3.2.1. Cruise Information and Hydrography

Data were collected on board the *RRS* Discovery during a research cruise (DY029) to the Celtic Sea between the 1st and 31st April 2015, coinciding with the boreal spring. Six sampling events took place at a station in the central Celtic Sea (CCS) over the course of the cruise (Fig. 3.1). During each sampling event, a Sea-Bird 9 plus

Conductivity-Temperature-Depth (CTD) and a CTG AquaTracka III fluorometer mounted on a 24-bottle rosette system collected vertical profiles of temperature, salinity, and chlorophyll fluorescence to observe how these parameters changed with depth. The data were subsequently screened and anomalous data was removed, averaged onto a 1 db grid and calibrated against samples of chlorophyll concentration and salinity. Discrete seawater samples were collected from depth using a 24-bottle rosette of 20 L Niskin bottles on a stainless-steel frame from CTD casts.

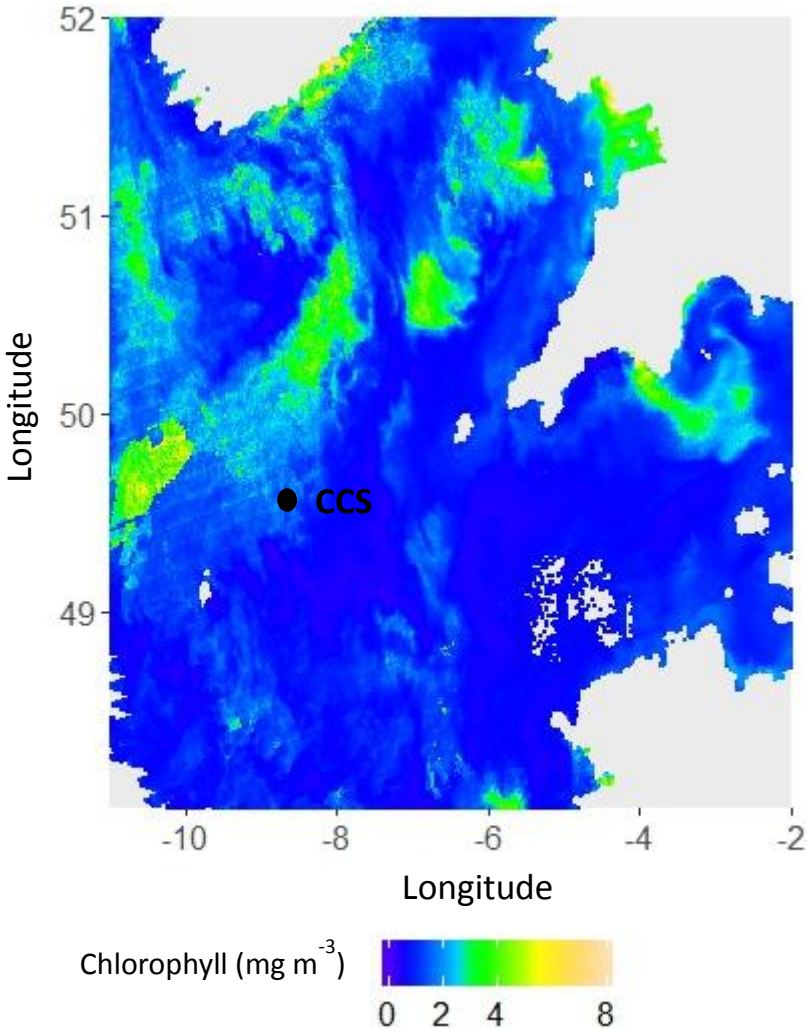

Figure 3.1. Satellite estimates of chlorophyll across the Celtic Sea with the location of the central Celtic Sea station. The background image is a 7-day Visible Infrared Imaging Radiometer Suite (VIIRS) OC5 chlorophyll data measured between the 15th and the 21st of April. VIIRS data were acquired from the NERC Earth Observation Data Acquisition and Analysis Service (NEODAAS)

Light measurements

Measurements of photosynthetically active radiation (PAR) were made using sensors mounted on both the ship's bridge and the top of the CTD frames, allowing the calculation of daily irradiance and the light attenuation coefficient (*k*). *k* was then estimated using profile data converted to a linear plot as ln E vs. depth, the slope of which was taken as -*k* and used to calculate the surface irradiance (E_0) and subsequently the E_Z:

$$E_Z = E_0 \ e^{-kz} \qquad \text{Eqn. 3.1}$$

where E_0 was estimated using the mean daily incident irradiance from the previous day, measured using the bridge PAR sensor, and 0.1 m as the depth (z):

$$E_0 = E_{sur} \ e^{-kz} \qquad \text{Eqn. 3.2}$$

Data from mid-day profiles (or within one hour) were used for the estimation of *k* and the upper 5 m were removed to reduce noise caused by wave action and surface reflectance. An individual value of *k*, E_Z and E_0 was obtained for each day on CCS; unless it lacked a daytime profile on station (yearday - Yday - 96 and 102) or suffered from poor quality light data (Yday 111). Percentage light levels ($E_{\%}$) were obtained using the E_Z and mean daily irradiance, these values were then grouped (0-20, 20-40, 40-60, 60+ % of surface irradiance) and used to analyse changes in photophysiology driven by light availability.

3.2.2. Fast Repetition Rate fluorometry

A multi-spectral Fast Repetition Rate fluorometer (FRRf; FastOcean™, Chelsea Technologies Group - CTG - Ltd, UK), fitted with an integrated FastAct™ bench-top unit (CTG Ltd), was used to measure phytoplankton photophysiology for seawater samples drawn from the ship's non-toxic underway system (approximately 4 m depth) and collected by Niskin during CTD casts. Samples were dark-acclimated at source temperature for a minimum of 30 minutes, before single turnover acquisitions were made using a protocol of 50 sequences of 100 2µs saturation flashes at 150 ms intervals. Data were processed using software provided by the instrument manufacturer (FASTpro8 V1.0.5, CTG Ltd.), with the minimum fluorescence (F_o), maximum fluorescence (F_m) and the functional absorption cross section of photosystem II (σ_{PSII}) provided by fitting the data to the KPF model (Kolber *et al.* 1998).

The dark-acclimated maximum quantum yield of photochemistry (F_v/F_m) was calculated as F_m- F_o/F_m. The RLC protocol consisted of 16 light steps, each of 2 minutes, with the FastAct actinic irradiance increasing from 10 to 1803 µmol photons m^{-2} s^{-1}. At each light step the fluorescence under actinic light (F'), the maximum fluorescence under actinic light (F_m') and the parameters F_q'/F_v', F_v'/F_m' and F_q'/F_m' were obtained. Non-photochemical quenching (NPQ) was calculated as the normalised Sterm-Volmer coefficient, discussed in McKew *et al*. (2013) and defined as:

$$NPQ_{NSV} = \left(\frac{Fm'}{Fv'}\right) - 1 = \left(\frac{Fo'}{Fv'}\right) \qquad \text{Eqn. 3.3}$$

where NPQ_{NSV} is the ratio of the nonphotochemical dissipation in the light-adapted state to the rate constant for photochemistry. The absolute rate of photosynthetic

electron transfer (ETR) through photosystem II (PSII) reaction centres was calculated from fast repetition rate fluorescence as follows:

$$ETR^{RCII} = 0.6023 \cdot a^{PSII} \cdot \left[F_q'/F_m'\right] \cdot E \qquad \text{Eqn. 3.4}$$

where ETR^{RCII} is the rate of charge separation by RCII (units of s^{-1} $RCII^{-1}$), $a^{PSII} = \sigma_{PSII}/(F_v/F_m)$ is the optical cross-section of PSII (units of nm^2 $RCII^{-1}$), where both σ_{PSII} and F_v/F_m were measured after dark-acclimation prior to starting the rapid light curve, F_q'/F_m' is the operating efficiency of PSII under actinic illumination, E is the photosynthetic photon flux density (units of µmol photons m^{-2} s^{-1}) and the constant 0.6023 is Avogadro's number divided by 10^{24} to allow ETR^{RCII} to be reported in units of inverse time (units of s^{-1} $RCII^{-1}$). Photosynthetic-irradiance (P vs. E) parameters were calculated from PAR-dependant changes in ETR^{RCII} calculated at each light-step before being fitted to a function adapted from Webb *et al*. (1974) shown in Eqn. 3.5 and discussed in Silsbe & Kronkamp (2012):

$$Webb\ model\ \ (ETR^{RCII}) = \ \alpha \cdot \frac{E}{E_K} \cdot \left[1 - \left(\frac{E}{E_K}\right)\right] \qquad \text{Eqn. 3.5}$$

where α represents the initial light-limited slope, E_K represents the light saturation parameter and the maximum light-saturated ETR^{RCII} (ETR_{max}) is calculated as $E_K \cdot \alpha$.

3.2.3. Total and Size-fractionated Fluorometric Chlorophyll

Water samples (0.2-0.25 L) for chlorophyll extraction were filtered onto 25mm Whatman glass fibre filters (effective pore sizes 0.7 µm) and extracted in 6-10 mL 90% acetone (HPLC grade, Sigma-Aldrich, UK) at 4 ^{o}C for 18-24 h. Fluorescence was measured on a Turner Designs Trilogy fluorometer using a non-acidification module

and calibrated with a solid standard and a pure chlorophyll *a* standard (Sigma-Aldrich, UK). Size fractionated chlorophyll was also analysed on parallel samples by filtering onto 47mm polycarbonate filters of various pore sizes (0.2, 2 and 20 µm) and following the same extraction protocol as total chlorophyll (Daniels *et al.* 2015)

3.2.4. Macronutrient Concentration

Water samples for dissolved inorganic nutrients were collected in 60 ml HDPE Nalgene bottles using clean handling techniques to avoid contamination. Analytical chemical methodologies used were Brewer and Riley (1965), Grasshoff (1976), Kirkwood (1989) and Mantoura and Woodward (1983). Nutrient concentrations were determined on board using a 5-channel Bran and Luebbe AAII segmented flow auto-analyser, following the molybdenum blue method or using a liquid waveguide capillary cell to check when phosphate concentrations were less than 50 nM.

3.2.5. Analytical Flow Cytometry

Cell numbers for the major phytoplankton groups were analysed from each sampling depth 328 within the euphotic zone, through flow cytometry (for *Synechococcus* pico-eukaryotes, nano-eukaryotes, coccolithophores, cryptophytes). Samples were collected in clean 250 mL polycarbonate bottles and analysed using a Becton Dickinson FACSort instrument (Tarran *et al.* 2006).

3.2.6. Light Microscopy

Samples for light microscopy were collected in 100 mL brown glass bottles and preserved in acidic Lugol's solution (2% final solution) until analysis under a Leica DM IRB 334 inverted microscope (Widdicombe *et al.* 2010).

3.2.7. Statistical Analyses

Two-way ANOVA tests were used to test for variation in photophysiological parameters (PSII turnover and P vs. E parameters) between sampling events and different light gradients (described in section 3.2.1 of this chapter). Significant differences between light gradients and sampling events were identified with Tukey-Kramer (T-K) tests.

Principal component analysis (PCA) was carried out to define the primary gradients of variability and identify multicollinearity in environmental and taxonomic parameters. Generalised linear modelling (GLM) was then used to explore the response of physiological parameters to multiple environmental and taxonomic variables. GLM was selected to allow the use of non-normally distributed data. The environmental variables were transformed (scaled and centred) to standardise the variance. Cell numbers measured using analytical flow cytometry (AFC) were normalised to chlorophyll concentration (measurements described in section 3.2.3), before being scaled and centred. Although multicollinearity between explanatory variables were identified and removed using PCA. A stepwise model selection procedure using Akaike Information Criterion (AIC) was employed to select the best model for the data set. All environmental and community parameters were also

modelled together, following the same optimising procedure, to view the combined effects. Following the optimisation and selection of the environmental, community and combined models, AIC was used again to indicate the best explanatory model for each physiological parameter.

3.3. Results

3.3.1. General Oceanography: Development of Bloom and Stratification

The central Celtic Sea station (CCS) was profiled on twelve days during the initiation, peak and decline stages of a large phytoplankton bloom. A temperature-driven pycnocline developed over the course of the cruise, altering the density and structure of the upper 50 m of the water column. The profiles of the first sampling event revealed that the water column was almost entirely homogenous in both temperature and salinity; salinity was stable at 35.30-35.35 ppt over the entire cruise. However, over the next three sampling events, warming in the upper 50 m led to a variable mixed layer forming, as temperatures increased by up to 1.5 ^{o}C (Fig. 3.2).

Stratification had started to take place at the time of the final sampling event with a weak thermocline developing at approximately 30 m (Fig 3.2). Initial surface water concentrations of nitrate, phosphate and silicate were 6.1 µM L^{-1}, 0.5 µM L^{-1} and 2.8 µM L^{-1} respectively and were almost entirely homogenous throughout the water column (nitrate was 0.7 µM L^{-1} higher below 50 m). A substantial drawdown of both nitrate (5 µM L^{-1}) and phosphate (0.3 µM L^{-1}) occurred in the upper 30 m between the 4th (Yday 94) and 28th (Yday 118) of April, representing a decrease of 80 % and 60 % respectively, from the concentrations recorded on the first day of sampling (Fig.

3.2). Silicate^{-} also decreased by 1.9 µM L^{-1} (50 %) over the course of the cruise (Fig. 3.2).

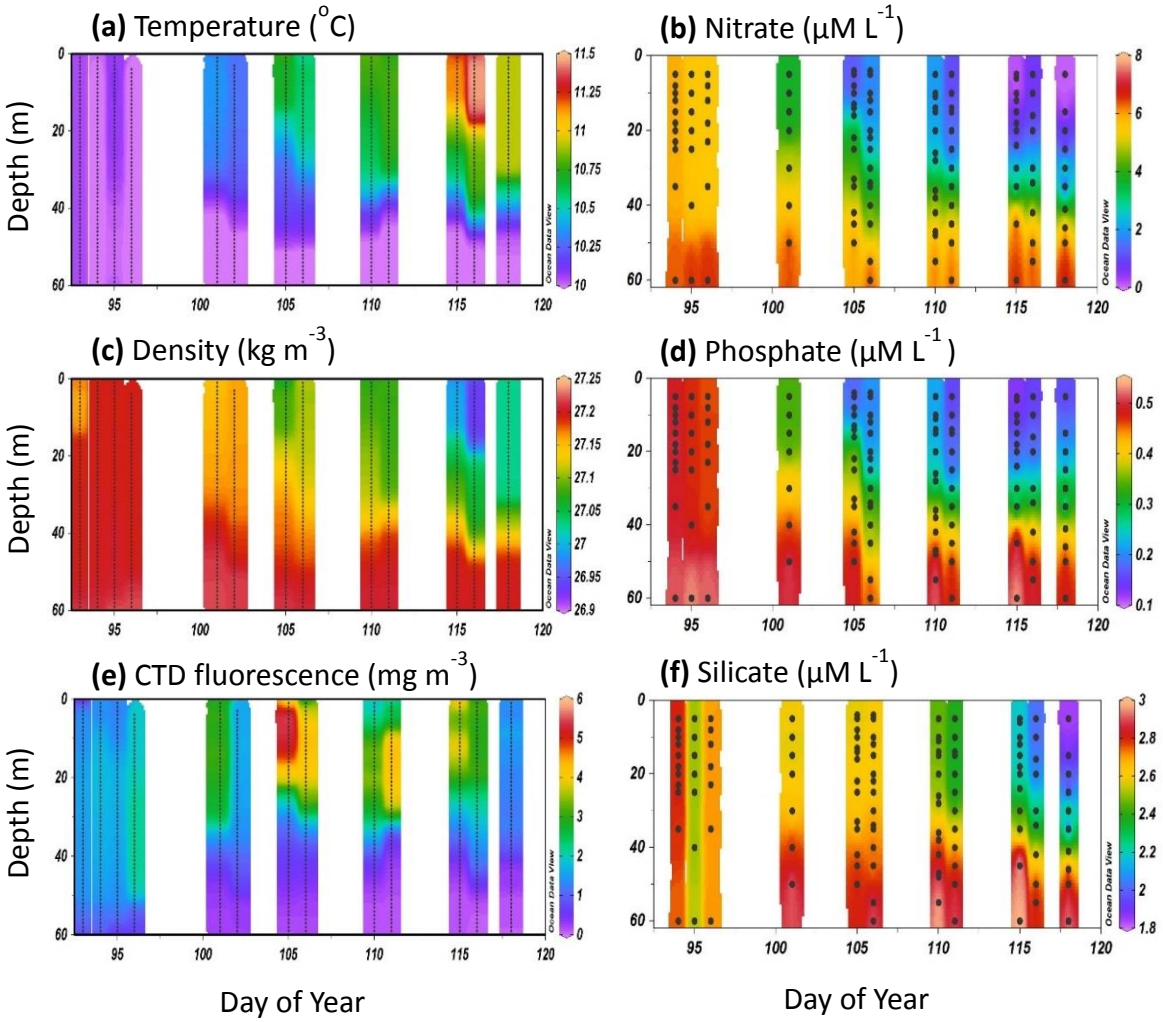

Figure 3.2. Upper water column profiles, for the central Celtic Sea station (CCS), of **(a)** temperature **(b)** salinity and **(c)** CTD fluorescence. Nutrient concentration at CCS measured during six sampling events. **(d)** Nitrate **(e)** phosphate and **(f)** silicate. Black dots indicate a sampling point

3.3.2. Plankton Biomass, Vertical Distribution and Taxonomy

Depth profiles of chlorophyll, measured with fluorescence via the CTD, changed substantially over the course of the cruise, indicating different stages of the phytoplankton bloom (Fig. 3.2). Like temperature, chlorophyll fluorescence profiles taken during the first sampling event showed a relatively homogenous distribution

throughout the water column with higher values in the upper 50 m (coupled with slightly reduced nitrate), which indicated an accumulation of photosynthetic biomass in the aphotic zone prior to the first sampling event. During the second sampling event (11th April, Yday 101), the maximum recorded chlorophyll fluorescence increased 1.5-fold and was found in the upper 30 m. The third sampling event (15th April, Yday 105) saw the greatest increase in chlorophyll fluorescence with the maximum value 2.5-fold higher than any observed during the first sampling event. The fourth and fifth visits to CCS on the 20th April (Yday 110) and 25th April (Yday 115) showed a gradual decrease in the maximum fluorescence through the water column.

Acetone extracted measurements of chlorophyll ranged from 0.2 to 8.4 mg m^{-3} (Fig. 3.3). There were peaks in concentration on two separate occasions: (i) the first peak on 15th April (third sampling event), chlorophyll was 5.5-fold greater than the maximum value from the first sampling event, which occurred 15 days previous and was followed by a steady decline until (ii) a secondary peak on the 25th of April. The highest chlorophyll values were consistently found in the upper surface waters, with concentrations not exceeding 2 mg m^{-3} in samples taken from depths of < 30 m.

The size-fractionated chlorophyll revealed changes in the composition of the community found in the upper 30 m of the CCS site, over the course of the cruise. The smallest fraction (picoplankton; 0.2 – 2 µm) was typically more abundant (> 25 % of the total chlorophyll) in the upper 20 m during the first sampling event, but declined as the cruise progressed and became more prevalent at greater depth (> 30 m). However, during the fifth sampling event the picoplankton component increased again in the upper surface waters. Over the course of the first five sampling events the 2 – 20 µm (nano) fraction often accounted for a large proportion (> 50 %) of the

total chlorophyll, but peaked in biomass in the upper 25 m (70 – 90 %) during the third sampling event. The > 20 µm size-fraction (microplankton) rarely featured in the first five sampling events. However, the final sampling event saw a substantial increase in the microplankton component to > 25 % at all depths.

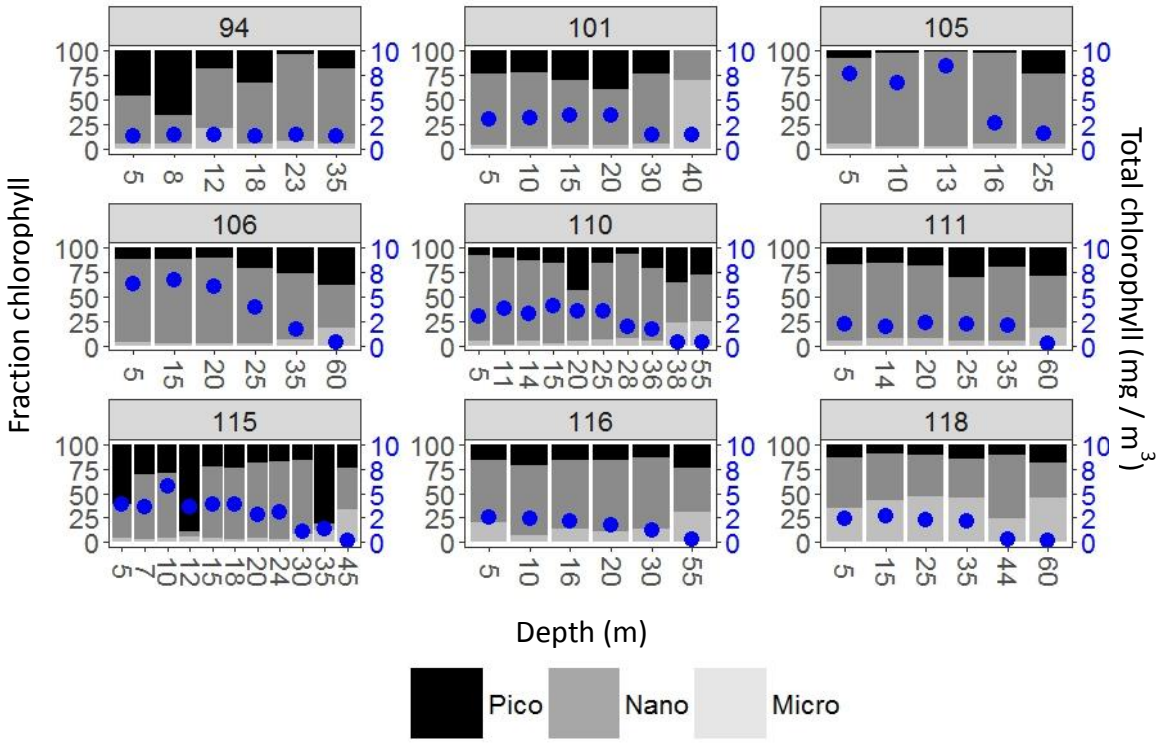

Figure 3.3. Total and size fractionated chlorophyll for samples taken from the CCS. The blue dots show total chlorophyll. The grey bars indicate the % contribution of each size class - pico (<0.2 µm), nano (2-20 µm) and micro (>20 µm). The year day (Yday is indicated above each plot

Analytical flow cytometry

Synechococcus, pico-eukaryotes (< 3 µm) and nano eukaryotes (approx. 3-12 µm) were found in the highest abundance at CCS over the course of the cruise, each having periods where they dominated the community (Fig. 3.4). During the first sampling event, pico-eukaryotes became increasingly abundant in the upper 35 m and peaked at 45 090 cells mL^{-1} on 6th April (Yday 96). Abundance was still high (> 44 000 cells mL^{-}

^{1}) during the second sampling event, but had started to decline (< 30 000 cells mL^{-1}) at depths between 25 – 35 m. This decline continued for the duration of the cruise until cells were regularly distributed throughout the water column at abundances < 1000 cells mL^{-1}. Like the pico-eukaryotes, *Synechococcus* spp. were also present in moderate abundances (27 000 cells mL^{-1}) throughout the upper 35 m during the first sampling event and peaked at 40 020 cells mL^{-1} on Yday 96, before a continuous and steady decline occurred. The nano-eukaryote component of the community was principally comprised of cryptophytes, coccolithophores and unidentified taxa.

Nano-eukaryotes abundance was consistently < 3 000 cells mL^{-1} throughout the water column during the first sampling event, but increased to > 4 500 cells mL^{-1} in the upper 20 m during the second. During the third sampling event nano-eukaryote abundance continued to increase in the upper surface waters (the highest value was 7 590 cells mL^{-1} at 13 m) but did not peak (> 8 500 cells mL^{-1} in the upper 10 m) until the 25th April (Yday 115). Cryptophyte abundance followed the same trend as the general nano-eukaryote component but peaked earlier (during the third sampling event) and remined high during the fourth, before declining. Coccolithophores were not common relative to the other nano-eukaryotes but were at highest abundance during the first and second sampling events, declining in number across the duration of the cruise.

Diatoms (identified by light microscopy) were only present in small numbers (< 3 cells ml^{-1}) for most of the cruise and were predominantly represented by *Pseudo-nitzchia sp.* and *Thalassiosira sp*. They were most abundant during the first sampling event and decreased in number during the development and peak of the bloom in chlorophyll biomass.

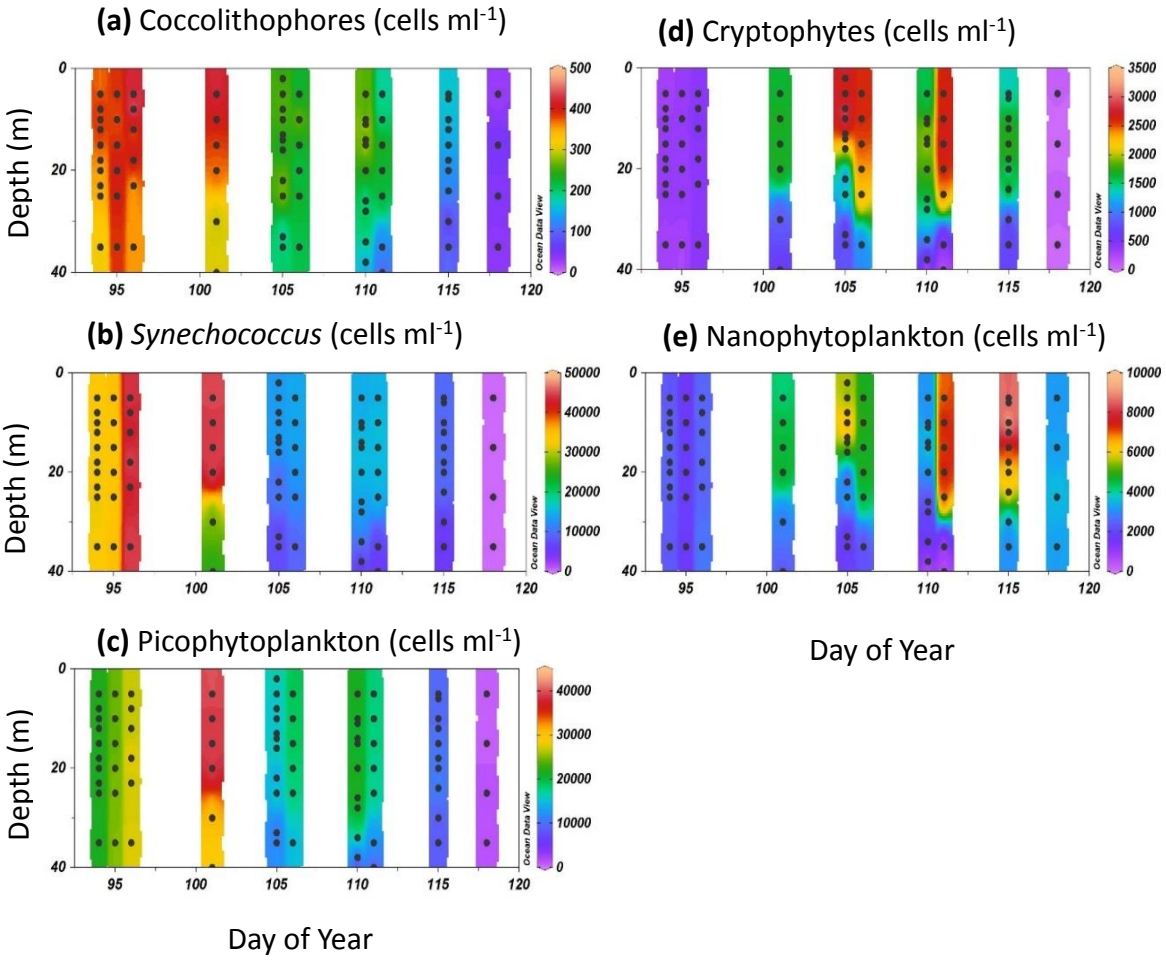

Figure 3.4. Analytical flow cytometry counts of nano and picoplankton at CCS **(a)** coccolithophores **(b)** *Synechococcus* **(c)** picophytoplankton **(d)** cryptophytes **(e)** nanophytoplankton (excluding coccolithophores and cryptophytes). Black dots indicate sampling points

3.3.3. Relationships Between Environmental Conditions and Phytoplankton Community Structure

Temperature was the main correlate with changes in nutrient availability and phytoplankton community composition. This was observed in PC1 of the PCA analysis, which showed a strong inverse relationship with nutrients, the abundance of some taxonomic groups (e.g. picoeukaryote, coccolithophore and *Synechococcus spp.*) and the depth of the surface mixed layer. PC2 was predominantly influenced by factors associated with the light climate (*k*, $E_{\%}$, previous days irradiance - PDI), chlorophyll concentration and the remaining taxonomic groups (cryptophytes and nano plankton). Together, these factors account for 67.6 % of the variation and revealed co-variance between taxonomic and environmental variables. Silicate concentration, Z_{mld}, chlorophyll, *k*, PDI and Elev were selected to represent the variance in the environment over the cruise, whilst cryptophytes and nano plankton abundance (normalised to chlorophyll) were selected to represent taxonomic changes.

The distribution of sample points on the biplot revealed temporal trends in variance between samples. Early sampling events (Yday 94, 95, 96) were tightly clustered to the right of the x-axis signifying cold, nutrient-rich conditions (Fig. 3.5). The cluster is also strongly associated with *Synechococcus*, coccolithophores and photosynthetic picoeukaryotes (PPEs). Changes started to occur on Yday 101, as the temperature increased and nutrient concentrations decreased. A similar trend was also observed in the samples from Yday 115 where the two deepest stations were

distinctly different from shallower samples. The taxonomy also changed from a high abundance of cryptophytes to nanoplankton.

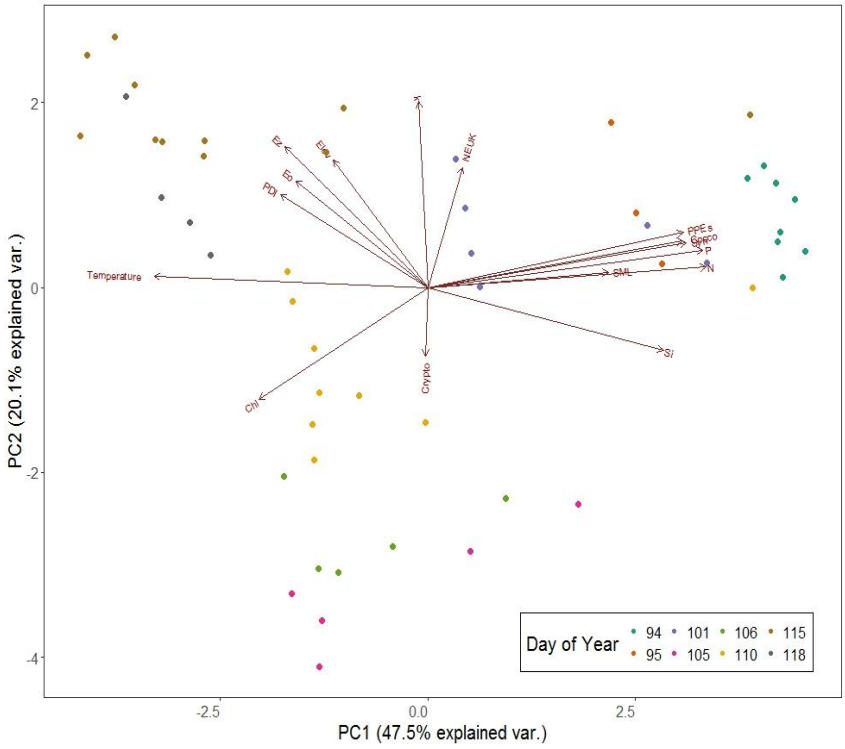

Figure 3.5. PCA ordination containing environmental parameters and analytical flow cytometry counts measured at CCS during eight sampling events. Measured parameters are described in the text. Data were scaled and centred. 47.5 %of the variance was explained by the principal component 1 (PC1) with the second (PC2) accounting for a further 20%

3.3.4. Variation in Photophysiology

P vs. E parameters were found to differ by several orders of magnitude over the course of the cruise, coinciding with large-scale changes in community composition (Fig. 3.6). Estimates of the maximum light utilisation efficiency (α) ranged from 0.14 - 0.41 over the course of the cruise, but unlike all other FRRf parameters, did not differ significantly over time (sampling period) or space (light depth) indicating a wide range and high variability between sampling events (Fig. 3.6). The saturating irradiance (E_K) and maximum electron transfer rate (ETR_{max}) both differed significantly between

sampling periods with values ranging 3-fold and 4-fold, respectively (ANOVA, T-K, p <0.05). A similar trend in spatial variability was observed in E_K and ETR_{max}. A considerable increase in both was observed towards the end of the cruise, following the decline of nanoplankton abundance. Cryptophyte abundance was the driving taxonomic influence and correlated strongly with ETR_{max} (-0.66) and E_K (-0.59). It was also a parameter in the optimised ETR_{max} model and the solitary explanatory variable for E_K.

Values of F_v/F_m and σ_{PSII} both varied 1.5-fold, with significant variance observed between the first sampling event and the rest of the cruise (ANOVA, T-K, p

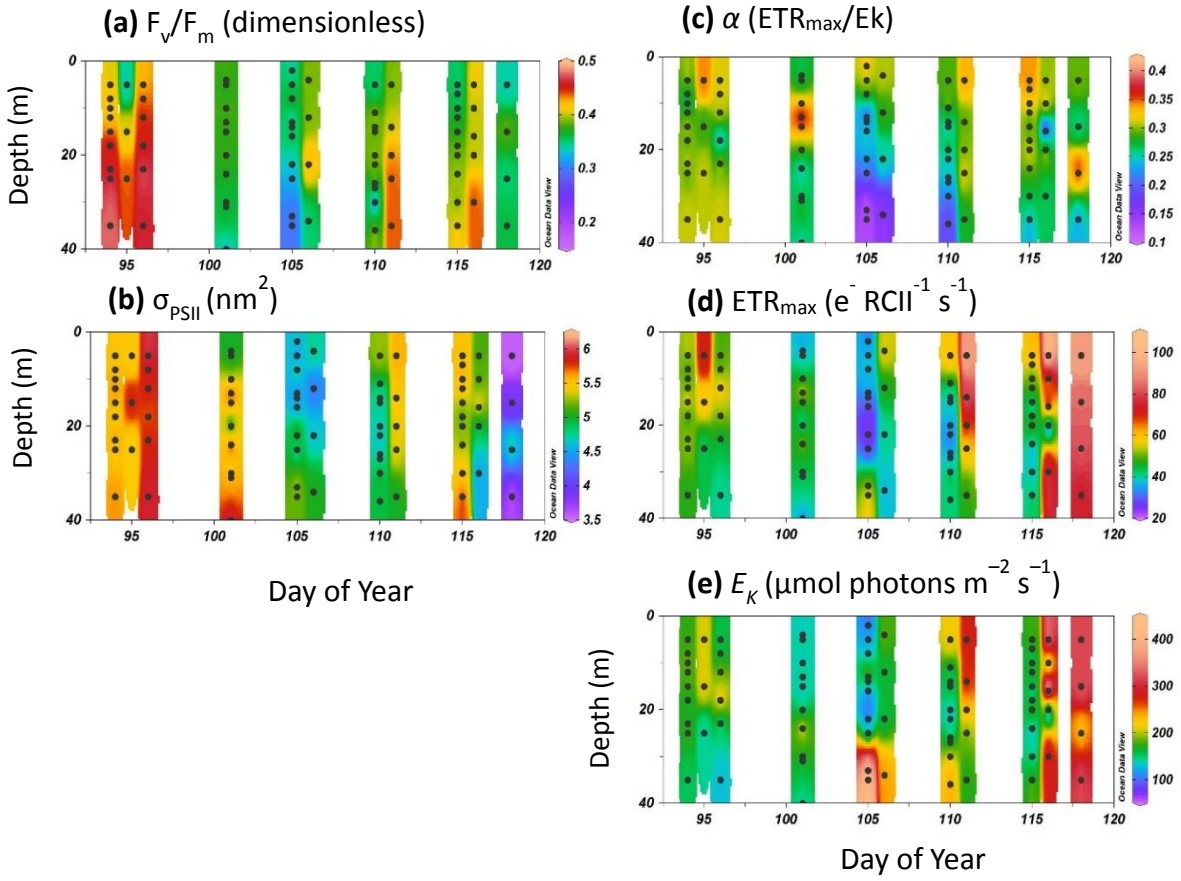

Figure 3.6. Photophysiological parameters measured at CCS. **(a)** Photosynthetic efficiency (F_v/F_m) **(b)** The functional cross section of Photosystem II (σ_{PSII}) **(c)** Maximum light-utilisation coefficient (α) **(d)** The PAR required to saturate photosynthesis (E_K) **(e)** The maximum electron transfer rate (ETR_{Max})

<0.05). During this period, the community composition at CCS changed from a high abundance of coccolithophores and picoplankton, towards a community dominated by nanoplankton. However, environmental parameters, not changes in taxonomy were revealed as the significant drivers behind the variance in both parameters.

Environmental Drivers of Photophysiology

F_v/F_m ranged from 0.26 – 0.50 (units dimensionless), showing significant spatial and temporal variability (ANOVA, T-K, p <0.01). High F_v/F_m values (> 0.40) were seen throughout the upper 40 m during the first sampling event (Yday 94 – 96), which was homogenously-mixed and nutrient replete. A suppression in F_v/F_m (< 0.40) occurred following the first sampling event, which coincided with a 5.5-fold increase in chlorophyll, decreasing nutrient availability and declining numbers of picoeukaryotes and coccolithophores. Despite moderate correlation with both coccolithophores (0.36) and picoeukaryote chlorophyll-normalised cell numbers (0.44), they were not present in the explanatory model; whilst nitrate and chlorophyll were (Table 3.1; Table 3.2). The other explanatory variables were percentage light level ($E_{\%}$), k, and the previous days mean irradiance (PDI). The light climate was an influential driver of F_v/F_m, with significant differences found between the 60+ and 20-40 $E_{\%}$ groupings. This was reflected by the suppressed values in the top 10 m (60+ $E_{\%}$) and by higher values of F_v/F_m at depths of ~20 m where most of the 20-40 $E_{\%}$ were found. Despite this relationship, the lowest F_v/F_m was measured on a day with one of the lowest average daily irradiance values.

Values of σ_{PSII} ranged from 3.5 - 6 (nm^2) and followed a similar trend to F_v/F_m, showing a substantial decrease following the first sampling event (ANOVA, T-K, p

<0.001). The σ_{PSII} model contained four explanatory parameters (k, N, Chl, PDI) also present in the F_v/F_m, but E_0 and Z_{MLD} were present and E_0 was not.

Table 3.1. Correlation between photophysiological and environmental parameters

	F_v/F_m	σ_{PSII}	α	E_k	ETR_{max}
Elev	-0.215	0.147	0.530***	0.081	0.377**
k	0.218	0.365*	0.321*	0.078	0.219
PDI	0.212	-0.107	0.279	0.139	0.252
Z_{MLD}	0.388**	0.217	-0.088	0.227	0.192
Chl	-0.308*	-0.401**	0.076	-0.103	-0.112
Si	0.271	0.578***	-0.172	-0.403**	-0.437**
NEUK	0.199	0.219	-0.13	-0.163	-0.207
Crypto	-0.168	0.007	-0.231	-0.593***	-0.661***

Computed correlation used pearson-method with listwise-deletion.

The substantial variance (~3-fold) observed in α values throughout the water column was strongly driven by changes in the light climate. The 60+ $E_{\%}$ grouping was found to differ significantly from both the 0-20 and the 20-40 $E_{\%}$ groups with much higher values observed in the upper 20 m. ETR_{max} also showed considerable variation (~5-fold) over the cruise with significant differences observed over both time and depth (ANOVA, T-K, p <0.001). A strong driver behind the variance in ETR_{max} was cryptophyte abundance, which correlated strongly (-0.66), but $E_{\%}$ level and the Z_{MLD} were also key explanatory parameters. There was a distinct difference in values of ETR_{max} between 20 and 30 m (approximately the bottom of the MLD) in comparison to the rest of the water column where the remaining measures of ETR_{max} appeared to be very heterogenous.

Table 3.2. Explanatory variables used in each model and the explained variance

FRRf parameter	Explanatory variables	r^2
F_v/F_m	*Elev + k + PDI + ZMLD + Chl + Si*	0.51
σ_{PSII}	*k + PDI + ZMLD + Si*	0.7
a	*Elev + k + Crypto*	0.3
E_k	*ZMLD + Si + Crypto*	0.44
ETR_{max}	*k + ZMLD + Si + Crypto*	0.53

3.4. Discussion

3.4.1. Interpreting Variation in Phytoplankton Photophysiology

Previous studies have highlighted the importance of considering both physiological and taxonomic signatures when interpreting FRRf data (Suggett *et al.* 2009a). This is supported by coastal and open-ocean field campaigns where large differences in FRRf measurements typically correspond with substantial shifts in community structure, whilst laboratory studies have also identified taxon-specific 'signatures' in F_v/F_m and σ_{PSII} (Suggett *et al.* 2004; Allen *et al.* 2005; Moore *et al.* 2005; Suggett *et al.* 2009).

Typically, diatoms exhibit the highest taxon-specific F_v/F_m, and an inversely low σ_{PSII}, leading to the assumption that diatom-dominated natural populations will possess this fluorescence signature. Communities of large, fast growing diatoms are often found in well-mixed, coastal waters, particularly during the onset of phytoplankton blooms, where their high efficiency in photosynthetic energy conversion may give them an advantage over another species (Halsey and Jones, 2015). As the bloom develops, a shift in phytoplankton taxonomy (from cyanobacteria and prymnesiophytes to cryptophytes and other nanoplankton) and PSII

characteristics (to low F_v/F_m and high σ_{PSII}) occurs, driven by water column stratification and changes in nutrient availability (Moore *et al.* 2005; Hickman *et al.* 2012; Daniels *et al.* 2015). However, during the entirety of this study diatoms were largely absent and changes in community structure merely reflected a succession of dominance by different nano-eukaryotic groups (first coccolithophores, then cryptophytes and finally an unidentified group). This may explain the lack of correlation between the taxonomic data and F_v/F_m or σ_{PSII} which were both high at the start of the cruise before an abrupt 1.5-fold change. However, size-dependent light-harvesting approaches could potentially be a more important driver in the variance observed in this study.

3.4.2. Effects of Phytoplankton Taxonomy on Photophysiology

Alternate approaches to light harvesting strategy are driven by the need to balance maximal energy absorption (and high metabolic rates) with minimal photodamage and the high energetic costs incurred through the need of constant PSII repair (Halsey and Jones, 2015). This leads to size-related changes in physiology with smaller cells often exhibiting higher growth rates, high metabolic capacity and large complex antennae that allow increased electron transfer through the limited available pool of PSII. In contrast, larger cells reduce their electron transport through lower pigment concentrations and antennae-to-reaction centre ratios (Finkel *et al.* 2004, 2009; Key *et al.* 2010). This often gives smaller cells or phytoplankton species a competitive advantage over larger cells in high nutrient environments where light is not limiting; much like the conditions encountered during this study. In his review, Marañón (2014) questioned why blooms are therefore not dominated by small cells, concluding top-

down control through grazing pressure was the most accepted explanation. This study, provides a scenario that confirms this hypothesis, revealing pico and nanophytoplankton as the dominant size classes with the latter regularly accounting for >70% of the chlorophyll biomass thorough the bloom.

During the early stages of this cruise, when the water column was well-mixed, pico- and nano-plankton were highly abundant and the highest values of both F_v/F_m (0.52, units dimensionless) and σ_{PSII} (8.2, nm^2) were measured. These observations suggest that despite the potentially fluctuant light climate (caused by vertical mixing) and increasing susceptibility of phytoplankton to photoinhibition, the phytoplankton community did not incur photodamage severe enough to reduce photosynthetic efficiency. It was only during the final sampling event that the community's size structure began to change and the microphytoplankton fraction accounted for >25% throughout the water column, corresponding with significant changes in σ_{PSII}, E_k and ETR_{max}. One potential explanation for the sudden change in E_K and ETR_{max} is the nanoplankton present during previous sampling events achieved acclimated growth to nutrient starvation and the photosynthetic apparatus adjusted accordingly.

3.4.3. Environmental Drivers of Photophysiology

The influence of macronutrient (N, P) starvation on photosynthetic efficiency in natural populations has been shown, through laboratory-based findings, to often result in a decreased PSII functionality and reduction in F_v/F_m (Kolber et al. 1988; Geider et al. 1993; Suggett et al. 2006). However, these results are uncommon in open-ocean phytoplankton populations, with many studies showing that under steady-state, nutrient-limited conditions, phytoplankton growth and physiology do

not reflect macro-nutrient limitation (Parkhill et al. 2001; Behrenfeld et al. 2006; Moore et al. 2008).

During this study, N and P availability transitioned from a state of high to low concentration between the first and third sampling events (12 days), coinciding with a 5.5-fold increase in chlorophyll and a decrease in F_v/F_m from 0.5 to 0.35. Over the following three sampling events (15 days) the N:P ratio in the upper 20 m remained below 10, signifying nitrogen limitation (Leonardos and Geider, 2004), but the F_v/F_m remained constant, only changing significantly at depths greater than 20 m. The suppression of F_v/F_m at surface waters is unsurprising as irradiance is highest and light stress could result in the down-regulation of PSII or a reduction in functional PSII reaction centres (Milligan et al. 2012). However, the relative lack of difference between the F_v/F_m of the surface waters, compared with those at depth, also suggest that nutrient limitation was not at the stage where it was impairing photorepair processes.

3.4.4. Photophysiology and Bloom Dynamics

In the introduction of this chapter it was highlighted that increasing irradiance often corresponds with stratification and bloom initiation (Franks, 2015). During the presented study, an isothermal layer that extended to approximately 40 m, developed between the first and second sampling events and seemed to trigger the greatest burst of phytoplankton growth. However, data collected over the course of the cruise showed no signs of stratification, meaning bloom initiation occurred following the alleviation of growth-limiting light conditions or a significant reduction in convective mixing (i.e. the critical turbulence hypothesis; Hopkins et al. 2017). As nitrate levels

within the isothermal layer were already lower than those at greater depth and chlorophyll was higher in the upper 50 m, it suggests growth had already become relieved of light-limitation and reduced mixing was the trigger (Fig. 3.2). Despite this, the significant changes that occurred in the fluorescence measurements may provide some insight into the factors driving taxonomic succession through the bloom.

Variation in σ_{PSII} is commonly observed when sampling natural communities and there is increasing evidence that suggests this is a taxonomical controlled adaptive parameter, which results in both inter- and intra-specific variability across a range of taxa (Suggett *et al.* 2004; Moore *et al.* 2005; Suggett *et al.* 2009b). In this study, the significant temporal variance in σ_{PSII} (and not spatial variance in σ_{PSII}) often occurred following substantial community structure changes, suggesting σ_{PSII} variation was a better indicator of taxonomy than of light history/stress. The highest values of σ_{PSII} were recorded in the first three sampling events when coccolithophores, *Synechococcus spp.* and other pico-phytoplankton were in high abundance. Although σ_{PSII} values correlated highly with all three groups, regular changes in taxonomy over the cruise likely resulted in a reduction of model's explanatory power.

Photoacclimation has previously been shown to induce a trade-off between light absorption and photoprotection in the coccolithophore species, *Emiliania huxleyi,* grown in nutrient replete conditions. The early stages of this cruise could be a reflection of this process in a natural environment (McKew *et al.* 2013, 2015). The studies revealed how *E. huxleyi* increased levels of proteins associated with light harvesting to enhance growth under suboptimal (30 µmol photons m^{-2} s^{-1}) light climates whilst increasing photoprotective proteins under supraoptimal (1000 µmol photons m^{-2} s^{-1}) light. This proteomic plasticity was shown to result in no significant

difference between light-saturated gross photosynthesis rates and could explain why coccolithophores were eventually dominated by other nanophytoplankton, which acclimated to changing light and nutrient conditions and dominated for the rest of the cruise.

3.5. Conclusions

FRRf measurements of phytoplankton photophysiology, made during a phytoplankton spring bloom in the central Celtic Sea, revealed spatial and temporal variability in fluorescence signatures (F_v/F_m and σ_{PSII}). In addition to spatial and temporal variability in F_v/F_m, data analyses and/or modelling showed that light may also have played a critical role in depth driven changes. Increases in phytoplankton biomass may have started before the first sampling event but the period of highest growth rate was triggered by the development of an isothermal layer that reduced convective mixing and resulted in cell dilution at the sea surface layer. Although the changes in F_v/F_m and σ_{PSII} were not influenced by environmental drivers or responsible for the initiation of the bloom, they do shed light on the potential dynamics that controlled the succession of taxa that dominated the upper 30 m.

Chapter 4 : Assessing Phytoplankton Distribution Using *in situ* Fluorescence and Satellite Ocean Colour

4.1. Introduction

Remote sensing offers the only approach to quantifying global primary production in response to climate change (Behrenfeld *et al.* 2005). However, the satellite-based determination of phytoplankton physiology has proven elusive, with satellite-derived estimates of primary production still reliant on empirical models to reflect physiological variability (Behrenfeld & Falkowski, 1997; Campbell *et al*. 2002). Consequently, the environmental controls on physiology have been studied extensively by the oceanography community and this thesis (Chapter 2; Chapter 3) to better inform these empirical models. However, in addition to physiology parameters, the measurement of biomass is also crucial in global productivity models and is reliant on satellite-derived data of ocean colour (Chapter 1).

Using further empirical approaches, ocean colour estimates are used to derive chlorophyll, which in turn provides the biomass component of satellite productivity estimates (Platt *et al.* 1988; Sathyendranath *et al.* 2017). Ocean colour data are therefore a key parameter in some productivity algorithms, but reliable estimates are difficult to obtain in coastal regions where optical properties are difficult to determine and hydrography is highly variable (Tilstone *et al.* 2005; Bracher *et al.* 2017). To assess the accuracy of ocean colour data in these regions, high resolution *in situ* datasets are required.

The use of *in vivo* fluorescence techniques allows oceanographers to measure the productivity and distribution of marine phytoplankton, frequently in time and space, leading to the regular incorporation of fluorometers into ecological monitoring systems (Falkowski & Kiefer 1985; Behrenfeld et al. 2009; Sauzède et al. 2015). The

relative ease and cost-effectiveness of *in vivo* fluorescence techniques has led to the assembly of global fluorescence databases. High-resolution fluorescence measurements have already started to alter our understanding of how photoacclimation and adaptation drive changes in primary productivity (Moore *et al.* 2003, 2006), but could also provide valuable comparative datasets for the ground truthing of remotely sensed data products (Huot et al. 2013; Browning et al. 2014; O'Malley et al. 2014).

The objectives of this study were (i) to quantify the extent of variability in phytoplankton distribution and concentration using chlorophyll fluorescence *in situ* and remote sensing data products (ii) compare the extent of variability detected by the two methods and (iii) compare the accuracy of both methods to each other and with measurements of extracted estimates of chlorophyll concentration.

4.2. Methods

4.2.1. Cruise Information and Hydrography

Data were collected on board the *RRS* Discovery during a research cruise (DY029) to the Celtic Sea between the 1st and 31st of April 2015 (Fig. 4.1). Two transects were sampled, the first between the CS2 and the CCS sites (O-transect) and the second between the Celtic Deep and the CCS (J-transect). The vessel's underway water supply was sampled continuously to provide measurements of salinity (S), temperature (T), chlorophyll fluorescence and incident photosynthetically active radiation (iPAR) for water in the surface mixed layer for the duration of the cruise (Table 4.1). Underway fluorescence data were collected using a WETStar WS3S fluorometer (Wet Labs Inc., USA) calibrated to the original manufacturing settings. Data output was in volts with

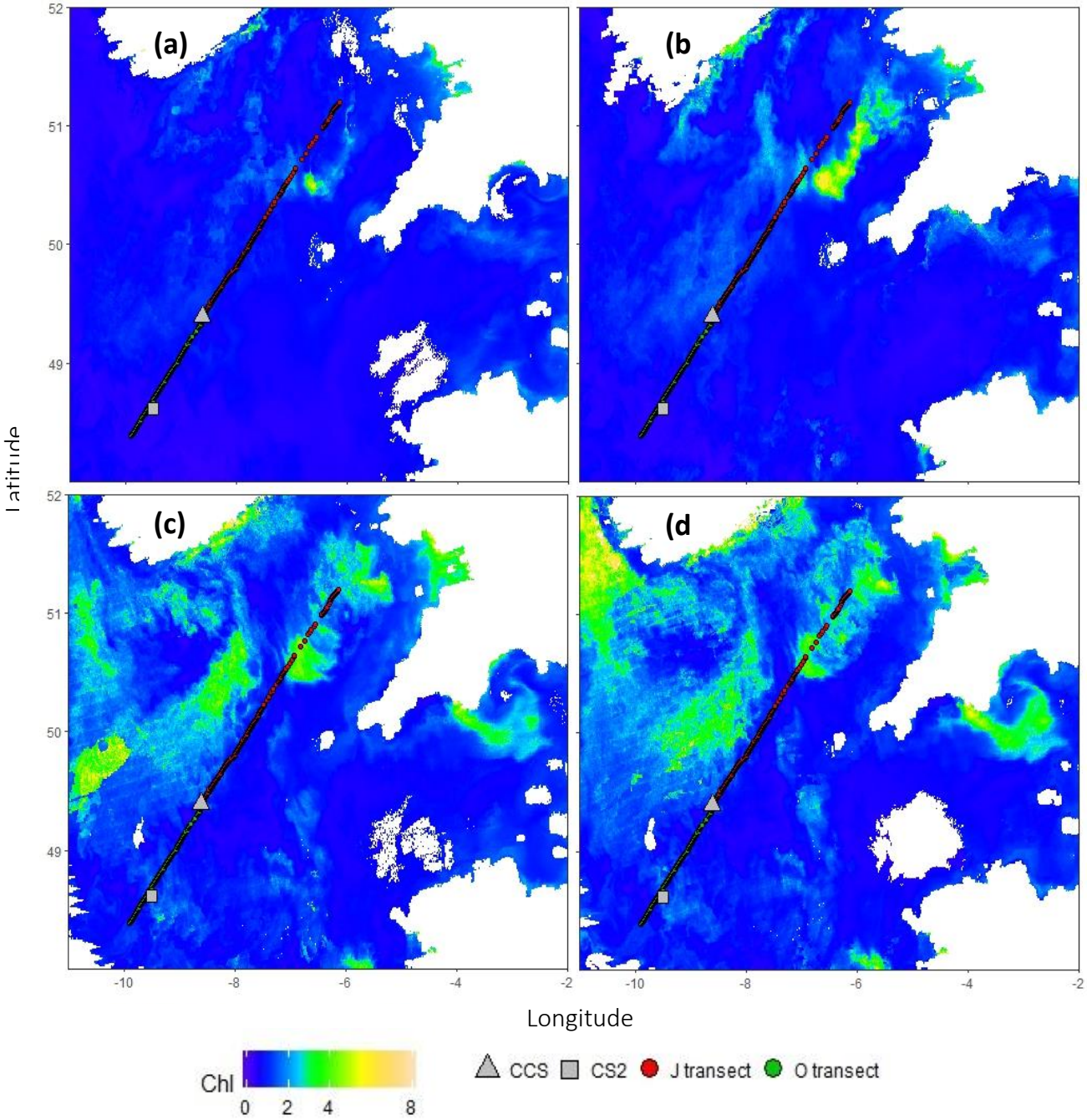

Figure 4.1. Satellite estimates of chlorophyll across the Celtic Sea with transect routes and process station locations. Background images are 7-day ocean colour estimates of chlorophyll (units in mg/m^3) formed of data collected between (**a**) the 1st and 8th of April (ST) (**b**) the 8th and 14th (**c**) 15th and the 21st and **(d)** the 21st and 27th. Each transect is plotted during the week of collection. The central Celtic Sea (CCS) and shelf break (CS2) stations are also shown.

the coefficients applied post-cruise. Scaling of underway chlorophyll fluorescence measurements was therefore necessary to account for the potential bias in factory-calibration of the fluorometer (Roesler *et al.* 2017).

Table 4.1. Data and statistics for the J and O transects carried out during the cruise. r represents the linear correlation coefficient between estimates of chlorophyll derived from ocean colour (OC) and in situ fluorescence approaches. Δ Chl represents the range of in situ and Δ OC Chl the ocean colour chlorophyll measurements recorded across the transect. All chlorophyll values are recorded in units of mg/m^3, means are presented ± 1 SD. Mean iPAR is the average incident irradiance measured over the course of the transect using the on-board PAR sensor, units are µmol photons m^{-2} s^{-1}.

Name	n	*r* (Chl:OC)	Mean OC Chl	Δ OC Chl	Mean Chl	Δ Chl	Mean iPAR
J 1	690	-0.07	1.16 (± 0.52)	2.45	5.29 (± 3.78)	18.24	247
J 2	931	0.68	1.56 (± 0.90)	3.72	2.79 (± 1.14)	5.78	689
J 3	847	-0.03	1.60 (± 0.96)	4.07	3.06 (± 1.02)	4.72	515
O 1	465	0.87	0.56 (± 0.21)	0.72	1.05 (± 0.42)	1.55	821
O 2	363	0.85	0.67 (± 0.24)	0.89	2.96 (± 1.24)	4.39	277
O 3	420	0.06	0.97 (± 0.22)	0.84	4.02 (± 1.63)	8.28	216
O 4	391	0.7	1.02 (± 0.42)	1.78	3.57 (± 2.22)	8.39	224
O 5	231	0.61	1.07 (± 0.38)	1.72	3.20 (± 1.14)	4.43	40
O 6	334	0.23	0.87 (± 0.25)	1.14	2.15 (± 0.91)	2.98	69

4.2.2. Fast Repetition Rate fluorometry

A multi-spectral FastOcean™ Fast Repetition Rate fluorometer (FRRf, Chelsea Technologies Group – CTG – Ltd.; West Mosley U.K.) fitted with an integrated FastAct unit (CTG Ltd.) was employed to measure phytoplankton fluorescence parameters for semi-continuous seawater samples drawn from the ship's non-toxic underway system. Single turnover acquisitions were made using a protocol of 32-50 sequences of 100 1.1-2 µs saturation flashes at 2.8 µs intervals followed by 40 µs relaxation flashes at 50 µs intervals. Data were processed using software provided by the instrument manufacturer (FASTpro8 V1.0.5, CTG Ltd.) with minimum fluorescence (F_o), maximum fluorescence (F_m) and the functional absorption cross section of Photosystem II (σ_{PSII}) obtained by fitting the data to the KPF model (Kolber *et al.* 1998). F_v/F_m was calculated as $(F_m-F_o)/F_m$. Non-linearity in instrument settings (gain and LED

intensity) was corrected for using updated software (FASTpro8 V1.0.5, CTG Ltd.). Non-photochemical quenching (NPQ) was calculated within the software as the normalised Sterm-Volmer coefficient (Eqn. 3.3).

4.2.3. Fluorometric Chlorophyll Measurements

Water samples (0.2-0.25 L) for chlorophyll extraction were filtered onto 25mm Whatman glass fibre filters (effective pore sizes 0.7 µm) and extracted in 6-10 mL 90% acetone (HPLC grade, Sigma-Aldrich, UK) at 4 ^{o}C for 18-24 h. Fluorescence was measured on a Turner Designs Trilogy fluorometer using a non-acidification module and calibrated with a solid standard and a pure chlorophyll *a* standard (Sigma-Aldrich, UK).

4.2.4. Ocean Colour

Visible Infrared Imaging Radiometer Suite (VIIRS) OC5 chlorophyll data were acquired from the NERC Earth Observation Data Acquisition and Analysis Service (NEODAAS) at daily, 3-day and 7-day resolution. The level 3 data (1.1 km reference resolution) were processed by NEODAAS from NASA OBPG L2 data using SeaDAS version 7.2. Poor quality data pixels were masked out during processing. Ocean colour data were obtained as NetCDF files and extracted and processed using the ncdf4 package in Rstudio (Pierce, 2017). Ocean colour data was strongly affected by high levels of cloud cover during the cruise period. Very few of the daily images of the study region were viable with > 70% of values undetectable due to cloud cover. Half of the 3-day composites contained viable data for most of the study region, but were still heavily influenced by cloud. Due to poor quality data in 1-day and 3-day composites, 7-day

estimates of ocean colour chlorophyll were used for the comparison with *in situ* measurements. The latitude and longitude of *in situ* and ocean colour chlorophyll measurements were truncated to two decimal places (1.1 km^2 precision) to allow for pixel match-up.

4.2.5. Statistical Analyses

Underway data from the full cruise was plotted versus distance and split by day to reveal linear transects for the analysis of spatial and temporal variation in chlorophyll estimates (Fig. 4.1). The most southerly coordinates of each transect were selected and used to calculate the distance for each measurement made along the transect using the Haversine formula and the geosphere package in R (Hijmans *et al.* 2016). The distance between each underway measurement, hereafter referred to as lag distance (*h*), was then calculated from data collected whilst the ship was in transit and identified as ~150 m. Measurements made at process stations were identified by an $h < 120$ m and removed from the transect datasets.

Three long (240-260 km) J-transects and six short (100-140 km) O-transects were identified and individually analysed using a semivariogram approach to examine the extent of spatial variability in chlorophyll concentration (Journel and Huijbregts, 1978). This approach allowed the investigation into whether the similarity between the chlorophyll measurements made along each transect was greater between densely spaced points compared to those that were more distant from each other, thereby providing insight into the extent of the heterogeneity encountered and how much was captured using the continuous sampling approach. All semivariogram analyses were conducted using the 'gstat' package in R (Pebesma and Graeler, 2017).

For the *in situ* analyses, 3 km distance bins were used when calculating the semivariogram, which resulted in 18 data pairs per bin. A spherical model was then fitted to the semivariogram data to provide the nugget, sill and autocorrelation range values (Fig. 4.2).

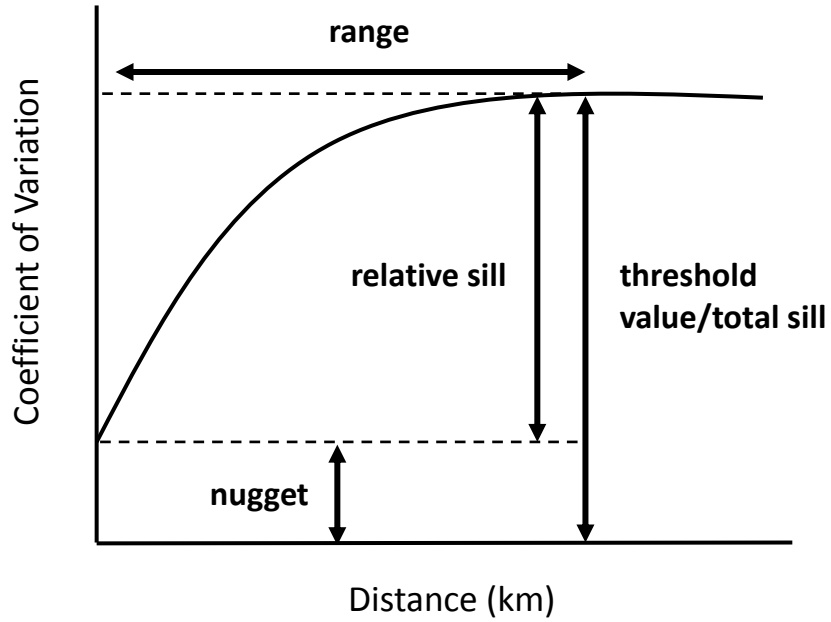

Figure 4.2. An example spherical semivariogram model fit showing the range, nugget and the total and relative sill.

The nugget effect of the model can be interpreted as measurement error or non-recorded microscale variability in the data. The total sill (or threshold value) is the maximum value of the semivariogram and indicates the point at which the measured values become spatially independent of each other. The range is defined as the distance (*h*) at which the total sill is reached (Lausch *et al*. 2013). The same approach to semivariogram analysis was used for ocean colour data. These data were binned with 30 pairs per bin at an *h* of ~9 km. All semivariograms were carried out over a *distance of reliability*, calculated as a third of the total transect distance.

The extent of temporal variance on chlorophyll estimations was explored using a time-series dataset collected at the Central Celtic Sea station, which consisted of

five visits of one or two full days (full diel cycle). To minimise the spatial influence on the time-series measurements, the most visited coordinates were selected for each day. The distance for each measurement from these coordinates was then calculated and all values > 5 km were removed. Data were then averaged by hour before analysis.

4.3. Results

4.3.1. Underway Chlorophyll Fluorescence Calibration

Previous studies that have utilised underway fluorescence data removed measurements made during periods of high light intensity, due to the influence of non-photochemical quenching (Roesler *et al.* 2017). In this study, no data were removed but chlorophyll in acetone extracts were compared with underway fluorescence data that had been scaled and corrected using a light correction

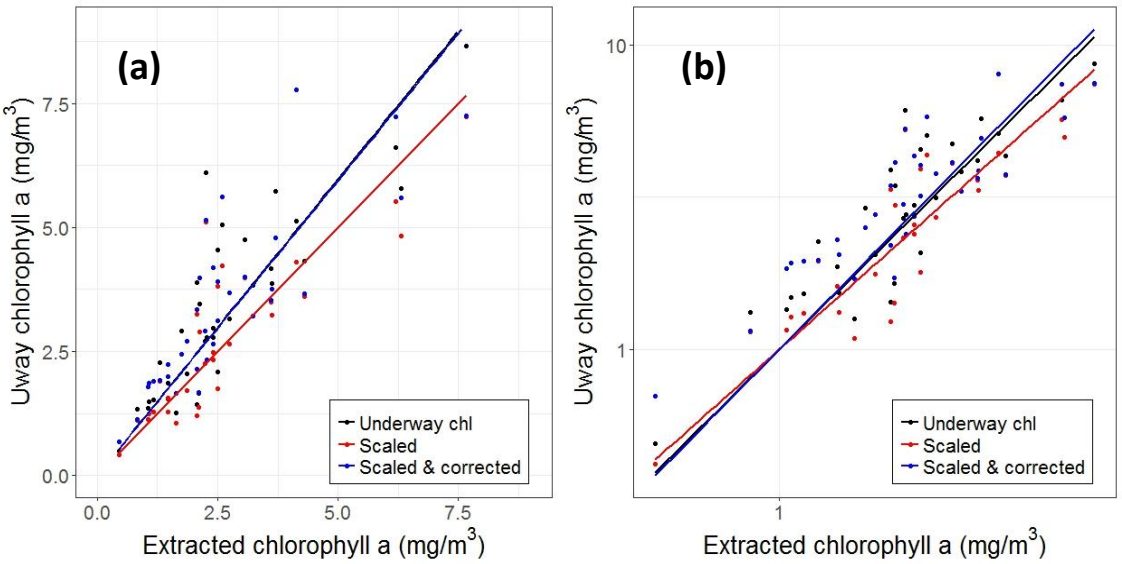

Figure 4.3. Regression between fluorescence-based chlorophyll estimates from underway (Uway) water samples paired with extracted chlorophyll estimates made using a Turner fluorometer on **(a)** a linear scale. Underway: slope = 1.20, r^2 = 0.93, scaled: slope = 1, r^2 = 0.93, scaled and corrected: slope = 1.19, r^2 = 0.92 and **(b)** a log-log scale. Underway: slope = 1.16, r^2 = 0.92, scaled: slope = 1.04, r^2 = 0.92, scaled and corrected: slope = 1.19, r^2 = 0.91 Regression was not forced through the origin.

parameter (Appendix). The results showed that the light-correction did not greatly increase the accuracy of fluorescence-based estimates, so underway measurements of chlorophyll discussed throughout this chapter were scaled but not corrected (Fig. 4.2).

Ocean colour versus in situ

Satellite chlorophyll estimations showed varying degrees of agreement with scaled *in situ* measurements, but were found to consistently underestimate the chlorophyll concentration by up to 4-fold (Fig. 4.4).

In situ data from the long transects (LT), largely collected in coastal and central locations, generally showed poor match-ups with the ocean colour estimates (r^2 =

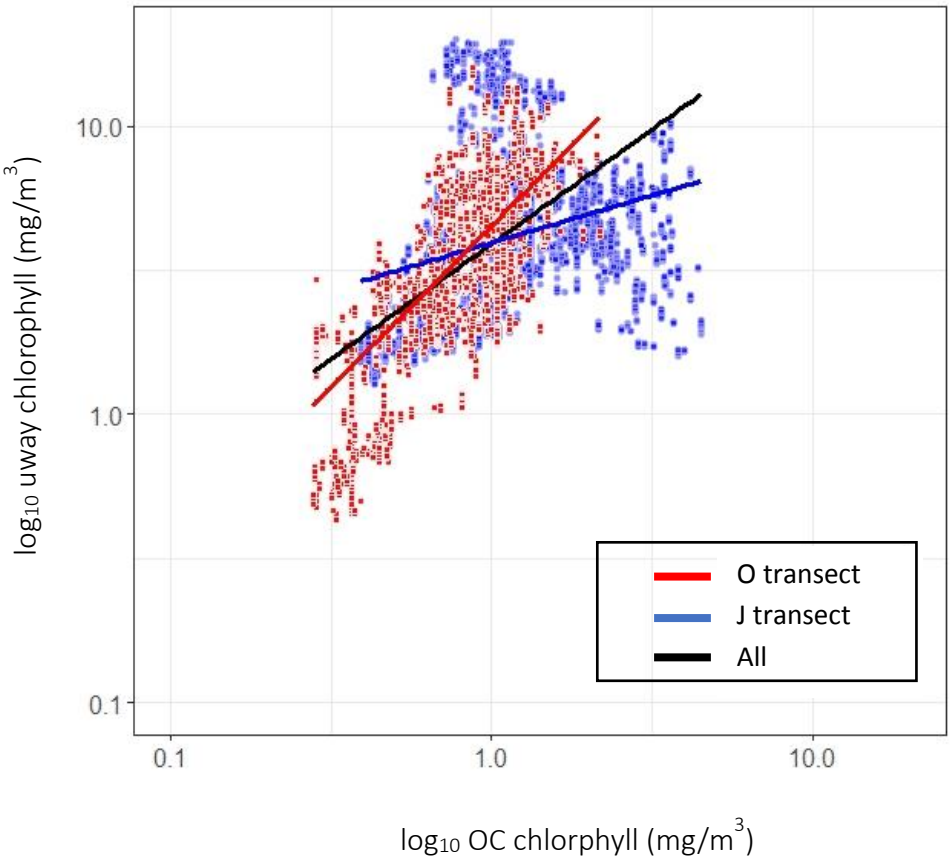

Figure 4.4. Ocean colour (OC) versus in situ fluorescence estimates of chlorophyll made during the nine transects. J transects: slope = 0.32, r^2 = 0.10, O transects: slope = 1.12, r^2 = 0.65, All: slope = 0.80, r^2 = 0.46

0.10). The shelf edge data collected during the short transects (ST) showing greater agreement (r^2 = 0.65). The strongest correlation was observed between the measurements of first short transect when the shelf-wide chl concentration was at its lowest. However, there were strong correlations between ocean colour and *in situ* measurements during periods of increased biomass (J2, O4) suggesting poor relationships were not driven by issues of saturation in the ocean colour data.

4.3.2. Spatial Variance in Chlorophyll Concentration During a spring phytoplankton bloom

Both *in situ* and ocean colour chlorophyll data indicate a large phytoplankton bloom initiated in the north-east (NE) region of the Celtic Sea during the first week, before spreading south-west (SW) towards the shelf break over the four weeks of the cruise (Fig. 4.1). The bloom was patchy and fluctuated in magnitude with mesoscale (10-200 km) features apparent in both concentration and distribution of chlorophyll measured *in situ* and via satellite. The long transects (LT) covered 240 km in a north-east to south-west direction, ranging from the shallow (~40 m depth) coastal region in the NE to the process station in the central Celtic Sea (CCS) region, which was slightly deeper (~150 m depth). Due to time constraints, the pre-bloom conditions along the length of the subsequent long transects were not captured *in situ*, but substantial differences in the chlorophyll concentration between the first and final transects indicate *in situ* sampling captured the bloom as it changed in magnitude across the central and northern regions of the shelf (Table 4.2).

The mean (5.8 ± 4.24, mean ± SD, units mg/m^3) and range (17.15 mg/m^3) in chlorophyll values recorded during LT1 were the highest recorded during any of the transects and ~2.5-fold higher than LT3, which took place nearly two weeks later;

indicating the bloom was most prevalent in the NE during the second week. A similar trend in bloom dynamics was shown in the six ST which took place over 18 days and covered the shelf-edge where phytoplankton growth and biomass was not as extensive as observed in the central and NE regions (Fig. 4.1). However, the increased frequency allowed the ST series to capture bloom conditions before, during and after a peak of the bloom in the shelf-edge region.

The mean and range of the chlorophyll values for ST1 were the lowest recorded during any transect and reflect the low concentrations detected across the entire shelf in the first week (Fig.4.1, Table 4.1). By the third week of the cruise the mean and range of the transects had increased by ~3.5-fold reflecting the shelf wide increase in biomass, spreading from the shallow regions out towards the shelf edge as the bloom developed. However, the *in situ* data indicated the bloom peaked in magnitude during the second week of the cruise (LT1), before declining over the course of the month (LT2 and LT3) was not supported by the ocean colour data which show the bloom continued to progress over the course of the month with the highest ocean colour transect mean recorded in the final week.

Semivariograms

The relative sill values of the LT semivariograms were consistent (0.40 – 0.46), indicating the magnitude of variance changed very little over the month of sampling (Fig. 4.4; Table 4.2). The autocorrelation distance (distance the sill was reached) varied more, nearly 2-fold, with the largest difference between LT2 and LT3. This was unusual due to the proximity in time (1 day apart) between the two transects and

provides some insight into the temporal fluctuations of the chlorophyll distribution over a very short time-frame.

Table 4.2. Semivariogram parameters with the physical and biological properties of the nine transects. The sill, nugget and range (km) are coefficients taken from spherical models fitted to semi variograms. Δ Chl and Δ Temp represent the range of temperature and chlorophyll measurements recorded during the transect. All chlorophyll values are recorded in units of mg/m^3. All temperature values are ^{o}C. Means are presented ± 1 SD

Name	Date	Sill	Range	Nugget	Dist (km)	Chl	Δ Chl	Temp	Δ Temp
LT 1	14/04/15	0.040	46	0.0008	244	5.8 (±4.24)	17.75	10.11 (±0.37)	1.56
LT 2	26/04/15	0.046	57	0	266	2.85 (±1.33)	5.62	10.88 (±0.46)	1.61
LT 3	27/04/15	0.042	32	0	266	2.59 (±1.02)	4.85	10.55 (±0.18)	0.91
ST 1	06/04/15	0.015	51	0	150	1.04 (±0.61)	2.17	10.85 (±0.62)	1.58
ST 2	10/04/15	0.010	23	0	114	2.44 (±1.40)	4.01	11.02 (±0.33)	1.05
ST 3	17/04/15	0.036	25	0	132	3.58 (±1.12)	8.25	11.81 (±0.35)	1.61
ST 4	19/04/15	0.095	40	0	123	2.16 (±1.49)	8.22	11.69 (±0.33)	1.37
ST 5	22/04/15	0.032	22	0	99	1.83 (±0.94)	4.73	12.35 (±0.56)	1.91
ST 6	24/04/15	0.034	24	0	115	2.55 (±0.92)	3.94	11.88 (±0.32)	1.86
OC 1	1-8/04/17	0.026	75	0.001	450	0.76 (±0.43)	5.54	NA	NA
OC 2	8-14/04-15	0.044	62	0	450	1.11 (±0.89)	6.88	NA	NA
OC 3	15-21/04/15	0.048	68	0.002	450	1.31 (±0.87)	5.27	NA	NA
OC 4	27-27/04/15	0.052	80	0.004	450	1.33 (±0.89)	5.5	NA	NA

LT1 was the only *in situ* semivariogram to produce a nugget effect which was low, relative to the sill value, but does indicate that some variance may have gone undetected due to measurement error or a lack of resolution. The sill values of the ST series showed much greater change with a 2-fold increase in the observed variance between the first and last transect and a large amount of fluctuation in-between. The autocorrelation also fluctuated extensively over the course of the series, but decreased 2-fold between the first and last transect. Despite the high levels of variance observed, no nugget effect was found in the ST semivariogram analyses.

The 7-day ocean colour data for the region of the cruise transect conformed with the *in situ* observations across the shelf, showing a phytoplankton bloom that

progressed in magnitude over the course of the cruise. The mean chlorophyll concentration increased over the course of the month, however, the range stayed relatively consistent – peaking during the second week. The relative sill of the ocean colour semivariograms also increased over the course of the month and nugget effects were observed in all but one (week 2) of the semivariogram analyses. The autocorrelation range decreased between the first and third week before increasing again in the fourth.

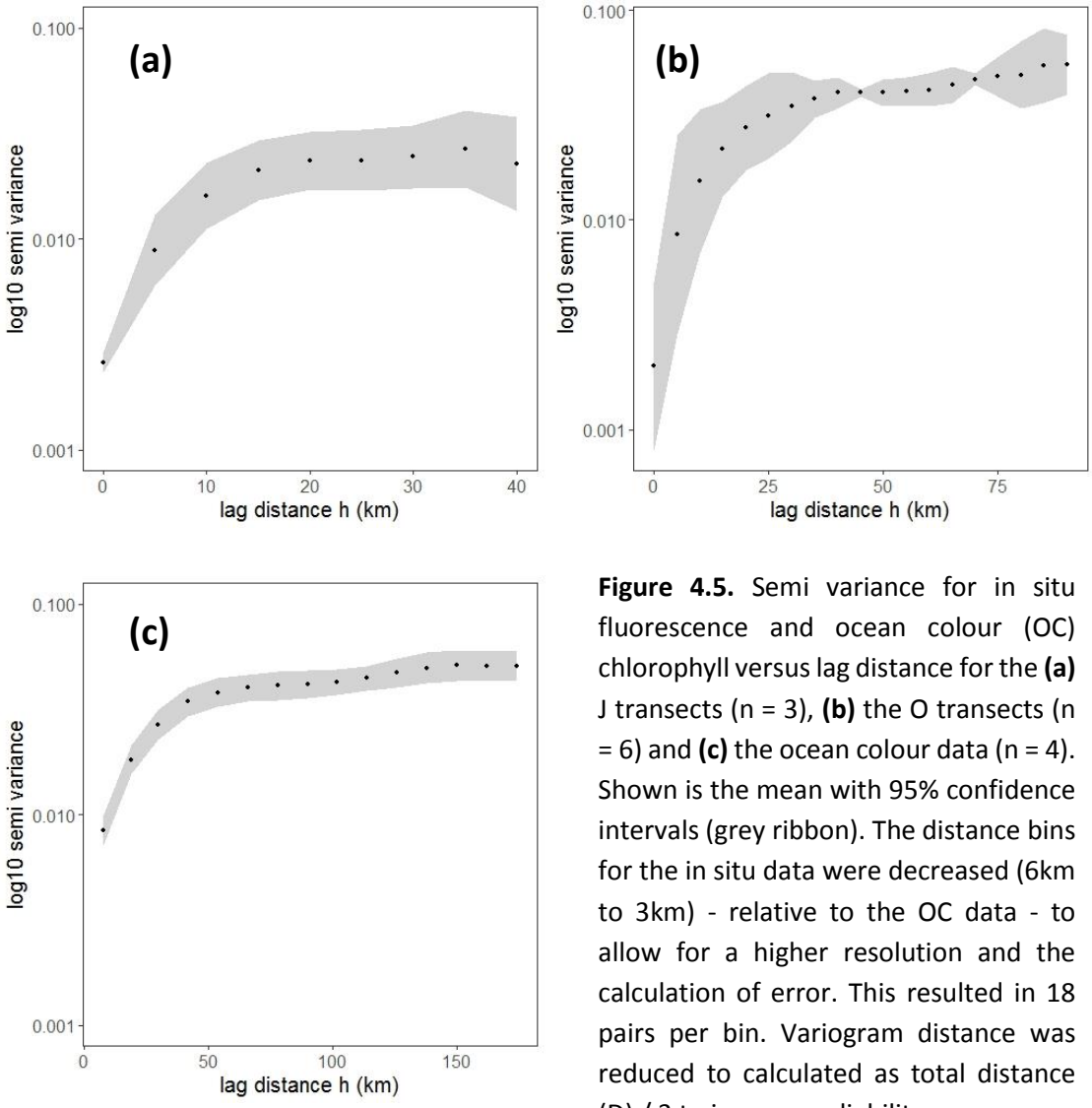

Figure 4.5. Semi variance for in situ fluorescence and ocean colour (OC) chlorophyll versus lag distance for the **(a)** J transects (n = 3), **(b)** the O transects (n = 6) and **(c)** the ocean colour data (n = 4). Shown is the mean with 95% confidence intervals (grey ribbon). The distance bins for the in situ data were decreased (6km to 3km) - relative to the OC data - to allow for a higher resolution and the calculation of error. This resulted in 18 pairs per bin. Variogram distance was reduced to calculated as total distance (D) / 3 to increase reliability.

Error in the semivariogram analyses showed an inverse trend between the short and long transects. The variability at *h0* of the ST analysis showed incredibly low error, which increased with distance. In contrast, the variance at *h0* for the LT was high and declined once the autocorrelation distance had plateaued. The ocean colour semivariogram analysis showed relatively little error at any distance. Due to the linear nature of all the transects almost no directional anisotropy was found in any of the semivariogram analyses.

4.3.3. Temporal Variance in Chlorophyll Concentration

The transects provided some insight into the temporal variance in chlorophyll as the bloom developed but greater understanding is offered by the time series measurements at the CCS process station. CCS was visited on five occasions which coincided with the initiation, peak and decline of the bloom. A 2.5-fold increase in chlorophyll occurred between the start of the cruise and the peak of the bloom on yearday (Yday) 105 in the second week. Following this peak, the chlorophyll concentration was substantially lower at the following sampling event, before returning to concentrations close to those seen during the peak of the bloom (Fig. 4.5, Table 4.3). The extent of diurnal variability ranged over the course of the time series and did not seem to be driven entirely by changes in fluorescence linked to photophysiology (e.g. midday nonphotochemical quenching).

Table 4.3. Variability of chlorophyll and temperature at the central Celtic Sea (CCS) station measured over the course of the time series. Δ Chl and Δ Temp represent the range of temperature and chlorophyll measurements recorded during the transect using the underway system. All chlorophyll values are recorded in units of mg/m^3. All temperature values are ^{o}C. Means are presented ± 1 SD

Station	Yday	Date	Distance (km)	Chl	Δ Chl	Temp	Δ Temp
CCS	94	04/04/2015	2	1.69 (± 0.30)	1.43	9.94 (± 0.05)	0.22
CCS	95	05/04/2015	4	1.62 (± 0.47)	1.75	10.00 (± 0.06)	0.29
CCS	101	11/04/2015	3	2.64 (± 0.57)	2.94	10.33 (± 0.07)	0.47
CCS	105	15/04/2015	5	4.67 (± 1.30)	5.10	10.72 (± 0.10)	0.64
CCS	110	20/04/2015	5	2.21 (± 1.13)	5.21	10.79 (± 0.12)	0.42
CCS	115	25/04/2015	5	4.08 (± 0.87)	4.60	11.39 (± 0.28)	1.95

During the first two days of sampling it was evident that non-photochemical quenching (NPQ) was suppressing the underway chlorophyll values around midday, when NPQ was highest (Fig. 4c & 4d). Following the midday suppression, a gradual reduction in the effects of NPQ led to the inferred chlorophyll concentration increasing, before stabilising over the rest of the day. The following four sampling events reveal a substantial amount of fluctuation in chlorophyll throughout the day which coincided with increased variance in temperature. During this time, there was no consistent relationship between chlorophyll concentration (as estimated from fluorescence) and NPQ during two sampling events (Yday 106 and 115), possibly indicating changing water bodies were the driving factor behind the variability rather than photophysiology.

Mean daily temperature at CCS increased by ~1.5 ^{o}C over the course of the time series and varied diurnally. Like the chlorophyll concentration, the diurnal range during the first three sampling events was minimal with some fluctuation around midday. The fourth sampling event showed a steady decrease of 0.5 ^{o}C over the

course of the day, with the fifth showing the opposite trend. The final sampling event showed the highest amount of fluctuation and a much greater range in values (1.95

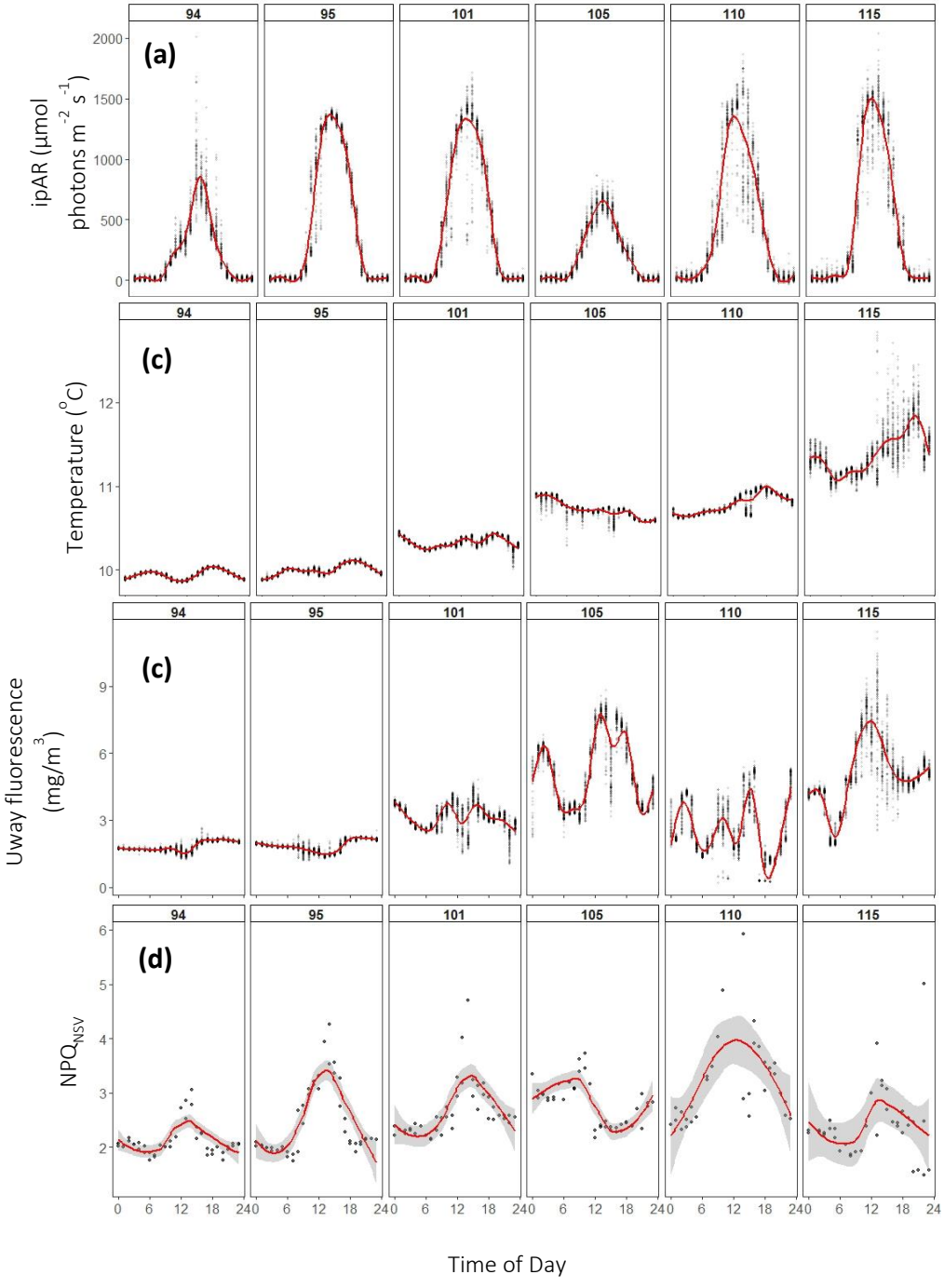

Figure 4.6. Diurnal changes **(a)** incident irradiance (iPAR), **(b)** underway temperature, **(c)** underway (Uway) fluorescence and **(d)** NPQ_{NSV} via FRRf at CCS during six sampling events. Number at the top of each panel indicates the yearday (Yday). The line is a local regression (LOESS) through the mean. The shaded area represents the smoothed 95 % confidence interval

^{o}C, Table 4.3) supporting the possibility of changing water bodies or a breakdown in the stratification.

4.4. Discussion

4.4.1. The Current and Potential Use of Chlorophyll Fluorescence

The results of this study provide insight into the advantages and limitations of the two principal approaches to measuring the biomass of phytoplankton in the marine environment: *in situ* bio-optical instrumentation and remote sensing. The deployment of chlorophyll fluorometers on ships or autonomous platforms provides oceanographers with the largest *in situ* global dataset for estimates of chlorophyll, but exploiting this data to understand the distribution and variability of phytoplankton is a difficult task, with many sources of uncertainty to address (Lin *et al.* 2016; Roesler *et al.* 2017). The first of these owes to the fact that chlorophyll fluorescence is not a direct estimate of chlorophyll concentration and is influenced by factors such as the status of phytoplankton growth and physiology, the light and nutrient climate and the optical properties of the water (Cullen and Davis, 2003; Behrenfeld *et al.* 2005; Xing *et al.* 2012).

In this study, data from the underway fluorometer and chlorophyll-in-acetone measurements revealed strong correlation between *in situ* fluorescence and extracted chlorophyll, with the fluorometer slightly overestimating the total concentration. These results conform with those found by Roesler *et al*. (2017), who conducted a comprehensive assessment of *in situ* fluorometry. It also offers insight into the accuracy of *in situ* fluorescence in a temperate shelf sea, a region not included in their analysis.

The influence of NPQ on *in situ* fluorescence measurements was also discussed by Roesler *et al*. (2017) who removed all observations subject to NPQ. That step was not taken in this study, to allow more complete assessment between the agreement of *in situ* fluorescence and remotely sensed chlorophyll estimates. As ocean colour measurements are made at midday, the period of most intense iPAR and NPQ, it was decided the *in situ* fluorescence measurements from this time should be included in the analysis. However, an exponential light correction (Appendix) of this thesis was applied to the data to explore the influence of quenching on *in situ* fluorescence. The increased slope of the corrected fluorescence values confirmed that NPQ led to a 20% underestimation, but increased the amount of scatter compared to uncorrected measurements. Despite this, the time series results of continuous measurements made on station at the CCS station reveal that the diurnal change in chlorophyll measurements driven by NPQ were minimal and indicated that a change in water-mass caused far greater fluctuations in the fluorescence measurements, with a 4-fold range observed on some days. This small scale spatial variability is not problematic for satellite observations that provide a mean value for relatively large areas at one point in time, but should be considered during *in situ* sampling campaigns in dynamic regions and highlights the importance of collecting continuous measurements of temperature alongside chlorophyll fluorescence. The diel variability in chlorophyll observed in this study indicates the extent of spatial/temporal variance that satellites cannot detect.

4.4.2. Observed Variance in Chlorophyll Concentration Measured in situ and Using Ocean Colour

The overarching aim of this study was to quantify the extent that phytoplankton biomass varied, using two different measurement techniques. The results offer insight into how they could be combined to provide more reliable and accurate estimates of chlorophyll concentration. Here the analysis of high resolution *in situ* fluorescence measurements shows increasing heterogeneity in the distribution and concentration of chlorophyll, as the magnitude of the bloom increased, resulting in high variance (relative sill) and a decrease in the autocorrelation distance (range). The same general trends were picked up by remote sensing, but high nugget effects reveal the increased likelihood that small scale variance was not detected by this approach.

High levels of heterogeneity in chlorophyll concentration are not uncommon, due to the influence of horizontal and vertical mixing on the biomass, physiology and growth of phytoplankton communities (Denman and Gargett, 1983; Sharples *et al.* 2001, 2007). This variability has been well documented since the 1970's, when some of the first *in situ* fluorescence studies attempted to quantify spatial variance using optical approaches much like those used in this study. Platt & Denman (1975) showed significant changes occurred between 1 – 100 m and these correlated strongly with changes in temperature. It is in the identification of this small-scale variability in chlorophyll and water masses that *in situ* sampling is in valuable and provides the most values to remote sensing.

In coastal areas in particular, hydrography is highly dynamic, with alterations to the physical structure influenced by salinity, temperature and the tide (Pingree *et al.* 2009; Williams *et al.* 2013). These factors combined with the potential for high

turbidity make estimating chlorophyll from space a very difficult process that relies heavily on direct measurements and highly developed bio-optical models (McClain, 2009). This is potentially problematic, due to the high levels of productivity in these regions, particularly during the seasonal phytoplankton blooms (Autumn and Spring), when high phytoplankton growth results in a huge amount of carbon sequestration and export. This study has shown that although remote sensing has the ability to capture shelf wide trends in phytoplankton distribution, it may sometimes underestimate the biomass and extent of the variability, constrained by resolution and the detail lost within each pixel and over time due to averaging.

4.5. Conclusions

Fluorescence provides a robust method for collecting chlorophyll estimates at a high temporal resolution, but an increase in the number of ships and platforms is necessary before the scientific community can take full advantage of their potential. Even in the event fluorometers are fitted to both commercial and research vessels with the intention of feeding into a global database, the spatial coverage will largely be concentrated in areas ecologically important regions around the coast

There are many obstacles that must be overcome to allow the formation of a global database of chlorophyll concentrations. One of the major benefits of fluorometers is the ease at which they can be employed and automated. As relatively simple instruments that require very little maintenance (relative to flow cytometers for example) they can be set up and monitored remotely with the data extracted digitally or manually when the ship returns. Maintenance and calibration of the fluorometers are other factors for consideration. Cleaning can be achieved through a

simple acid wash through the ships underway system or manually whilst calibration could follow the methods outlined in Roesler *et al*. (2017). Most research ships are setup with continuous data collection for temperature, fluorescence and other parameters such as turbidity – that are instantaneously logged along with the location, time and date. This makes data processing relatively simple and only requires the screening of data to flag and/or remove anomalous values. Some correction of the data may be required (Appendix) or removal of data collected at high light intensity. The analysis of and interpretation of the data will likely change according to the party of interest. Those with a potentially vested interest include the remote sensing community (for validation) and environmental institutes or governmental departments (for monitoring purposes). There are already many programs in place that utilise this approach for fixed platforms (e.g. CEFAS smart buoy), but the community is yet to exploit the full potential of ship-based measurements.

Chapter 5 : Synthesis and Conclusions

The broad objective of this thesis was to provide further understanding of the environmental factors that regulate phytoplankton stocks and rates, with particular focus on temperate shelf seas (Chapter 1). These regions are vulnerable to anthropogenic influence (e.g. eutrophication) and climate change (Gröger *et al.* 2013; Morris *et al.* 2014; Burson *et al.* 2016). Consequently, they are the subject of interest to environmental agencies, who require estimates of phytoplankton biomass and productivity to assess fisheries and regional carbon budgets (Thomas *et al.* 2005; Emeis *et al.* 2015).

To address some of the gaps in our understanding of productivity in the shelf seas three cruises took place, during which, I conducted a series of experiments and collected over 3500 FRRf P vs. E curves and over 120 000 individual measurements of environmental parameters (e.g. temperature, chlorophyll and light). This rich dataset has allowed me to answer questions about the variability of primary producers and the factors that affect their photophysiology. It also shed light on the potential promises and challenges of using fluorescence-based measurements of biomass and productivity, particularly when compared to satellite-based measurements. This dataset also holds promise to eventually contribute to the answer of novel questions raised in this thesis and beyond.

To understand the scale of variability in nutrient concentration and its effect on photophysiology, I first tested the influence of nutrient addition on phytoplankton photophysiology and growth using bioassay experiments (Chapter 2). My study took place in the thermally stratified North Sea, where geographically distinct regimes of nutrient availability were identified, giving rise to taxonomically diverse communities. The response to nutrient addition was found to vary between the experiments,

indicating the combination of initial community composition and nutrient availability influenced the capacity for photosynthesis and growth, following the alleviation of nutrient limitation. These findings suggest that biogeochemical models must account for small scale variation in nutrient availability and community composition to adequately represent nutrient limitation of phytoplankton primary productivity and its response to eutrophication and other environmental change.

To test these experimental findings of variation in photophysiology across a broader range of natural conditions, I then employed a surveying approach to obtain high-resolution measurements of phytoplankton physiology during a spring bloom in the Celtic Sea (Chapter 3). Simple modelling approaches were employed to quantify the extent environmental parameters could account for changes in FRRf-derived measurements of phytoplankton photophysiology (F_v/F_m and σ_{PSII}) and productivity (α, E_K and ETR_{max}). This provided insight into the factors that drive both spatial (depth) and temporal (monthly) variance in P vs. E. The changes in photosystem II (PSII) characteristics (F_v/F_m and σ_{PSII}) during the bloom did not match with the substantial decrease in nutrient (N+P) concentration but instead coincided with sequential changes in taxonomy, as the community shifted from a dominance in prymnesiophytes to cryptophytes. The models for these parameters revealed these changes were correlated with the light environment and the mixed layer depth, which were also correlated with the observed variability in community composition (Chapter 3). These results conform to previous observations of phytoplankton physiology made using FRRf in shelf sea regions (Moore *et al.* 2003, 2005), providing further support that the physiological state of PSII can be used as an indicator of bloom status and community composition.

The use of *in vivo* fluorescence techniques allows the measurement of phytoplankton biomass and distribution frequently in time and space, but requires careful interpretation (Falkowski and Kiefer, 1985). At present, there is currently no consensus on the approach that should be taken to correct ship-based fluorescence data collected using continuous systems, even for the basic parameter of ambient irradiance at time of measurement. To address this, I provided a simplistic approach to ambient light correction for ship-based fluorescence measurements (Appendix). This correction was applied to underway data from another region but proved ineffective at vastly improving the accuracy of ship-based measurements (Chapter 4), highlighting the need for further research into this area. The incorporation of additional data (e.g. temperature, NPQ, F_v/F_m) would result in a more robust correction parameter and highlights the importance of auxiliary measurements of photophysiological to be collected alongside biomass estimations. By providing greater confidence in these high-resolution fluorescence datasets, they could be effectively used to increase monitoring efforts in response to climate or anthropogenic impacts; or for validation and error estimation in remote sensing approaches.

I employed ship-based fluorescence measurements to compare *in situ* estimates of biomass with satellite estimations (Chapter 4). Using semivariogram approaches and ship-based fluorescence estimates of biomass, the variability of phytoplankton distribution was presented (Chapter 4). I showed how both approaches possess the ability to capture mesoscale variability, yet ocean colour estimates lose accuracy in highly heterogenous (e.g. bloom) conditions. This raises questions as to the potential resolution lost through satellite averaging during these

highly productive bloom periods. Accurate satellite-derived estimates of chlorophyll are crucial in global predictions of productivity but it is particularly hard to obtain reliable data in coastal regions, where optical properties are difficult to determine and hydrography is highly variable (Tilstone *et al.* 2005; Bracher *et al.* 2017). However, the contribution of these coastal regions to the global carbon cycle is significant, putting increased significance on reliable and accurate productivity estimates (Chapter 1). For this reason, the wealth of information provided by ship-based measurements could prove highly valuable and should be further exploited.

The collection of these measurements is a common occurrence on research ship and a global database of thousands of fluorescence measurements already exists. However, as discussed, a robust correction and quality control procedure are necessary for an accurate interpretation of the data (Appendix). To achieve this, multiple sensors would be required for the collection of auxiliary data; this, to shed light on the environmental controls of fluorescence. A key measurement would be non-photochemical quenching (NPQ); used to protect the photosynthetic apparatus in periods of high light.

The effects of environmental factors on NPQ were only briefly investigated in this study and revealed minimal changes in response to different nutrient availability (Chapter 2), but strong diurnal changes when continuous sampling using FRRf was employed (Chapter 4). The capacity for NPQ has been linked to the process of electron transfer and carbon fixation in areas of limited nutrient availability, further highlighting the necessity to better parameterise NPQ for productivity and biomass estimations (Schuback *et al.* 2016).

Automated data collection is an emerging force in marine science with many projects now utilising buoys and moorings for stationary measurements whilst floats, gliders and ships are employed for extensive spatial coverage. The ARGO project is something of a model study when it comes to a global initiative established to observe changes in the global ocean and specific regional impacts. Established in 2000 to monitor the changing state of the upper ocean ARGO now consists of nearly 4000 floats that provide global coverage and over 100 000 temperature/salinity profiles a year. This international collaborative effort sees 30 countries and 50 research/operational agencies work together towards the goal of building a global array of floats and the open data policy held by ARGO. Over the 17 years of operation this program has contributed to hundreds of theses and papers and remains one of the most potent datasets when it comes to observing climate-related change, although the project does acknowledge the dataset is not yet long enough to reliable observe these global change signals, with its greatest contribution expected in the future.

At present, there is no ship-based program or data repository that rivals the spatial coverage or collaborative effort of the ARGO project. The continuous plankton recorded dataset (CPR) operated by the Sir Alastair Hardy Foundation for Ocean Science (SAHFOS) remains one of the longest and most extensive marine ecological surveys but lacks auxiliary measurements to provide biogeochemical context to its findings. The FerryBox system offers a glimpse into the potential future of autonomous ship-based data collection. Much like the CPR, the automated instrument package of FerryBox capitalises on the routes covered by ships of opportunity to provide a range of biogeochemical information. FerryBox data

featured in every chapter of this thesis which hopefully goes some way in displaying the potential approaches towards the use of the data. To fully exploit this unexplored fluorescence data and those collected by others to improve our understanding of the variability in phytoplankton stocks and rates directives for future research are suggested below:

1. An evaluation of how FRRf has progressed over the past decade (e.g. the development of new multi-spectral sensors and FRRf-based productivity algorithms), that culminates in a standardised method for the collection of light-response (P vs. E) parameters.
2. A quantitative assessment (e.g. meta-analysis) that provides better understanding of the controlling environmental factors of light, nutrients and taxonomy on (i) F_v/F_m and σ_{PSII} and (ii) FRRf-derived P vs. E parameters (e.g. P_m, α and E_K), complimenting the previous reviews and analyses of Suggett et al. (2009) and Lawrenz et al. (2013)
3. Advances towards (i) a robust quality control procedure for the correction of *in situ* fluorescence transect data measured using ship-based monitoring systems and (ii) the collection and synthesis of a global database of ship-based fluorescence transects

I have contributed a small, yet important step towards capturing the extent of spatial and temporal variability in phytoplankton stocks and rates in temperate shelf seas, in part, by providing a better understanding of the strengths and limitations of the use of fluorescence based measurements. Instrument development and a growing understanding of phytoplankton eco-physiology holds the promise that the spatial

and temporal variability of marine primary production will be directly measured and adequately accounted for in future generations of biogeochemical models. Such advancements will provide us with the means to predict and manage far ranging ecosystem services, from fisheries to carbon sequestration.

Appendix: The Influence of Ambient Irradiance on Ship-based In Situ Fluorescence Measurements

A.1 Introduction

The use of *in vivo* fluorescence techniques allows oceanographers to measure the productivity and distribution of marine phytoplankton frequently in time and space (Falkowski & Kiefer 1985; Behrenfeld *et al*. 2009; Sauzède *et al*. 2015). Fluorescence measurements have already started to alter our understanding of how photoacclimation and adaptation influence marine photosynthesis in different hydrodynamic conditions (Chapter 3; Moore *et al*. 2003; Moore *et al*. 2006); in different nutrient regimes (Chapter 2; Browning, *et al*. 2014; Schuback *et al*. 2016) and different light climates (Wagner *et al.* 2006; Giovagnetti *et al.* 2014). These measurements are crucial to improve our understanding of phytoplankton physiology for the improved parameterisation of productivity algorithms and predictive models. However, very few recent studies have exploited the high-resolution data available from underway chlorophyll fluorometers to examine the biomass and distribution of phytoplankton communities.

There are many reasons for the a improve estimates of satellite but could also provide valuable comparative datasets for the ground truthing of remotely sensed data products (Huot *et al*. 2013; Browning *et al*. 2014; O'Malley *et al*. 2014). However, the analysis and interpretation of *in vivo* fluorescence relies on a number biological and environmental assumptions (Suggett *et al*. 2009; Sauzède *et al*. 2015).

Both biological and environmental variability and variability in environmental conditions can affect the fluorescence signal. Sources of variability in fluorescence measurements include the differences in the pigment structure of the light harvesting antennae between major taxa (Suggett *et al.* 2001; Ragni *et al.* 2010), the influence of

nutrient stress on the photosynthetic apparatus (Geider *et al.* 1993) and photoinhibition caused by prolonged exposure to high light intensities (Long *et al.* 1994; Murata *et al.* 2007). Differences in instruments calibration or the excitation wavelength can also lead to a bias in inferred chlorophyll fluorescence values, which the fluorescence community is starting to address (Roesler *et al.* 2017). Robust quality control procedures have also been developed to correct *in situ* profiles for the contribution of fluorescence non-algal matter (Xing *et al.* 2017) and community composition (Sauzède *et al.* 2015). Similar approaches have been taken to correct for the influence of ambient light intensity that causes quenching of fluorescence measurements acquired by autonomous platforms (Xing *et al.* 2012). Fluorometers still differ in their reported measurements of chlorophyll and there is currently no consensus on the approach that should be taken to correct ship-based fluorescence data collected using continuous systems, even for the basic parameter of ambient irradiance at time of measurement. (e.g. FerryBox; Petersen 2014).

The main objectives of this study are (i) to compare the accuracy of two fluorescence techniques used to estimate chlorophyll concentration, (ii) to investigate the influence of the ambient light environment on automated fluorescence measurements and (iii) correct data subject to quenching effects and determine the extent of change in the North Sea.

A.2 Methodology

A.2.1 General Sampling and Hydrography

Data were collected on board the RV *Cefas Endeavour* (CEND_1815) during a research cruise to the North Sea between the 9th of August and 3rd of September 2015. 74 sites

were visited and profiled using a Falmouth Scientific NXIC conductivity, temperature, depth (CTD) and LI-192 underwater quantum light sensor. The presence of thermal stratification was calculated using temperature difference throughout the water column (≥2^{o}C indicating stratification, <2^{o}C indicating mixed conditions).

An automated FerryBox sampling system connected to the vessel's underway water supply - approximately 4m depth - provided continuous measurements of salinity (S), temperature (T), turbidity, chlorophyll fluorescence, photosynthetic quantum efficiency and pH for near-surface waters (Peterson *et al.* 2014). Diel influence on data was assessed by grouping as 'night' or 'day', subject to the levels of ambient irradiance at the time of collection. Using photosynthetically active radiation (PAR) data from a sensor on the ship's bridge, night values were assigned to data collected at < 10 µmol photons m^{-2} s^{-1} whilst data collected at an ambient PAR => 10 µmol photons m^{-2} s^{-1} was considered daylight. Discrete near-surface water samples were collected from the ship's non-toxic underway water supply for nutrient and pigment analysis.

A.2.2 Phytoplankton Pigments and Community Structure

Water samples for phytoplankton pigment composition were collected on station in clean Nalgene bottles and filtered through 47 mm Whatman® GF/F filters before immediate storage at -80 ^{o}C. 55 samples were selected and sent for pigment analysis using high performance liquid chromatography (HPLC) at the DHI Institute for Water and Environment (Hørsholm, Denmark). Pigment data were statistically analysed and quality assured (QA) following the methods of Aiken *et al.* (2009). Upon completion

of QA, data from two stations were removed from further analysis due to an unusual ratio of total chlorophyll a to accessory pigments.

A.2.3 Fast Repetition Rate fluorometry

A multi-spectral FRRf (*FastOcean™*, Chelsea Technologies Group - CTG - Ltd, UK) fitted with an integrated FastAct™ bench-top unit (CTG Ltd) was used to measure phytoplankton photophysiology for discrete seawater samples collected from the ship's non-toxic underway water supply. Samples were dark-acclimated at source temperature for a minimum of 30 minutes before single turnover FRRf measurements were made using a 32-sequence protocol of 100 1.1 µs saturation flashes at 2.8 µs intervals followed by 40 µs relaxation flashes at 50 µs intervals.

Data were processed using software provided by the instrument manufacturer (FASTpro8 V1.0.5, CTG Ltd) with the minimum (F_o) and maximum (F_m) fluorescence and effective absorption cross section provided by fitting single acquisition data to the KPF model (Kolber *et al.* 1998). The dark-acclimated maximum quantum yield of photochemistry (F_v/F_m) was calculated as F_m- F_o/F_m. Non-linearity in instrument settings (gain and LED intensity) was corrected for using updated software (FASTpro8 V1.0.5, CTG Ltd.) and further characterised using a chlorophyll in acetone (extracted from cultured algal species) dilution series conducted post-cruise, at the University of Essex, with results showing the software effectively corrected values measured using different gain and LED intensities.

A.3 Results

A.3.1 Comparative Chlorophyll Estimates

Chlorophyll estimates made using three techniques - HPLC, FRRf (derived from the F_o) and the Seapoint chlorophyll fluorometer (SCF) of the *FerryBox* showed different degrees of linear correlation (Table A.1). FRRf chlorophyll estimates (derived from F_o) and values of F_v (F_q' under actinic light, Table A.1) were compared for two reasons. Firstly, changes in F_o and F_m should respond proportionally to fluorescent artefacts in the sample, thus eliminating the over or underestimation of the baseline fluorescence and removing the necessity for correction. Secondly, F_o increased substantially (25 - 30 %), relative to measurements made in total darkness, following exposure to low levels of actinic light. This increase continued during the RLC until the PAR reached approximately 150 µmol photons m^{-2} s^{-1} where it peaked and began to exponentially decline as the PAR increased. Although F_v exhibited a similar trend it was not of the same magnitude. The *FerryBox* SCF measurements showed the weakest relationship with HPLC values (r^2 = 0.45) but a strong correlation with dark acclimated FRRf values of chl (r^2 = 0.78) and F_v (r^2 = 0.77). The two FRRf measurements also revealed a strong correlation with the HPLC values but F_v (r^2 = 0.73) had a greater correlation than F_o derived estimates (r^2 = 0.70; Table A.1).

Table A.1. Correlations for chlorophyll estimates and fluorescence measurements. All correlations are significant at 99 % confidence. FRRf chl, fast repetition rate fluorometry (FRRf) chlorophyll estimation; HPLC, high performance liquid chromatography; Fv, variable fluorescence (Fm – Fo) measured using FRRf; FerryBox SCF, FerryBox Seapoint chlorophyll fluorometer.

Figure	Correlation	n	R^2	Slope	Intercept
Appendix. 5a	FRRf chl vs HPLC	54	0.70	3.64	1.00
Appendix. 5b	Fv vs HPLC	54	0.73	0.29	0.43
Appendix. 5c	*FerryBox* SCF vs HPLC	54	0.45	0.68	0.68
Appendix. 5d	FRRf chl vs *FerryBox* SCF	71	0.78	3.69	1.33
Appendix. 5e	Fv vs *FerryBox* SCF	71	0.77	0.31	0.07
NA	Corrected *FerryBox* vs HPLC	71	0.55	0.85	0.17

A.3.2 Ambient Light on Fluorescence Measurements

Trends in fluorescence measurements made using the *FerryBox* SCF followed those seen in the HPLC data, revealing a wide range of values and widespread spatial heterogeneity, albeit at a much higher resolution. Diel fluorescence cycles were also observed in the data, characterised by an exponential suppression of fluorescence values by increasing PAR (Fig. A.1). The extent of this PAR-driven depression in FerryBox SCF data was calculated by linear regression of the log-transformed fluorescence vs. PAR relationship. The proportion of variance explained by the model was low ($r^2 = 0.19$), most likely due to the large spatial scale over which the data were collected and subsequent variance in taxonomy and environmental parameters (e.g. nutrients, temperature, salinity). The model coefficients were used to calculate a simple correction algorithm (Corrected *F*) which was applied to the raw SCF data:

$$Corrected\ F\ = F \cdot exp(x \cdot PAR) \qquad \text{Eqn. A.1}$$

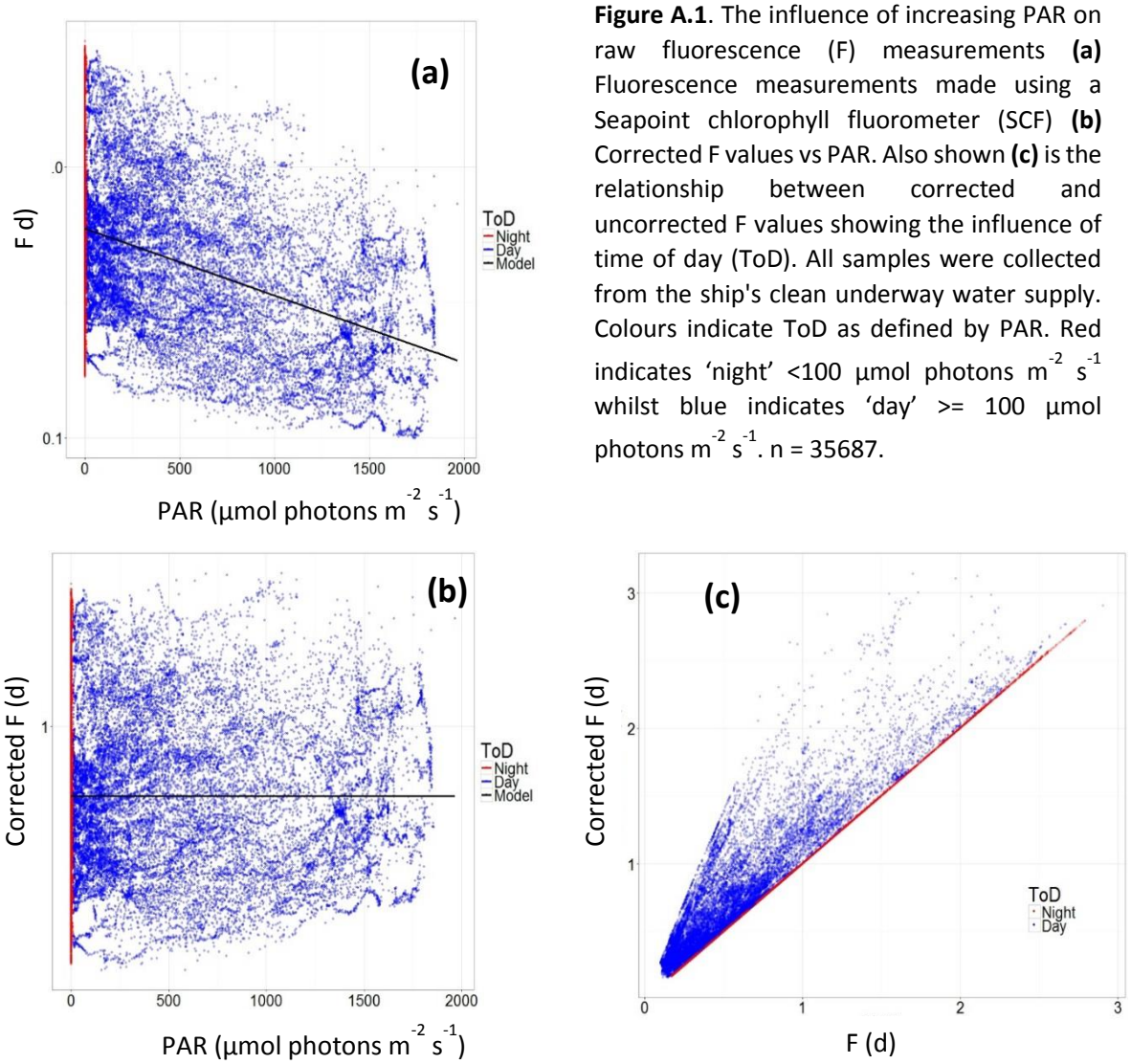

Figure A.1. The influence of increasing PAR on raw fluorescence (F) measurements **(a)** Fluorescence measurements made using a Seapoint chlorophyll fluorometer (SCF) **(b)** Corrected F values vs PAR. Also shown **(c)** is the relationship between corrected and uncorrected F values showing the influence of time of day (ToD). All samples were collected from the ship's clean underway water supply. Colours indicate ToD as defined by PAR. Red indicates 'night' <100 µmol photons m^{-2} s^{-1} whilst blue indicates 'day' >= 100 µmol photons m^{-2} s^{-1}. n = 35687.

where *F* is the raw fluorescence data, *x* is the slope and PAR is the value measured on the bridge of the ship. Following correction, the average for all fluorescence values was found to increase 15 % (0.71 ± 0.48, mean ± SD) compared to the raw data (0.60 ± 0.45) and the reduction previously observed along an increasing gradient of PAR was removed.

The spatial distribution of chlorophyll estimated by both corrected and uncorrected fluorescence values revealed elevated concentrations in the coastal areas with small pockets of particularly high levels in the north-west and south-east regions where the

water column was homogenously mixed. There was a noticeable increase in the corrected fluorescence values of the southern regions (Fig. A.2).

When normalised to Tchla (F : Tchla), raw fluorescence values measured at 54 discrete stations reveal a decrease over the course of the day before increasing again in the afternoon. Following the correction of the fluorescence measurements the mid-day suppression (common trend observed in fluorescence measurements) was greatly reduced (Fig. 4b). The linear correlation of corrected SFC against HPLC values also increased (r^2 = 0.55, slope = 0.85).

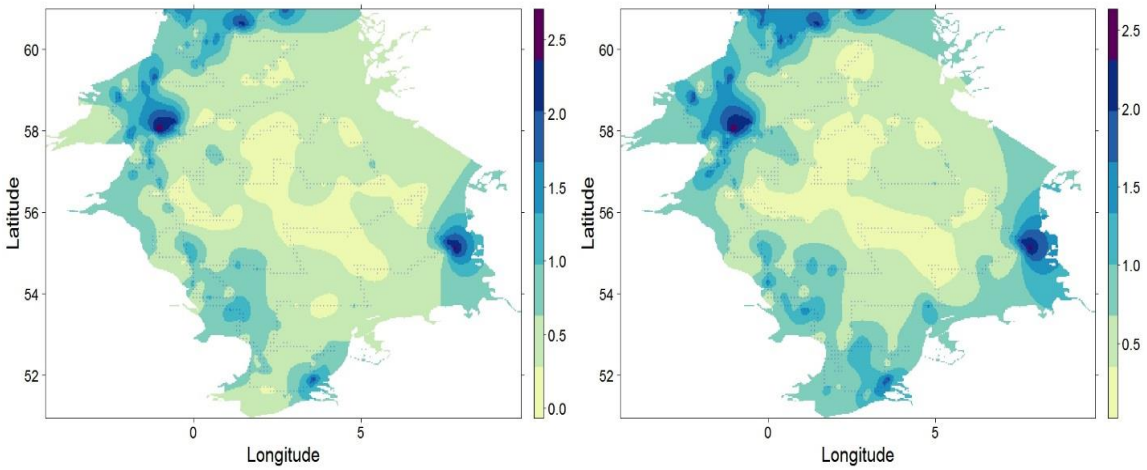

Figure A.2. Mapped values of fluorescence-based chlorophyll estimates measurements revealing the influence of ambient light on fluorescence data **(a)** The influence of increasing PAR on raw fluorescence (F) measurements. These data were modelled using linear regression and the coefficients used to create a correction algorithm **(b)** Samples were measured in situ and obtained from a depth of approximately 3m between August 9th and September 4th 2015 (n = 35500). Light blue points indicate the cruise transect and the background shows the values interpolated using ordinary kriging

A.4 Discussion

In this study, an automated fluorescence-based approached was utilised to evaluate the spatial variability of phytoplankton biomass in the North Sea. The results provide further evidence that automated fluorescence methods can effectively be used to obtain high resolution *in situ* datasets for both phytoplankton biomass and provide statistical methods for the correction of fluorescence data. Within this study the SCF provided high resolution estimates of chlorophyll across the entire North Sea.

Areas of increased phytoplankton biomass were found in the coastal regions, particularly the south-east and north west, and coincide with stations that were shown to have a homogenously mixed water column and elevated nutrients levels in the surface mixed layer. Despite this, the regression between the SCF estimates and samples of Tchla (HPLC) measured at all stations was weak in comparison to the FRRf. One potential explanation for this for this is the suppression of the fluorescence signal in responses to increasing light. Fluorescence based-measurements, made in situ, over the course of a diurnal cycle have previously shown diel patterns that include a nocturnal decrease (Seen in FvFm and associated with Fe limitation) and a mid-day suppression associated with photoprotective mechanisms and photoinhibition (Behrenfeld & Kolber 1999; Behrenfeld *et al*. 2006a).

Results showed PAR had a highly significant influence on SCF, causing an exponential decrease in fluorescence values, even in areas of higher biomass and increased nutrient concentration. This is somewhat consistent with previous studies that attributed spatial heterogeneity fluorescence measurements to three factors; chlorophyll concentration, pigment packaging effects on light absorption and light

dependent energy processes (Behrenfeld *et al.* 2009). As previously stated, corrected fluorescence values normalised to Tchla were shown to increase at mid-day (Fig. 4). In both the corrected and uncorrected data the concentration of Tchla appeared to have no influence either the magnitude of mid-day suppression or correction, respectively. However, regression analysis between uncorrected SCF and HPLC values shows much greater agreement at lower concentrations with higher values of Tchla being grossly over-and-under estimated as fluorescence (Appendix, Fig. 4a). This could suggest pigment composition or packaging effects have influenced the absorption.

The final factor discussed in Behrenfeld *et al*. (2009) was the influence light dependent energy quenching processes that phytoplankton employ to drive photosynthesis prevent or minimise photoinhibition (Müller *et al.* 2001; Baker, 2008). Under ambient light conditions it is important to consider both photochemical quenching (qP) and nonphotochemical forms of quenching in order to determine the chlorophyll fluorescence yield (Browning *et al.* 2014). Absorbed excitation energy within photosystem II (PSII) to drive electron transfer and is termed qP, whilst nonphotochemical quenching (NPQ) occurs when there is an excess of excitation energy within PSII with is dissipated as heat (Baker, 2008). These two processes, along with chlorophyll fluorescence are all in direct competition for excitation energy so a change in rate of one will directly influence the other two (Kramer *et al.* 2004).

Unlike other chlorophyll fluorometers the SCF used in this study does not have the capacity to calculate qP or NPQ so quenching processes cannot be separated and are grouped as a single effect when discussing SCF data. The PAR-driven reduction in fluorescence SCF data collected in ambient light over the cruise was shown to account

for a 15 % underestimation with the largest changes coming in well mixed, shallow areas. This is highlights the importance for the correction of fluorescence data sets collected in ambient light over large spatial scales. Firstly, for the accuracy of the primary data but also, in case of use for remote sensing comparison. As all ocean colour data for chlorophyll calculation are collected at mid-day the correction of quenching for comparative must be considered.

A.4.1 Influence of Taxonomy, Turbidity and Temperature

Although the correction model was made using only simple linear regression and one explanatory variable (PAR) other factors could be considered to try and improve the explanatory power of the observed spatial variability in fluorescence measurements. Increasing temperature was found to have similar negative effects on normalised fluorescence measurements. Another potential driver in the observed variation between fluorescence-based values and HPLC could be phytoplankton community composition. Differences in the taxonomic composition within a sample has previously been shown to influence fluorescence measurements primarily due to alternate light harvesting strategies employed by different phytoplankton taxa (Litchman and Klausmeier, 2008).

A.4.2 Instrument Calibration

A final consideration should be the instruments used and the pre-deployment processes that should be carried out. Fluorometers differ in the excitation wavelength used to stimulate active fluorescence. Despite differences in the dark-acclimated state of samples, and potential influence of quenching, values from the two

fluorescence techniques showed a strong linear relationship. This is most likely due to the common use of a blue LED excitation light which would target the same algal groups. There was a pronounced difference in the slopes of the regressions of FRRF and Seapoint fluorescence estimates of Tchla versus HPLC measurements which may be related to the calibration procedure carried out for each instrument. A pre-cruise calibration should be carried out to allow greater confidence in comparison between instruments.

A.5 Conclusions

Research vessels are often deployed with on board fluorometers in automated systems that consistently collect data at high temporal resolution (seconds) over large geographical distances. Although further work is needed there is the potential for the access to large volumes of data that could prove attractive to a those in water quality assessment, remote sensing and biogeochemical modelling. However, with these datasets also come caveats, the need for correction and pre-and-post calibration procedures. These corrections are driven primarily by differences in fluorometer specifications (calibration and excitation wavelength), natural diversity in taxonomy and nutrients, differences in temperature and finally the influence of diel processes on the fluorescence cycles of phytoplankton.

References

Abrantes, F., Cermeno, P., Lopes, C., Romero, O., Matos, L., Van Iperen, J., Rufino, M. and Magalhães, V. (2016) 'Diatoms Si uptake capacity drives carbon export in coastal upwelling systems', *Biogeosciences*, 13(14), pp. 4099–4109.

Aiken, J., Pradhan, Y., Barlow, R., Lavender, S., Poulton, A., Holligan, P. and Hardman-Mountford, N. (2009) 'Phytoplankton pigments and functional types in the Atlantic Ocean: A decadal assessment, 1995–2005', *Deep Sea Research Part II: Topical Studies in Oceanography*, 56(15), pp. 899–917.

Allen, J. T., Brown, L., Sanders, R., Mark Moore, C., Mustard, A., Fielding, S., Lucas, M., Rixen, M., Savidge, G., Henson, S. and Mayor, D. (2005) 'Diatom carbon export enhanced by silicate upwelling in the northeast Atlantic', *Nature*, 437(7059), pp. 728–732.

Arrigo, K. (2005) 'Molecular diversity and ecology of microbial plankton', *Nature*, 437(7057), pp. 349–355.

Artioli, Y., Friedrich, J., Gilbert, A. J., McQuatters-Gollop, A., Mee, L. D., Vermaat, J. E., Wulff, F., Humborg, C., Palmeri, L. and Pollehne, F. (2008) 'Nutrient budgets for European seas: A measure of the effectiveness of nutrient reduction policies', *Marine Pollution Bulletin*, 56(9), pp. 1609–1617.

Bailey, S. and Grossman, A. (2008) 'Photoprotection in cyanobacteria: regulation of light harvesting.', *Photochemistry and photobiology*, 84(6), pp. 1410–20.

Baker, N. R. (2008) 'Chlorophyll Fluorescence: A Probe of Photosynthesis In Vivo', *Annual Review of Plant Biology*, 59(1), pp. 89–113.

Bauer, J. E., Cai, W.-J., Raymond, P. a, Bianchi, T. S., Hopkinson, C. S. and Regnier, P. a G. (2013) 'The changing carbon cycle of the coastal ocean.', *Nature*, 504(7478), pp. 61–70.

Beardall, J., Young, E. and Roberts, S. (2001) 'Approaches for determining

phytoplankton nutrient limitation', *Aquatic Sciences*, 63(1), pp. 44–69.

Behrenfeld, M. and Falkowski, P. (1997) 'Photosynthetic rates derived from satellite-based chlorophyll concentration', *Limnology and Oceanography*, 42(1), pp. 1–20.

Behrenfeld, M. J. (2010) 'Abandoning Sverdrup's Critical Depth Hypothesis on phytoplankton blooms', *Ecology*, 91(4), pp. 977–989.

Behrenfeld, M. J. and Boss, E. S. (2014) 'Resurrecting the Ecological Underpinnings of Ocean Plankton Blooms', *Annual Review of Marine Science*, 6(1), pp. 167–194.

Behrenfeld, M. J., Boss, E., Siegel, D. a. and Shea, D. M. (2005) 'Carbon-based ocean productivity and phytoplankton physiology from space', *Global Biogeochemical Cycles*, 19(1).

Behrenfeld, M. J. and Falkowski, P. G. (1997) 'Photosynthetic rates derived from satellite-based chlorophyll concentration', *Limnology and Oceanography*, 42(1), pp. 1–20.

Behrenfeld, M. J. and Kolber, Z. (1999) 'Widespread Iron Limitation of Phytoplankton in the South Pacific Ocean', *Science*, 283(5403), pp. 840–843.

Behrenfeld, M. J., O'Malley, R. T., Siegel, D. a, McClain, C. R., Sarmiento, J. L., Feldman, G. C., Milligan, A. J., Falkowski, P. G., Letelier, R. M. and Boss, E. S. (2006) 'Climate-driven trends in contemporary ocean productivity.', *Nature*, 444(7120), pp. 752–5.

Behrenfeld, M. J., Westberry, T. K., Boss, E. S., O'Malley, R. T., Siegel, D. a., Wiggert, J. D., Franz, B. a., McClain, C. R., Feldman, G. C., Doney, S. C., Moore, J. K., Dall'Olmo, G., Milligan, a. J., Lima, I. and Mahowald, N. (2009) 'Satellite-detected fluorescence reveals global physiology of ocean phytoplankton', *Biogeosciences*, 6(5), pp. 779–794.

Behrenfeld, M. J., Worthington, K., Sherrell, R. M., Chavez, F. P., Strutton, P., McPhaden, M. and Shea, D. M. (2006) 'Controls on tropical Pacific Ocean productivity revealed through nutrient stress diagnostics.', *Nature*, 442(7106), pp. 1025–1028.

Berges, J. A., Charlebois, D. O., Mauzerall, C. C. and Falkowski, P. G. (1996) 'Differential effects of nitrogen limitation on photosynthetic efficiency of photosystems I and II in microalgae', *Plant physiology*, 973, pp. 689–696.

Blackman, F. F. (1903) 'Optima and Limiting Factors on JSTOR', *Annals of Botany*, XIX(Lxxiv).

Borges, A. V, Delille, B. and Frankignoulle, M. (2005) 'Budgeting sinks and sources of CO 2 in the coastal ocean: Diversity of ecosystems counts', *Geophysical Research Letters*, 32(14), p. n/a-n/a.

Bracher, A., Bouman, H. A., Brewin, R. J. W., Bricaud, A., Brotas, V., Ciotti, A. M., Clementson, L., Devred, E., Di Cicco, A., Dutkiewicz, S., Hardman-Mountford, N. J., Hickman, A. E., Hieronymi, M., Hirata, T., Losa, S. N., Mouw, C. B., Organelli, E., Raitsos, D. E., Uitz, J., Vogt, M. and Wolanin, A. (2017) 'Obtaining Phytoplankton Diversity from Ocean Color: A Scientific Roadmap for Future Development', *Frontiers in Marine Science*, 4(April).

Brewer, P. G. and Riley, J. P. (1965) 'The automatic determination of nitrate in sea water', *Deep Sea Research and Oceanographic Abstracts*, 12(6), pp. 765–772.

Brewin, R. J. W., Sathyendranath, S., Hirata, T., Lavender, S. J., Barciela, R. M. and Hardman-Mountford, N. J. (2010) 'A three-component model of phytoplankton size class for the Atlantic Ocean', *Ecological Modelling*, 221(11), pp. 1472–1483.

Browning, T. J., Bouman, H. A. and Moore, C. M. (2014) 'Satellite-detected fluorescence: Decoupling nonphotochemical quenching from iron stress signals in the South Atlantic and Southern Ocean', *Global Biogeochemical Cycles*, 28(5), pp. 510–524.

Brunet, C., Conversano, F., Margiotta, F., Dimier, C., Polimene, L., Tramontano, F. and Saggiomo, V. (2013) 'Role of light and photophysiological properties on phytoplankton succession during the spring bloom in the north-western Mediterranean Sea', *Advances in Oceanography and Limnology*, 4(1), pp. 1–19.

Burson, A., Stomp, M., Akil, L., Brussaard, C. P. D. and Huisman, J. (2016) 'Unbalanced reduction of nutrient loads has created an offshore gradient from

phosphorus to nitrogen limitation in the North Sea', *Limnology and Oceanography*, 61(3), pp. 869–888.

Campbell, J., Antoine, D., Armstrong, R., Arrigo, K., Balch, W., Barber, R., Behrenfeld, M., Bidigare, R., Bishop, J., Carr, M.-E., Esaias, W., Falkowski, P., Hoepffner, N., Iverson, R., Kiefer, D., Lohrenz, S., Marra, J., Morel, A., Ryan, J., Vedernikov, V., Waters, K., Yentsch, C. and Yoder, J. (2002) 'Comparison of algorithms for estimating ocean primary production from surface chlorophyll, temperature, and irradiance', *Global Biogeochemical Cycles*, 16(3), pp. 1–15.

Chen, C.-T. A., Huang, T.-H., Chen, Y.-C., Bai, Y., He, X. and Kang, Y. (2013) 'Air–sea exchanges of CO_2 in the world's coastal seas', *Biogeosciences*, 10(10), pp. 6509–6544.

Cruz, S. and Serôdio, J. (2008) 'Relationship of rapid light curves of variable fluorescence to photoacclimation and non-photochemical quenching in a benthic diatom', *Aquatic Botany*, 88(3), pp. 256–264.

Cullen, J. J. (1991) 'Hypotheses To Explain High-Nutrient Conditions in the Open Sea', *Limnology and Oceanography*, 36(8), pp. 1578–1599.

Cullen, J. J. and Davis, R. F. (2003) 'The Blank can Make a Big Difference in Oceanographic Measurements', *Limnology and Oceanography: Bulletin*, 12(2), pp. 29–35.

Daniels, C. J., Poulton, a J., Esposito, M., Paulsen, M. L., Bellerby, R., St John, M. and Martin, a P. (2015) 'Phytoplankton dynamics in contrasting early stage North Atlantic spring blooms: composition, succession, and potential drivers', *Biogeosciences*, 12, pp. 2395–2409.

Denman, K. L. and Gargett, A. E. (1983) 'Time and space scales of vertical mixing and advection of phytoplankton in the upper ocean', *Limnology and Oceanography*, 28(5), pp. 801–815.

Elser, J. J., Bracken, M. E. S., Cleland, E. E., Gruner, D. S., Harpole, W. S., Hillebrand, H., Ngai, J. T., Seabloom, E. W., Shurin, J. B. and Smith, J. E. (2007) 'Global analysis of nitrogen and phosphorus limitation of primary producers in freshwater, marine and

terrestrial ecosystems', *Ecology Letters*, 10(12), pp. 1135–1142.

Emeis, K. C., van Beusekom, J., Callies, U., Ebinghaus, R., Kannen, A., Kraus, G., Kr??ncke, I., Lenhart, H., Lorkowski, I., Matthias, V., M??llmann, C., P??tsch, J., Scharfe, M., Thomas, H., Weisse, R. and Zorita, E. (2015) 'The North Sea - A shelf sea in the Anthropocene', *Journal of Marine Systems*. Elsevier B.V., 141, pp. 18–33.

Falkowski, P. G., Katz, M. E., Knoll, A. H., Quigg, A., Raven, J. a, Schofield, O. and Taylor, F. J. R. (2004) 'The evolution of modern eukaryotic phytoplankton.', *Science (New York, N.Y.)*, 305(5682), pp. 354–60.

Falkowski, P. G. and Kiefer, D. a (1985) 'Chlorophyll a fluorescence in phytopankton: relationship to photosynthesis and biomass', *Journal of Plankton Research*, 7(5), pp. 715–731.

Falkowski, P. G. and LaRoche, J. (1991) 'Acclimation to spectral irradiance in algae', *Journal of Phycology*, 27(1), pp. 8–14.

Falkowski, P. and Kiefer, D. A. (1985) 'Chlorophyll a fluorescence in phytoplankton : relationship to photosynthesis and biomass * Outer Chloroplast Membrane Inner Membrane', 7(5), pp. 715–731.

Falkowski, P. and Kolber, Z. (1995) 'Variations in chlorophyll fluorescence yields in phytoplankton in the world oceans', *Australian Journal of Plant Physiology*, 22, pp. 341–355.

Finkel, Z., Irwin, A. and Schofield, O. (2004) 'Resource limitation alters the 3/4 size scaling of metabolic rates in phytoplankton', *Marine Ecology Progress Series*, 273, pp. 269–279.

Finkel, Z. V., Beardall, J., Flynn, K. J., Quigg, A., Rees, T. a. V. and Raven, J. a. (2009) 'Phytoplankton in a changing world: cell size and elemental stoichiometry', *Journal of Plankton Research*, 32(1), pp. 119–137.

Fogg, G. E. and Calvario-Martinez, O. (1989) 'Effects of bottle size in determinations of primary productivity by phytoplankton', *Hydrobiologia*. Kluwer Academic Publishers, 173(2), pp. 89–94.

Ford, D. A., Van Der Molen, J., Hyder, K., Bacon, J., Barciela, R., Creach, V., McEwan, R., Ruardij, P. and Forster, R. (2017) 'Observing and modelling phytoplankton community structure in the North Sea', *Biogeosciences*, 14(6), pp. 1419–1444.

Frank, K. T., Petrie, B. and Shackell, N. L. (2007) 'The ups and downs of trophic control in continental shelf ecosystems', *Trends in Ecology & Evolution*, 22(5), pp. 236–242.

Franks, P. J. S. (2015) 'Has Sverdrup's critical depth hypothesis been tested? Mixed layers vs. turbulent layers', *ICES Journal of Marine Science: Journal du Conseil*, 72(6), pp. 1897–1907.

Geider, R. J., Delucia, E. H., Falkowski, P., Finzi, A. C., Grime, J. P., Grace, J., Kana, T. M., La Roche, J., Long, S. P., Osbourne, B. A., Platt, T., Prentice, I. C., Raven, J. a., Schlesinger, W. H., Smetacek, V., Stuart, V., Sathyendranath, S., Thomas, R. B., Vogelmann, T. C., Williams, P. and Woodward, F. I. (2001) 'Primary productivity of planet earth: biological determinants and physical constraints in terrestrial and aquatic habitats', *Global Change Biology*, (7), pp. 849–882.

Geider, R. J., La Roche, J., Greene, R. M. and Olaizola, M. (1993) 'Response of the photosynthetic apparatus of Phaeodactylum tricornatum (Bacillariophycea) to nitrate, phosphate, or iron starvation', *Journal of Phycology*, pp. 755–766.

Geider, R. and La Roche, J. (2002) 'Redfield revisited: variability of C:N:P in marine microalgae and its biochemical basis', *European Journal of Phycology*, 37(1), pp. 1–17.

Giovagnetti, V., Flori, S., Tramontano, F., Lavaud, J. and Brunet, C. (2014) 'The velocity of light intensity increase modulates the photoprotective response in coastal diatoms', *PLoS ONE*, 9(8), pp. 1–12.

Greene, R., Geider, R. and Falkowski, P. (1991) 'Effect of iron limitation on photosynthesis in a marine diatom.', *Limnology and Oceanography*, 36, pp. 1772–1782.

Greenwood, N., Parker, E. R., Fernand, L., Sivyer, D. B., Weston, K., Painting, S. J., Kröger, S., Forster, R. M., Lees, H. E., Mills, D. K. and Laane, R. W. P. M. (2010)

'Detection of low bottom water oxygen concentrations in the North Sea; Implications for monitoring and assessment of ecosystem health', *Biogeosciences*, 7(4), pp. 1357–1373.

Grizzetti, B., Bouraoui, F. and Aloe, A. (2012) 'Changes of nitrogen and phosphorus loads to European seas', *Global Change Biology*, 18(2), pp. 769–782.

Gröger, M., Maier-Reimer, E., Mikolajewicz, U., Moll, A. and Sein, D. (2013) 'NW European shelf under climate warming: Implications for open ocean - Shelf exchange, primary production, and carbon absorption', *Biogeosciences*, 10(6), pp. 3767–3792.

Grosse, J., van Breugel, P., Brussaard, C. P. D. and Boschker, H. T. S. (2017) 'A biosynthesis view on nutrient stress in coastal phytoplankton', *Limnology and Oceanography*, 62(2), pp. 490–506.

Guillard, R. R. L. (1975) 'Culture of Phytoplankton for Feeding Marine Invertebrates', *Culture of Marine Invertebrate Animals*, pp. 29–30.

Halsey, K. H. and Jones, B. M. (2015) 'Phytoplankton Strategies for Photosynthetic Energy Allocation', *Annual Review of Marine Science*, 7(1), pp. 265–297.

Harpole, W. S., Ngai, J. T., Cleland, E. E., Seabloom, E. W., Borer, E. T., Bracken, M. E. S., Elser, J. J., Gruner, D. S., Hillebrand, H., Shurin, J. B. and Smith, J. E. (2011) 'Nutrient co-limitation of primary producer communities', *Ecology Letters*, 14(9), pp. 852–862.

Hedges, L. V, Gurevitch, J. and Curtis, P. S. (1999) 'The Meta-Analysis of Response Ratios in Experimental Ecology', *Ecology*, 80(4), pp. 1150–1156.

Hickman, A. E., Moore, C., Sharples, J., Lucas, M., Tilstone, G., Krivtsov, V. and Holligan, P. (2012) 'Primary production and nitrate uptake within the seasonal thermocline of a stratified shelf sea', *Marine Ecology Progress Series*, 463, pp. 39–57.

Hijmans, R. J., Williams, E. and Vennes, C. (2016) 'Package " geosphere "'.

Houliez, E., Simis, S., Nenonen, S., Ylöstalo, P. and Seppälä, J. (2017) 'Basin-scale spatio-temporal variability and control of phytoplankton photosynthesis in the Baltic

Sea: The first multiwavelength fast repetition rate fluorescence study operated on a ship-of-opportunity', *Journal of Marine Systems*. Elsevier B.V., 169, pp. 40–51.

Huot, Y., Babin, M. and Bruyant, F. (2013) 'Photosynthetic parameters in the Beaufort Sea in relation to the phytoplankton community structure', *Biogeosciences*, 10(5), pp. 3445–3454.

Huot, Y., Brown, C. a and Cullen, J. J. (2005) 'New algorithms for MODIS sun-induced chlorophyll fluorescence and a comparison with present data products', *Limnology and Oceanography: Methods*, 3, pp. 108–130.

Huot, Y., Franz, B. a. and Fradette, M. (2013) 'Estimating variability in the quantum yield of Sun-induced chlorophyll fluorescence: A global analysis of oceanic waters', *Remote Sensing of Environment*. Elsevier Inc., 132, pp. 238–253.

Kavanaugh, M. T., Emerson, S. R., Hales, B., Lockwood, D. M., Quay, P. D. and Letelier, R. M. (2014) 'Physicochemical and biological controls on primary and net community production across northeast Pacific seascapes', *Limnology and Oceanography*, 59(6), pp. 2013–2027.

Key, T., Mccarthy, A., Campbell, D. A., Six, C., Roy, S. and Finkel, Z. V (2010) 'Cell size trade-offs govern light exploitation strategies in marine phytoplankton', 12, pp. 95–104.

Kolber, Z. and Falkowski, P. G. (1993) 'Use of active fluorescence to estimate phytoplankton photosynthesis in situ', *Limnology and Oceanography*, 38(8), pp. 1646–1665.

Kolber, Z., Prasil, O. and Falkowski, P. (1998) 'Measurements of variable chlorophyll fluorescence using fast repetition rate techniques: defining methodology and experimental protocols', *Biochimica et biophysica acta*, 1367(1–3), pp. 88–106.

Kolber, Z., Zehr, J. and Falkowski, P. (1988) 'Effects of Growth Irradiance and Nitrogen Limitation on Photosynthetic Energy Conversion in Photosystem II.', *Plant physiology*, 88(3), pp. 923–9.

Kramer, D. M., Johnson, G., Kiirats, O. and Edwards, G. E. (2004) 'New fluorescence

parameters for the determination of Q A redox state and excitation energy fluxes', *Photosynthesis Research*, 79, pp. 209–218.

Lawrenz, E., Silsbe, G., Capuzzo, E., Ylöstalo, P., Forster, R.M., Simis, S.G., Prášil, O., Kromkamp, J.C., Hickman, A.E., Moore, C.M.,Forget, M.H., Geider, R., Suggett, D. (2013) Predicting the electron requirement for carbon fixation in seas and oceans. *PLoS One*, *8*(3), p.e58137

van Leeuwe, M. a., Villerius, L. a., Roggeveld, J., Visser, R. J. W. and Stefels, J. (2006) 'An optimized method for automated analysis of algal pigments by HPLC', *Marine Chemistry*, 102(3–4), pp. 267–275.

van Leeuwen, S., Tett, P., Mills, D. and van der Molen, J. (2015) 'Stratified and nonstratified areas in the North Sea: Long-term variability and biological and policy implications', *Journal of Geophysical Research: Oceans*, 120(7), pp. 4670–4686.

Lenhart, H. J., Mills, D. K., Baretta-Bekker, H., van Leeuwen, S. M., der Molen, J. van, Baretta, J. W., Blaas, M., Desmit, X., Kühn, W., Lacroix, G., Los, H. J., Ménesguen, A., Neves, R., Proctor, R., Ruardij, P., Skogen, M. D., Vanhoutte-Brunier, A., Villars, M. T. and Wakelin, S. L. (2010) 'Predicting the consequences of nutrient reduction on the eutrophication status of the North Sea', *Journal of Marine Systems*, 81(1–2), pp. 148–170.

Leonardos, N. and Geider, R. J. (2004) 'Responses of elemental and biochemical composition of Chaetoceros muelleri to growth under varying light and nitrate : phosphate supply ratios and their influence on critical N : P', *Limnol. Oceanogr*, 49(6), pp. 2105–2114.

Lin, H., Kuzminov, F. I., Park, J., Lee, S., Falkowski, P. G. and Gorbunov, M. Y. (2016) 'The fate of photons absorbed by phytoplankton in the global ocean', *Science*, 351(6270), pp. 264–267.

Litchman, E. and Klausmeier, C. a. (2008) 'Trait-Based Community Ecology of Phytoplankton', *Annual Review of Ecology, Evolution, and Systematics*, 39(1), pp. 615–639.

Long, S. P., Humphries, S. and Falkowski, P. (1994) 'Photoinhibition of

photosynthesis in nature', *Annual review of plant physiology and plant molecular biology*, 45, pp. 633–662.

MacIntyre, H., Kana, T., Anning, T. and Geider, R. J. (2002) 'Photoacclimation of photosynthesis irradiance response curves and photosynthetic pigments in microalgae and cyanobacteria', *Journal of …*, 38(July 2000), pp. 17–38.

MacIntyre, H. L., Kana, T. M. and Geider, R. J. (2000) 'The effect of water motion on short-term rates of photosynthesis by marine phytoplankton.', *Trends in plant science*, 5(1), pp. 12–7.

Mackey, K. R. M., Paytan, A., Grossman, A. R. and Bailey, S. (2008) 'A photosynthetic strategy for coping in a high-light, low-nutrient environment', *Limnology and Oceanography*, 53(3), pp. 900–913.

Mahadevan, A., D'Asaro, E., Lee, C. and Perry, M. J. (2012) 'Eddy-Driven Stratification Initiates North Atlantic Spring Phytoplankton Blooms', *Science*, 337(6090), pp. 54–58.

Marañón, E. (2015) 'Cell Size as a Key Determinant of Phytoplankton Metabolism and Community Structure', *Annual Review of Marine Science*, 7(1), pp. 241–264.

McClain, C. R. (2009) 'A Decade of Satellite Ocean Color Observations', *Annual Review of Marine Science*, 1(1), pp. 19–42.

McKew, B. a, Davey, P., Finch, S. J., Hopkins, J., Lefebvre, S. C., Metodiev, M. V, Oxborough, K., Raines, C. a, Lawson, T. and Geider, R. J. (2013) 'The trade-off between the light-harvesting and photoprotective functions of fucoxanthin-chlorophyll proteins dominates light acclimation in Emiliania huxleyi (clone CCMP 1516).', *The New phytologist*, 200(1), pp. 74–85.

McKew, B. a, Metodieva, G., Raines, C. a, Metodiev, M. V and Geider, R. J. (2015) 'Acclimation of E miliania huxleyi (1516) to nutrient limitation involves precise modification of the proteome to scavenge alternative sources of N and P', *Environmental Microbiology*, 17(10), pp. 4050–4062.

Melrose, D. and Oviatt, C. (2006) 'Comparisons of fast repetition rate fluorescence

estimated primary production and 14C uptake by phytoplankton', *Marine Ecology Progress Series*, 311, pp. 37–46.

Milligan, A. J., Aparicio, U. A. and Behrenfeld, M. J. (2012) 'Fluorescence and nonphotochemical quenching responses to simulated vertical mixing in the marine diatom Thalassiosira weissflogii', *Marine Ecology Progress Series*, 448, pp. 67–78.

Mills, M. M., Ridame, C., Davey, M., La Roche, J. and Geider, R. J. (2004) 'Iron and phosphorus co-limit nitrogen fixation in the eastern tropical North Atlantic.', *Nature*, 429(6989), pp. 292–4.

Moore, C. M. (2014) 'Microbial proteins and oceanic nutrient cycles', *Science*, 345(6201), pp. 1120–1121.

Moore, C. M., Lucas, M. I., Sanders, R. and Davidson, R. (2005) 'Basin-scale variability of phytoplankton bio-optical characteristics in relation to bloom state and community structure in the Northeast Atlantic', *Deep-Sea Research Part I: Oceanographic Research Papers*, 52(3), pp. 401–419.

Moore, C. M., Mills, M. M., Arrigo, K. R., Berman-Frank, I., Bopp, L., Boyd, P. W., Galbraith, E. D., Geider, R. J., Guieu, C., Jaccard, S. L., Jickells, T. D., La Roche, J., Lenton, T. M., Mahowald, N. M., Marañón, E., Marinov, I., Moore, J. K., Nakatsuka, T., Oschlies, A., Saito, M. a, Thingstad, T. F., Tsuda, A. and Ulloa, O. (2013) 'Processes and patterns of oceanic nutrient limitation', *Nature Geoscience*. Nature Publishing Group, 6(9), pp. 701–710.

Moore, C. M., Seeyave, S., Hickman, A. E., Allen, J. T., Lucas, M. I., Planquette, H., Pollard, R. T. and Poulton, A. J. (2007) 'Iron–light interactions during the CROZet natural iron bloom and EXport experiment (CROZEX) I: Phytoplankton growth and photophysiology', *Deep Sea Research Part II: Topical Studies in Oceanography*, 54(18–20), pp. 2045–2065.

Moore, C. M., Suggett, D. J., Hickman, A. E., Kim, Y.-N., Tweddle, J. F., Sharples, J., Geider, R. J. and Holligan, P. M. (2006) 'Phytoplankton photoacclimation and photoadaptation in response to environmental gradients in a shelf sea', *Limnology and Oceanography*, 51(2), pp. 936–949.

Moore, C., Mills, M. M., Langlois, R., Milne, A., Achterberg, E. P., La Roche, J. and Geider, R. J. (2008) 'Relative influence of nitrogen and phosphorous availability on phytoplankton physiology and productivity in the oligotrophic sub-tropical North Atlantic Ocean', *Limnology and oceanography*, 53(1), pp. 291–305.

Moore, C., Suggett, D., Holligan, P., Sharples, J., Abraham, E., Lucas, M., Rippeth, T., Fisher, N., Simpson, J. and Hydes, D. (2003) 'Physical controls on phytoplankton physiology and production at a shelf sea front: a fast repetition-rate fluorometer based field study', *Marine Ecology Progress Series*, 259, pp. 29–45.

Morris, D. J., Speirs, D. C., Cameron, A. I. and Heath, M. R. (2014) 'Erratum to "Global sensitivity analysis of an end-to-end marine ecosystem model of the North Sea: Factors affecting the biomass of fish and benthos" [Ecol. Model. 273 (2014) 251-263]', *Ecological Modelling*, 279, pp. 114–117.

Müller, P., Li, X. and Niyogi, K. (2001) 'Non-photochemical quenching. A response to excess light energy', *Plant Physiology*, 125, pp. 1558–1566.

Murata, N., Takahashi, S., Nishiyama, Y. and Allakhverdiev, S. I. (2007) 'Photoinhibition of photosystem II under environmental stress.', *Biochimica et biophysica acta*, 1767(6), pp. 414–21.

Muylaert, K., Gonzales, R., Franck, M., Lionard, M., Van der Zee, C., Cattrijsse, A., Sabbe, K., Chou, L. and Vyverman, W. (2006) 'Spatial variation in phytoplankton dynamics in the Belgian coastal zone of the North Sea studied by microscopy, HPLC-CHEMTAX and underway fluorescence recordings', *Journal of Sea Research*, 55(4), pp. 253–265.

Nielsen, E. (1952) 'The use of radio-active carbon (C14) for measuring organic production in the sea', *Journal du Conseil*, (1919).

Niyogi, K. K. and Truong, T. B. (2013) 'Evolution of flexible non-photochemical quenching mechanisms that regulate light harvesting in oxygenic photosynthesis', *Current Opinion in Plant Biology*. Elsevier Ltd, 16(3), pp. 307–314.

O'Malley, R. T., Behrenfeld, M. J., Westberry, T. K., Milligan, A. J., Shang, S. and Yan, J. (2014) 'Geostationary satellite observations of dynamic phytoplankton

photophysiology', *Geophysical Research Letters*, 41(14), pp. 5052–5059.

O'Reilly, J. E., Maritorena, S., Mitchell, B. G., Siegel, D. a., Carder, K. L., Garver, S. a., Kahru, M. and McClain, C. (1998) 'Ocean color chlorophyll algorithms for SeaWiFS', *Journal of Geophysical Research*, 103(C11), p. 24937.

OSPAR (2003) *OSPAR Integrated Report 2003 on the Eutrophication Status of the OSPAR Maritime Area Based Upon the First Application of the Comprehensive Procedure*, *Eutrophication Series*.

Oxborough, K., Moore, C. M., Suggett, D. J., Lawson, T., Chan, H. G. and Geider, R. J. (2012) 'Direct estimation of functional PSII reaction center concentration and PSII electron flux on a volume basis: a new approach to the analysis of Fast Repetition Rate fluorometry (FRRf) data', *Limnology and Oceanography: Methods*, 10, pp. 142–154.

Pahlow, M. & Oschlies, A. (2009). Chain model of phytoplankton P, N and light co-limitation. *Marine Ecolology Progress Series*, 376, pp. 69–83

Parkhill, J. P., Maillet, G. and Cullen, J. J. (2001) 'Fluorescence-based maximal quantum yield for PSII as a diagnostic of nutrient stress', *Journal of Phycology*, 37(4), pp. 517–529.

Pebesma, E. and Graeler, B. (2017) 'Spatial and Spatio-Temporal Geostatistical Modelling, Prediction and Simulation', pp. 1–82.

Petersen, W. (2014) 'FerryBox systems: State-of-the-art in Europe and future development', *Journal of Marine Systems*. Elsevier B.V., 140(PA), pp. 4–12.

Pierce, D. (2017) 'Package "ncdf4"'.

Pingree, R. D., Holligan, P. M., Mardell, G. T. and Head, R. N. (2009) 'The influence of physical stability on spring, summer and autumn phytoplankton blooms in the Celtic Sea', *Journal of the Marine Biological Association of the United Kingdom*, 56(4), pp. 845–873.

Platt, T. and Denman, K. L. (1975) 'Spectral Analysis in', pp. 189–211.

Platt, T., Sathyendranath, S., Caverhill, C. M. and Lewis, M. R. (1988) 'Ocean primary

production and available light: further algorithms for remote sensing', *Deep Sea Research Part A. Oceanographic Research Papers*, 35(6), pp. 855–879.

Ragni, M., Airs, R., Hennige, S., Suggett, D., Warner, M. and Geider, R. (2010) 'PSII photoinhibition and photorepair in Symbiodinium (Pyrrhophyta) differs between thermally tolerant and sensitive phylotypes', *Marine Ecology Progress Series*, 406, pp. 57–70.

Ragni, M., Airs, R. L., Leonardos, N. and Geider, R. J. (2008) 'Photoinhibition of Psii in Emiliania Huxleyi (Haptophyta) Under High Light Stress: the Roles of Photoacclimation, Photoprotection, and Photorepair', *Journal of Phycology*, 44(3), pp. 670–683.

Ralph, P. J. and Gademann, R. (2005) 'Rapid light curves: A powerful tool to assess photosynthetic activity', *Aquatic Botany*, 82(3), pp. 222–237.

Redfield, A. C. (1958) 'The biological control of chemical factors in the environment', *American Scientist*, 46(3), pp. 205–221.

Robinson, C., Suggett, D. J., Cherukuru, N., Ralph, P. J. and Doblin, M. a. (2014) 'Performance of Fast Repetition Rate fluorometry based estimates of primary productivity in coastal waters', *Journal of Marine Systems*. Elsevier B.V., 139, pp. 299–310.

Robinson, C., Tilstone, G., Rees, A., Smyth, T., Fishwick, J., Tarran, G., Luz, B., Barkan, E. and David, E. (2009) 'Comparison of in vitro and in situ plankton production determinations', *Aquatic Microbial Ecology*, 54(January), pp. 13–34.

Robison, J. D. and Warner, M. E. (2006) 'Differential Impacts of Photoacclimation and Thermal Stress on the Photobiology of Four Different Phylotypes of Symbiodinium (Pyrrhophyta)1', *Journal of Phycology*, 42(3), pp. 568–579.

Roesler, C., Uitz, J., Claustre, H., Boss, E., Xing, X., Organelli, E., Briggs, N., Bricaud, A., Schmechtig, C., Poteau, A., D'Ortenzio, F., Ras, J., Drapeau, S., Haëntjens, N. and Barbieux, M. (2017) 'Recommendations for obtaining unbiased chlorophyll estimates from in situ chlorophyll fluorometers: A global analysis of WET Labs ECO sensors', *Limnology and Oceanography: Methods*, 15(6), pp. 572–585.

Ruben, S., Randall, M., Kamen, M., Hyde and JL (1941) 'Heavy oxygen (O18) as a tracer in the study of photosynthesis', *Journal of the American Chemistry Society*, pp. 9–11.

Saito, M. a., Goepfert, T. J. and Ritt, J. T. (2008) 'Some thoughts on the concept of colimitation: Three definitions and the importance of bioavailability', *Limnology and Oceanography*, 53(1), pp. 276–290.

Sakshaug, E., Bricaud, A., Dandonneau, Y., Falkowski, P. G. and Kiefer, D. A. (1997) 'Parameters of photosynthesis : definitions , theory and interpretation of results', 19, pp. 1637–1670.

Sanders, R., Henson, S. A., Koski, M., De La Rocha, C. L., Painter, S. C., Poulton, A. J., Riley, J., Salihoglu, B., Visser, A., Yool, A., Bellerby, R. and Martin, A. P. (2014) 'The Biological Carbon Pump in the North Atlantic', *Progress in Oceanography*, 129, pp. 200–218.

Sathyendranath, S., Brewin, R. J. W., Jackson, T., Mélin, F. and Platt, T. (2017) 'Ocean-colour products for climate-change studies: What are their ideal characteristics?', *Remote Sensing of Environment*. Elsevier Inc.

Sauzède, R., Lavigne, H., Claustre, H., Uitz, J., Schmechtig, C., D'Ortenzio, F., Guinet, C. and Pesant, S. (2015) 'Vertical distribution of chlorophyll a concentration and phytoplankton community composition from in situ fluorescence profiles: A first database for the global ocean', *Earth System Science Data*, 7(2), pp. 261–273.

Schuback, N., Flecken, M., Maldonado, M. T. and Tortell, P. D. (2016) 'Diurnal variation in the coupling of photosynthetic electron transport and carbon fixation in iron-limited phytoplankton in the NE subarctic Pacific', *Biogeosciences*, 13(4), pp. 1019–1035.

Sharples, J., Moore, M. C., Rippeth, T. P., Holligan, P. M., Hydes, D. J., Fisher, N. R. and Simpson, J. H. (2001) 'Phytoplankton distribution and survival in the thermocline', *Limnology and Oceanography*, 46(3), pp. 486–496.

Sharples, J., Tweddle, J., Green, J., Palmer, M., Kim, Y., Hickman, A., Holligan, P., Moore, C., Rippeth, T., Simpson, J. and Krivtsov, V. (2007) 'Spring-neap modulation

of internal tide mixing and vertical nitrate fluxes at a shelf edge in summer', *Limnology and Oceanography*, 52(5), pp. 1735–1747.

Silsbe, G. M. and Kromkamp, J. C. (2012) 'Modeling the irradiance dependency of the quantum efficiency of photosynthesis', *Limnology and Oceanography: Methods*, 10(2002), pp. 645–652.

Smyth, T. J., Pemberton, K. L., Aiken, J. and Geider, R. J. (2004) 'A methodology to determine primary production and phytoplankton photosynthetic parameters from Fast Repetition Rate Fluorometry', *Journal of Plankton Research*, 26(11), pp. 1337–1350.

Suggett, D. J., MacIntyre, H. L. and Geider, R. J. (2004) 'Evaluation of biophysical and optical determinations of light absorption by photosystem II in phytoplankton', *Limnology and Oceanography: Methods*, 2(10), pp. 316–332.

Suggett, D. J., Moore, C. M., Marañón, E., Omachi, C., Varela, R. a., Aiken, J. and Holligan, P. M. (2006) 'Photosynthetic electron turnover in the tropical and subtropical Atlantic Ocean', *Deep Sea Research Part II: Topical Studies in Oceanography*, 53(14–16), pp. 1573–1592.

Suggett, D. j., Stambler, N., O, P., Kolber, Z., Quigg, A., Vázquez-Dominguez, E., Zohary, T., Berman, T., Iluz, D., Levitan, O., Lawson, T., Meeder, E., Lazar, B., Bar-Zeev, E., Medova, H. and Berman-Frank, I. (2009) 'Nitrogen and phosphorus limitation of oceanic microbial growth during spring in the Gulf of Aqaba', *Aquatic Microbial Ecology*, 56, pp. 227–239.

Suggett, D., Kraay, G., Holligan, P., Davey, M., Aiken, J. and Geider, R. (2001) 'Assessment of photosynthesis in a spring cyanobacterial bloom by use of a fast repetition rate fluorometer', *Limnology and Oceanography*, 46(4), pp. 802–810.

Suggett, D., MacIntyre, H., Kana, T. and Geider, R. (2009) 'Comparing electron transport with gas exchange: parameterising exchange rates between alternative photosynthetic currencies for eukaryotic phytoplankton', *Aquatic Microbial Ecology*, 56(September), pp. 147–162.

Suggett, D., Moore, C., Hickman, A. E. and Geider, R. (2009) 'Interpretation of fast

repetition rate (FRR) fluorescence: signatures of phytoplankton community structure versus physiological state', *Marine Ecology Progress Series*, 376, pp. 1–19.

Sverdrup, H. U. (1953) 'On Conditions for the Vernal Blooming of Phytoplankton', *ICES Journal of Marine Science*, 18(3), pp. 287–295.

Teeling, H., Fuchs, B. M., Becher, D., Klockow, C., Gardebrecht, A., Bennke, C. M., Kassabgy, M., Huang, S., Mann, A. J., Waldmann, J., Weber, M., Klindworth, A., Otto, A., Lange, J., Bernhardt, J., Reinsch, C., Hecker, M., Peplies, J., Bockelmann, F. D., Callies, U., Gerdts, G., Wichels, A., Wiltshire, K. H., Glöckner, F. O., Schweder, T. and Amann, R. (2012) 'Substrate-controlled succession of marine bacterioplankton populations induced by a phytoplankton bloom.', *Science (New York, N.Y.)*, 336(6081), pp. 608–11.

Thomas, H., Bozec, Y., de Baar, H. J. W., Elkalay, K., Frankignoulle, M., Schiettecatte, L.-S., Kattner, G. and Borges, A. V. (2005) 'The carbon budget of the North Sea', *Biogeosciences*, 2(1), pp. 87–96.

Thomas, H., Bozec, Y., de Baar, H. J. W., Elkalay, K., Frankignoulle, M., Schiettecatte, L.-S. and Vieira Borges, a. (2004) 'The carbon budget of the North Sea', *Biogeosciences Discussions*, 1(1), pp. 367–392.

Thyssen, M., Alvain, S., Lefèbvre, A., Dessailly, D., Rijkeboer, M., Guiselin, N., Creach, V. and Artigas, L.-F. (2015) 'High-resolution analysis of a North Sea phytoplankton community structure based on in situ flow cytometry observations and potential implication for remote sensing', *Biogeosciences*, 12(13), pp. 4051–4066.

Tilstone, G. H., Smyth, T. J., Gowen, R. J., Martinez-Vicente, V. and Groom, S. B. (2005) 'Inherent optical properties of the Irish Sea and their effect on satellite primary production algorithms', *Journal of Plankton Research*, 27, pp. 1127–1148.

Venrick, E. L., Beers, J. R. and Heinbokel, J. F. (1977) 'Possible consequences of containing microplankton for physiological rate measurements', *Journal of Experimental Marine Biology and Ecology*, 26(1), pp. 55–76.

Wagner, H., Jakob, T. and Wilhelm, C. (2006) 'Balancing the energy flow from captured light to biomass under fluctuating light conditions.', *The New phytologist*,

169(1), pp. 95–108.

Westberry, T., Behrenfeld, M.J., Siegel, D.A. and Boss, E. (2008). Carbon-based primary productivity modeling with vertically resolved photoacclimation. *Global Biogeochemical Cycles*, *22*(2)

Weston, K., Fernand, L., Mills, D. K., Delahunty, R. and Brown, J. (2005) 'Primary production in the deep chlorophyll maximum of the central North Sea', *Journal of Plankton Research*, 27(9), pp. 909–922.

Williams, C., Sharples, J., Mahaffey, C. and Rippeth, T. (2013) 'Wind-driven nutrient pulses to the subsurface chlorophyll maximum in seasonally stratified shelf seas', *Geophysical Research Letters*, 40(20), pp. 5467–5472.

Xing, X., Claustre, H. and Blain, S. (2012) 'for in vivo chlorophyll fluorescence acquired by autonomous platforms: A case study with instrumented elephant seals in the Kerguelen region (Southern Ocean', *Limnol. Oceanogr. …*, pp. 483–495.

Xing, X., Claustre, H., Boss, E., Roesler, C., Organelli, E., Poteau, A., Barbieux, M. and D'Ortenzio, F. (2017) 'Correction of profiles of in-situ chlorophyll fluorometry for the contribution of fluorescence originating from non-algal matter', *Limnology and Oceanography: Methods*, 15(1), pp. 80–93.

Zapata, M., Rodriguez, F. and Garrido, J. (2000) 'Separation of chlorophylls and carotenoids from marine phytoplankton: a new HPLC method using a reversed phase C8 column and pyridine-containing mobile', *Marine Ecology Progress Series*, 195, pp. 29–45.